Progress in Materials Science 58 (2013) 261–326

Contents lists available at SciVerse ScienceDirect

Progress in Materials Science

journal homepage: www.elsevier.com/locate/pmatsci

# Engineering biocompatible implant surfaces Part I: Materials and surfaces

Sebastian Bauer [a], Patrik Schmuki [a,*], Klaus von der Mark [b], Jung Park [c]

[a] Department of Materials Science, Institute for Surface Science and Corrosion (LKO), University of Erlangen-Nuremberg, 91058 Erlangen, Germany
[b] Department of Experimental Medicine I, Nikolaus-Fiebiger-Center of Molecular Medicine, University of Erlangen-Nuremberg, 91054 Erlangen, Germany
[c] Department of Pediatrics, Division of Molecular Pediatrics, University Hospital Erlangen, Germany

ARTICLE INFO

*Article history:*
Available online 3 October 2012

ABSTRACT

During recent decades vast and continuously increasing numbers of biomedical implants have been introduced for continuous use in the human body. Since the early cemented hip replacements in the 1960s there has been a constant spread of new materials, and ever more complex designs are being used in these implant devices. But still the rate of failure and loss of implants is undesirably high and leaves space for improvements. The challenge is to understand the interactions of implant surface with the surrounding tissue sufficiently, to actively tailor desired interactions. Bulk and surface properties of biomaterials used for implants have been shown to directly influence, and in some cases, control the dynamic interactions that take place at the tissue–implant interface. It is critical to recognize that synthetic materials have specific bulk and surface properties or characteristics that determine their in vitro and in vivo characteristics.

This article reviews the interdisciplinary field of biocompatible implant surfaces from the viewpoint of materials science, biochemistry and cell biology. It compiles an overview on basic information about bulk and surface properties of implants based on metallic materials (particularly titanium and its alloys) and surface modification including functionalization with adhesion and growth promoting species. It describes how cells recognize surfaces and respond to different biomaterials, outlines common

* Corresponding author.
*E-mail addresses:* sebastian.bauer@ww.uni-erlangen.de (S. Bauer), schmuki@ww.uni-erlangen.de (P. Schmuki), kvdmark@molmed.uni-erlangen.de (K. von der Mark), jpark@molmed.uni-erlangen.de (J. Park).

0079-6425/$ - see front matter 
http://dx.doi.org/10.1016/j.pmatsci.2012.09.001

assays on cell behavior in culture, and reports on cell types and proteins involved in tissue response, acute and chronic responses to implanted biomaterials.



**Contents**

**Table 1**
Definitions for Biomaterials [3,5].

| | |
|---|---|
| Biomaterial | A non-viable material, used in a medical device, intended to interact with biological systems |
| Implant | Any medical device made from one or more materials that is intentionally placed within the body, either totally or partially buried beneath an epithelial surface |
| Prosthesis | A device that replaces a limb, organ or tissue of the body |
| Artificial organ | A medical device that replaces, in part or in whole, the function of one of the organs of the body |

## 1. What are biomaterials?

### *1.1. Introduction to biomaterials*

Biomaterials are commonly characterized as materials used to construct artificial organs, rehabilitation devices, or implants to replace natural body tissues. More specific, biomaterials are materials that are used in close or direct contact with the body to augment or replace faulty materials.

In general biomaterials can be classified into living or once living materials, which fit into the division of for example tissue engineering, and materials that are of a synthetic origin [1]. Such biomaterials can be defined as inorganic or organic materials that are biocompatible and can be implanted in the human body to replace or repair failing tissue. The concept extends to the materials used in drug-delivery systems, biosensors or devices operating outside the body but in communication with it – for example artificial heart systems [2]. In recent years, progress in many different fields has paved the way to creating innovative biomaterials to improve existing treatments and develop new ones for a higher quality of life.

In 1986 the European Society for Biomaterials compiled a set of "Definitions in Biomaterials". Some definitions for biomaterials and most important terms in the field are listed in Table 1.

Especially materials known from the field of implantology that are used for the fixation or the replacement of diseased hard tissue have run through numerous inventions. Particularly, as this class of biomaterials includes certain materials systems such as metals, ceramics and polymers, which are used for example in reconstructing bones, joints or for teeth replacement, the diversity of inventions and modifications on bulk as well as surface properties, has reached an enormous quantity.

To successfully apply implants in the human body, an adequate level of tolerance of the material used with the living organism is required, in other words a high grade of biocompatibility [1].

Biocompatibility has been defined as "the ability of a material to perform with an appropriate host response in a specific application" [3,4]. This means that the material or any leachable products from it do not cause cell death, chronic inflammation or other impairment of cellular or tissue functions. Implants not only have to be biosafe and biostable in terms of cytotoxicity and degradation, they also have to match with the biological requirements of any structural biocompatibility. In other words, shape, inner structure and design of an implant need to be adapted to the characteristics of the tissue to be replaced [5]. Besides these bulk requirements, the biocompatibility of surfaces plays a crucial role as the surface is directly exposed to the living organism. Therefore it is necessary to tailor exposed surfaces in view of their chemical, physical, biological and morphological features [5]. Goal of implant

**Table 2**
Classification of interactions of implants with hard tissue [5,7].

| | |
|---|---|
| Incompatible | Release of substances in toxic concentrations that lead to inharmonious effects with the living organism that may result in a rejection of the implant |
| Biotolerant | Release of substances but not in toxic concentrations that may lead to an encapsulation within connective tissue |
| Bioinert | No release of toxic substances |
| Bioactive | Positive interaction with differentiation of tissue that leads to a close adhesion and interconnection along the interface of implant and tissue |

surface engineering is not only to fit the demands of avoiding negative effects of implanted materials on the surrounding tissue but even more to enhance the interplay between the designed technical material and the living matter [6]. Possible interactions of implants with hard tissue are listed below (Table 2 [5,7]).

In best case the physical and chemical properties of the chosen implant material should be in accord with the replaced tissue. One of the most challenging tasks is that living tissue has the ability to renew itself continuously, whereas implant materials typically lack this ability [5]. To reach a maximum in implant success it is necessary to combine the synergistic effects of various biomedical material systems.

### 1.2. Structural hierarchies

Designing a synthetic material which is dedicated to successfully replace tissue in a living organism, the length scales of the key structural hierarchy must be considered. The hierarchical structure of tissue in the living organism spans approximately eight orders of magnitude; starting at the molecular scale of, for example, cell adhesion receptors embedded in the cell membrane that interact with extracellular proteins or surfaces, towards organells leading to cells, which range in the 100 μm scale, and tissue and higher structures as organs that are of a macroscopic level [1,8]. This means that for engineering appropriate synthetic materials for the use as a biomedical material system, the whole length scale from the nanoscale up to macroscale needs to be taken into account.

For example, human compact bone is a natural composite which can be described roughly as follows. Starting from the macroscopic shape it exhibits a rich hierarchical structure [9,10] (see Fig. 1 [11]). On the microstructural level one can observe osteons [12], which are large (200 μm diameter) hollow fibers composed of concentric lamellae and of pores. The lamellae are built of fibers, and these fibers contain fibrils. At the ultra structural level of the nanoscale the fibers are a composite of the mineral hydroxyapatite and the protein collagen. These nanoscale building blocks produced through self-assembly yield a nested structure. These nested structures themselves may be formed by self-assembly, often with help of cells. In the field of implantology understanding the hierarchical structures (of e.g. bone) is a basic matter to finally obtain implant materials that fit to given structural demands.

The length scales in multiscale living organism can be matched with synthetic materials using various strategies. Structure in solids occurs in a hierarchy of sizes. The primary chemical structure of

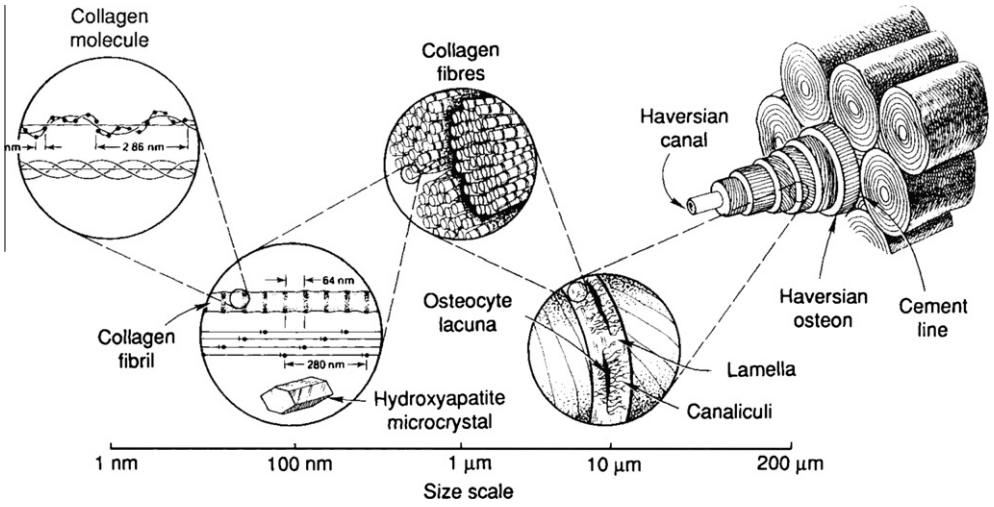


**Fig. 1.** Structural hierarchy of compact bone [11].

materials at the length scale of bonds can strongly be influenced by the choice of the material, i.e. it can be based on ionic, covalent or metallic bonds, and additionally provide secondary intramolecular effects such as electrostatic, H-bonding, van der Waals or hydrophobic interactions. The compatibility of an implant material is strongly determined by the primary chemical structure as for example properties like corrosion resistance, strength, wear resistance, flexibility or the solubility in water are derived to a large extent from the molecular arrangement [1].

The higher order in the bulk structure (1–100 nm) of materials can be utilized to tailor tissue specific properties of implants, as for example the crystal structure for controlled degeneration of polymers, the short range order of loose network structures as found in bioactive glasses, or the self-assembly of amphiphilic molecules as used in liposomal drug delivery systems [1,5].

The structure at the micrometer level (>1 μm) of materials bears another variable in the correlation between the influences of the length scale on the properties of the material and the effect on tissue. Grain size effects or second phase precipitates can affect strength, ductility or wear resistance and metallurgical methods can be used to adjust these properties. Another feature that plays an important role at the micron-scale of implant materials is the presence of porosity, cavities or channels that may allow a controlled ingrowth of tissue into the synthetically formed material. Thus not only a well interlinked connection between the synthetically formed material and the tissue from the living organism can be formed but also means for the ingrowth of blood vessels (vascularization) can be provided.

Both synthetic materials and biological systems possess functionally relevant over broad length scales, allowing for wide range of adjustability in case of biomedical materials. Typically the higher order structures as well as the microstructure strongly dictate the kinetic processes and mechanical responses. In early hard tissue implant materials mostly bulk properties of such systems (e.g. Young's modulus, tensile stress, bending strength, shear strength, fatigue strength, stiffness) were considered. Meanwhile the world wide thrust in this field has laid the foundation for a more advanced design of implant materials that is based on a drastically improved understanding of natural materials and the material/biological organism interface.

### *1.3. Materials choice for implants*

The choice of adequate materials for applications in the living organism is defined by their application. In case of implants that are dedicated for the replacement of bone tissue, key targets are the mechanical properties that can take high loads. For blood vessel implants the key requirement lies in the surface properties, primary the chemical composition, to maximally reduce thrombogenicity. On the other hand, for a material if used as contact lens or intraocular lens obviously the optical transparence is a major criterion for the selection of the material. For the success of an implant material introduced to the living organism, besides the need of biocompatibility of the material itself, also criteria such as sterilizability, required physical and chemical strength, or very simplified the ability to process the material have to be provided. It has to be considered that biocompatibility for implants is not only defined by the intrinsic properties of the material but also by the manufacturing process as well as by possible post-treatments such as sterilization. This means that for example in case of polymers a sterilization process must be employed that does not influence the molecular structure of the material itself [5]. Table 3 summarizes these requirements roughly.

**Table 3**
Material specifications for biomedical applications [13].

| Property | Desirables |
|---|---|
| Biocompatibility | Non-inflammatory, non-toxic, noncarcinogenic, nonpyrogenic, blood compatible, non-allergic |
| Sterilizability | Not destroyed by typical sterilizing techniques like autoclaving, dry heat, ethylene oxide, radiation |
| Physical characteristics | Strength, elasticity, durability |
| Manufacturability | Machinable, extrudable, moldable |

**Table 4**
Time scale over which the host is exposed to the material [13].

| Material | Contact time |
|---|---|
| Syringe needle | 1–2 s |
| Tongue depressor | 10 s |
| Contact lens | 12 h to 30 days |
| Bone screw/plate | 3–12 months |
| Total hip replacement | 10–15 years |
| Intraocular lens | 30+ years |

**Table 5**
Metals commonly used for implants [2].

| Metal | Application |
|---|---|
| Cobalt–chromium alloys | Artificial heart valves, dental prosthesis, orthopedic fixation plates, artificial joint components, vascular stents |
| Stainless steel | Dental prostheses, orthopedic fixation plates, vascular stents |
| Titanium alloys | Artificial heart valves, dental implants, artificial joint components, orthopedic screws, pacemaker cases, vascular stents |
| Gold or platinum | Dental fillings, electrodes for cochlear implants |
| Silver–tin–copper alloys | Dental amalgams |

Besides the recommendations for the biocompatibility of implants there is no general set of criteria, that if met, qualify a material as being biocompatible. The time scale over which a material is exposed to the living organism must be considered. Table 4 shows some examples of biomedical applications regarding the contact times with the living organism. It can be seen that for example in case of syringe needles the contact times are rather short, within seconds, so that chemical stability or toxicity do not play such a prior role. However, for intraocular lenses or total hip replacements where the desired time scale of contact with the host tissue is in the range of more than 15 years, the recommendations for the material are much more miscellaneous [1,13].

With these general requirements for implant materials it is one of the primary roles of the biomaterials specialist to choose appropriate materials for a specific application. In general, materials fall into the three categories metals, ceramics and polymers [2].

### *1.3.1. Metals*

Metals are inorganic materials possessing non-directional metallic bonds with highly mobile electrons. In addition to their ability to conduct electricity, metals are strong and relatively easily formed into complex shapes [2]. Implants based on metals are mainly used in two fields of application either for the total joint replacement as hip, knee or shoulder, or for the fixation of fractures or vessels in the form of nails, screws or stents. Moreover, in the field of oral surgery also noble metals are used in terms of dental fillings. In most other fields the low mechanical stability of noble metals is not sufficient [2,5]. The demand for metallic implant materials is characterized by many clinical trials. A high mechanical resistance is recommended to ensure a good load transmission over a long time as well as mechanical stiffness close to bone. The corrosion resistance of metals in the living organism is one of the major prerequisites to avoid impairment of the materials properties due to degradation. Moreover, the biocompatibility must be guaranteed so that any damage of the host tissue must be avoided that could be caused from leaking corrosion products or abrasive particles [5]. A list of commonly used biomedical applications of metals is given in Table 5.

### *1.3.2. Ceramics*

Ceramics are inorganic materials composed of non-directional ionic or covalent bonds and which are generally formed at elevated temperatures. The class of biocompatible ceramics consists mainly of the crystalline materials such as alumina, zirconia, calcium phosphates and bioactive glasses and

**Table 6**
Commonly used ceramics in biomedical applications [2,17].

| Ceramic | Application |
|---|---|
| Aluminum oxides | Orthopedic joint replacement, orthopedic load-bearing implants, implant coatings, dental implants |
| Zirconium oxides | Orthopedic joint replacement, dental implants |
| Calcium phosphates | Orthopedic and dental implant coatings, dental implant materials, bone graft substitute materials |
| Bioactive glasses | Orthopedic and dental implant coatings, dental implants, facial reconstruction components, bone graft substitute materials, bone cements |

glass ceramics [14,15]. Ceramics are very hard and more resistant to degradation in many environments than metals. However, they are quite brittle due to the nature of ionic bonds. The similarity in the chemistry of ceramics and that of native bone, makes ceramics often used as a part of orthopedic implants or as dental materials [2]. Mostly biocompatible ceramics are used in coherence with the human skeleton, bones, joints and teeth. In dental medicine ceramic materials are used as replacement of teeth. Due to the high abrasive strength ceramics are used as bearing balls in artificial joints or as bone conductive coatings on metal based implants [5,16]. Most frequently used ceramic biomaterials are listed in Table 6 [2,17].

### *1.3.3. Polymers*

In contrary to the other two classes of biocompatible materials polymers are organic materials possessing long chains with a large number of small repeating units (monomers) that are held together by directional covalent bonds. Polymers are widely used in biomedical applications due to the range of physical and chemical properties possible with these materials [18]. Polymers can be easily fabricated to various complex shapes and structures and additionally surface properties can be easily tuned. Polymers that are used as implant materials can be either derived from natural sources such as proteins or from synthetic sources [2]. When using polymers in biomedical devices several points are typically critical issues. Polymers tend to easily absorb water and biomolecules from the surroundings and thereby may alter the surface chemistry. Moreover, polymers are in comparison to metals or ceramics soft materials that may undergo mechanical wear and breakdown. For the processing of polymers usually additives such as flexibilizer, antioxidizer or stabilizers are needed. Therefore it is necessary to avoid any leaching of these, often harmful, compounds into the organism [19,20]. The sterilization of polymers bears some difficulties as the commonly used sterilization procedures may influence the chemical and mechanical properties [5].

Independent of the origin of the polymer used as biomedical material there are several polymer sub-classes that may be particularly suited to be used in certain tissues. At low stresses elastomers show the ability to sustain substantial deformation and return rapidly into their initial dimensions [21] as recommended for example in cardiovascular applications where tissue elasticity is an important property [2]. Another previously mentioned property of some polymers is the ability to uptake water and as a result a swollen hydrogel can be used for a variety of soft tissue applications [21]. Examples for synthetic and natural polymers are listed in Table 7.

In practice, division along material classes does not hold up well, as for example a heart valve may be fabricated from polymers, metals and carbons, while a hip joint will also be composed of metals and polymers and may be interfaced to the body via polymeric bone cement [1,5]. Nevertheless, the above described classes of materials for biomedical applications show that a wide range of materials is routinely used. This variety of material systems makes it virtually impossible for a single researcher to be experienced in synthesizing, designing and applying all these material classes in the biomaterials field. Ratner et al. therefore pointed out that there is a tendency to group the materials into the "hard tissue replacement biomaterials" (mainly metals and ceramics), typically represented by those involved in orthopedic and dental materials, and the "soft tissue replacement biomaterials"

**Table 7**
Polymers commonly used in biomedical applications derived synthetically and naturally [2,5].

| Polymer | Application |
|---|---|
| Synthetically derived | |
| Polyethylene | Orthopedic joint implants, syringes |
| Polypropylene | Heart valves, sutures, syringes |
| Polydimethylsiloxane | Breast implants, contact lenses, knuckle replacements, heart valves, artificial hearts |
| Polyethyleneterephthalate | Vascular grafts, sutures, blood vessles |
| Polymethylmethacrylate | Bone cements, intraocular contact lenses, dental implants |
| Polyethyleneglycol | Pharmaceutical fillers, wound dressings |
| Poly-2-hydroxylethylmethacrylate | Contact lenses, urinary bladder catheter |
| Polytetafluoroethylene | Vascular grafts, sutures |
| Polylactic-co-glycolic acid | Resorbable meshes and sutures |
| Poly-$\varepsilon$-caprolactone | Drug delivery devices, sutures |
| Polyvinylchloride | Blood bags, blood tubes |
| Polyisoprene | Gloves |
| Naturally derived | |
| Collagen | Orthopedic repair matrices, nerve repair matrices, tissue engineering matrices |
| Hyaluronic acid | Orthopedic repair matrices |
| Glycosaminoglycan | Orthopedic repair matrices |
| Elastin | Skin repair matrices |
| Fibrin | Hemostatic products, tissue sealants |
| Chitosan | Wound dressing |
| Alginate | Wound dressing |

(mainly polymers), which are often associated with cardiovascular and general plastic surgery materials [1].

The focus of the following paragraphs in this article will mainly focus on ''hard tissue replacement biomaterials'' and herein the properties and especially the modification and functionalization of surfaces and interfaces. Emphasis is given to the fact that biofunctionality of biomedical materials to a large extent is defined by the interactions between the implant surface and the surrounding biological matter.

## 2. Mechanical aspects of implant materials

### *2.1. Some general aspects*

Hard tissue is often damaged due to accidents, aging, and similar other causes. It is a common practice to surgically substitute damaged hard tissues with artificial replacements. Biomedical materials that are intended for the replacement of hard tissue must fulfill besides a proper biocompatibility, also key requirements such as favorable mechanical properties. Depending on the regions of the body in which the implants are inserted and the functions to be provided, the requirements of different endoprosthetic materials are varying. Medical progress calls for the development of increasingly specialized properties of biomaterials.

The adequate choice of a material for a specific mechanical application can be guided by the mechanical material constants such as Young's modulus, ductility, tensile strength, fracture strength, yield strength, or fatigue strength. These parameters not only define the processability of a material, but also are key to the rate of success and biocompatibility of an implant in the field of hard tissue replacement. A goal may be matching of Young's modulus of implants and bone, the latter for compact bone ranges 10–30 GPa. If the Young's modulus for example of a hard tissue implant material is much higher than that of cortical bone, the load bearing is not ideal and the risk of stress shielding occurs [5]. In particular this may lead to a mechanical insulation of the synthetic material from the tissue, so that the typically observed balance of tension induced remodeling of bone is hampered, and as a direct result the loosening of the prosthetic device may occur [22]. Besides the mechanical aspects of the

chosen material system, the structural compatibility of a device in terms of implant geometry must be considered as well [5,23]. In order to engineer an implant device not only in terms of biocompatibility but also in terms of safeness to mechanical or structural failure, it is important to consider degradation of materials such as fatigue, wear debris or yield strength under compression. These are important parameters, as for example in a hip implant or any joint replacement it is expected that the chosen material systems withstand numerous cyclic loadings during service without failure or fracture for long time [24].

Due to the fact that in some applications materials are exposed over long time periods to cyclic loading, the resistance to fatigue is an important request for load bearing orthopedic materials as well as for example vascular implants such as heart valves [1,24]. Besides the high number of cyclic loadings, fatigue failure can also appear if the tensile stress during service is of a sufficiently high value or if the fluctuations or variations of the loaded stress are adequately high [25,26].

In load bearing titanium based biomedical alloys fatigue is often considered as the major reason of failure. Thus, a cyclic loading, as apparent in joint replacements, may result in alternating plastic deformation of stress induced superelevations produced by grooves or microstructural inhomogeneities. Such zones of stress induced superelevations are the regions where the crack initiates, propagates, and finally fractures due to prolonged cyclic loading [24,27,28]. Not only for metallic biomedical materials, but also for polymers fatigue failure plays a fundamental role in designing fail-proof implant applications. In case of total hip replacements for the loaded bearing surfaces, medical grade ultra high molecular weight polyethylene (UHMWPE) is used. The cyclic loadings during service over long times may trigger a softening of the polymer and thus lead to a shift in Young's modulus and yield strength to much lower values [5,29].

The use of alumina as counterpart of the UHMWPE bearing surface in joint replacement devices is based on the high Young's modulus and the very high yield strength of this material under compression. A key advantage at this material combination is that the friction coefficient of this interplay of a ceramic femoral head and a UHMWPE acetabular cup in hip implant prostheses is sufficiently low. For many implant combinations materials fatigue and wear are crucial failure mechanisms. Fatigue failure or more specified wear may be elevated in saline or aqueous environment as apparent in the living organism [30]. Wear is known as a removal process and thus a damage of a surface originated by the motion of two surfaces in close contact. Thereby the rate of lost material depends on the hardness and applied load as well as the surface roughnesses [31,32]. Table 8 shows a comparison of wear of commonly used material pairings for bearings in artificial femoral heads and acetabular cups [33,34]. It is obvious that dissimilar material pairings bear a high risk of wear. It was found that a ceramic–ceramic pairing did show a minimum wear loss [35]. Also metal–metal pairings were reported to show much lower rates of lost material compared to dissimilar ones with UHMWPE [30]. However, in a recent statistical assesment of metal-on-metal bearing total hip replacements it has been shown that even by implanting large diameter bearing surfaces, high rates of failure were observed [36].

High material abrasion may result in an inflammatory response of the host tissue (Table 8). As joint replacements are located directly in the bone tissue any leaking substances from the surfaces may enter the periprosthetic tissue and be attacked by macrophages. As a result, a complex reaction of the immune system is started in which amongst others, macrophages release pro-inflammatory cytokines that may stimulate osteoclastic bone resorption and thus leading to osteolysis and in worst case a loosening of the implant [37]. As a direct consequence in recent joint replacements similar material pairings as metal-on-metal [38,39] and ceramic-on-ceramic [40] are developed to reduce the risk of wear debris.

**Table 8**
Comparison of lost material by wear per year for different material pairings in hip implants [33,34].

| Material pairing | Rate of abrasive wear [μm/year] |
|---|---|
| Co–Cr–Mo/UHMWPE | 200 |
| $Al_2O_3$/UHMWPE | 20–130 |
| $Al_2O_3/Al_2O_3$ | 1–10 |

### 2.2. Latest developments

As this work concentrates on modifications and functionalizations of surface of implant materials used in hard tissue replacements, in this paragraph only the mechanical aspects of materials really used in bone replacement will be addressed. This means the mechanical properties of bioinert metallic material systems and the class of bioinert ceramics will be accentuated, other classes such as calcium-phosphates, bioglasses and glass–ceramics rather belong to the field of bioactive and bioresorbable materials. Moreover, the mechanical behavior of polymers will be treated only briefly as polymers are mainly used for soft tissue implantation.

#### 2.2.1. Metals

Mechanical properties of metals depend, except for the chemical and physical nature of the material, on the microstructural features such as for example on grain size. For alloys, two different types of materials exist, in which the mechanical properties are influenced by different strengthening mechanisms: homogeneous alloys (single phase solid solutions of different metals or metals and nonmetals) and heterogeneous alloys (multiphase alloys). In homogeneous alloys the strengthening is due to solid solution hardening, whereas in heterogeneous alloys the mechanical properties are determined by the size and distribution of the different phases in the alloys. Further mechanisms leading to metal strengthening are work-hardening or strengthening by reducing the grain size of the material. Therefore, the manufacturing process of a technical device such as casting, forging, annealing, cold working or solidification influences the mechanical behavior [41]. A summary of some representative mechanical properties of stainless steels, CoCr-alloys or titanium and its alloys in relation to the processing conditions are listed in Table 9 [1,5,25,42].

Many different types of stainless steels are available which differ in their chemical composition and microstructure: typically stainless steels are classified according to the crystal structure into martensitic, ferritic, austenitic and duplex (austenitic–ferritic) stainless steels. The different types of alloys differ in their corrosion resistance and in the mechanical properties. In biomedical applications several stainless steels are used, however, AISI 316L, a single phase austenitic stainless steel, is one of the most popular materials for implant applications [22,41]. Usually this alloy is ordinarily used in a 30% cold-worked state because cold-worked metal has a markedly increased yield, ultimate tensile and fatigue strength relative to the annealed state [1]. The alloy contains about 17–19% Cr, 12–14% Ni and 2–3% of Mo – the latter increasing the localized corrosion resistance in chloride-containing environments. The "L" in the designation refers to "low carbon", which decreases the risk of intergranular corrosion due to formation of Cr-rich $M_{23}C_6$ carbides in the microstructure. The elastic modulus of stainless steel is

**Table 9**
Characteristic mechanical properties of various metallic biomedical materials [1,5,25,42].

| Material | Condition | Young's modulus (GPa) | Yield strength (MPa) | Tensile strength (MPa) |
|---|---|---|---|---|
| X2CrNiMo17122 | Annealed | 190 | 331 | 586 |
| (AISI 316L) | 30% Cold worked | 190 | 792 | 930 |
| | Cold forged | 190 | 1213 | 1351 |
| Co28Cr6Mo | Cast | 210 | 448–517 | 655–889 |
| | Hot forged | 210 | 896–1200 | 1399–1586 |
| Co20Cr15W10Ni | Hot forged | 210 | 484–648 | 951–1220 |
| | 44% Cold forged | 210 | 1606 | 1896 |
| Co35Ni35Cr20Mo10 | As wrought | 232 | 965–1000 | 1206 |
| cp-Ti | Grade 2 | 105–110 | 250 | 390–540 |
| Ti6Al4V | Cold worked | 100–110 | 830–1070 | 920–1140 |
| Ti6Al7Nb | – | 110 | 810–1010 | 870–101 |
| Ti5Al2.5Fe | – | 110–115 | 780 | 860 |
| Ti12Mo6Zr2Fe | – | 74–85 | 1000–1060 | 1060–1100 |
| Ti13Nb13Zr | – | 64–83 | 435–905 | 705–1035 |
| Ti29Nb13Ta4.6Zr | – | 65 | 400 | 1000–1050 |
| Ti30Nb | – | 63–80 | 500 | 700 |
| Ti30Ta | – | 60–70 | 590 | 740 |

about 200 GPa, which is >10 times higher than the cortical bone. Therefore, using stainless steel for load-bearing bone implants, stress shielding effects must be considered.

CoCr-alloys have a long history in biomedical implant engineering with the main attribute to enhance corrosion resistance in chloride environments, which is related to surface oxide formation which is strongly enriched with $Cr_2O_3$. Alloying of other elements such as nickel, molybdenum, or tungsten improve for example mechanical properties and the abrasion resistance [43]. Major differences in the mechanical properties exist between cast and wrought (forged) alloys, as well as between low- and high-carbon containing alloys. For the fabrication of implants casting of Co–Cr based alloys is not a preferred technique, as solidification during casting may result in large dendritic grains [44] and thus decrease the yield strength of the alloy. Moreover, casting defects such as inclusions and micropores cannot be avoided and may act as stress risers and thereby result in the overall decrease of fatigue strength of the material [44–46]. To avoid these problems with casting, powder metallurgical methods have been used to improve the alloys' microstructure and mechanical properties. For example, in hot isostatic pressing, a fine powder of the alloy is compacted and sintered together under appropriate pressure and temperature and then forged to final shape [47]. The typical microstructure shows much smaller grain sizes of about 8 μm than the as cast alloy [1]. The CoCrMo cast alloy (ASTM F75) has been used since the 1950s for orthopaedic implants. To improve the mechanical properties of the castings, two approaches are used: Hot-isostatic-pressing (HIP) to densify possible closed porosities in the castings, and homogenization heat treatments. However, such post-treatments are only of a limited effect in improving the mechanical properties, as especially the scatter from one casting charge to another also can be substantial. The cast alloys have a high C-content (≈0.2%), therefore the alloys contain primary carbides in the matrix. These carbide precipitates increase the wear resistance of CoCrMo cast alloys. The forged CoCrMo alloys show improved mechanical properties in comparison to the cast alloy (see Table 9). The alloys exist in "low carbon" (C < 0.08%) and "high carbon" (C ≈ 0.2%) variations. As in the case of cast alloys, the high carbon content leads to the formation of carbide precipates, which are advantageous for the wear resistance. Therefore, the forged alloy is a preferential material choice for biomedical application encountering strong tribological loads.

Design and thermo mechanical processing control of titanium alloys have allowed to offer implant materials with enhanced mechanical properties as generally shown in Table 9 by the Young's modulus, yield strength or tensile strength for these orthopedic alloys. Up to today the commercially most used titanium based implant materials are pure titanium and Ti6Al4V [41]. However, there has been a concern about the high elastic modulus of these alloys as compared to bone (10–30 GPa) [5]. Commercially pure titanium is still selected for applications where corrosion resistance is of prime importance other than its mechanical properties, for example in dental applications. The mechanical behavior and chemical stability as well as the microstructure of the α-ß alloy Ti6Al4V can be altered via heat treatment or mechanical processing [24,48–50]. A recent trend in research and development of titanium alloys specifically for biomedical applications addresses concerns of toxic effects of the dissolution of aluminum and vanadium ions into the host tissue as a result of corrosion wear of Ti6Al4V [24,51]. Recently, new titanium alloy compositions, specifically intended for biomedical applications, have been developed. These orthopedic alloys include Ti6Al7Nb [52] and Ti5Al2.5Fe [53], two alloys with properties similar to Ti6Al4V that were developed in response to concerns related with Vanadium to show a potential cytotoxicity [54,55] and adverse reactions with the host tissue [56]. Therefore, a common goal in this field is to develop single phase ß-titanium alloys composed of non-toxic and non-allergic elements with excellent mechanical properties and good workability. Another advantage is that these ß-phase titanium alloys show an inherently lower elastic modulus than the α-phase materials [24,28]. Biocompatibility enhancement and lower modulus have been achieved through the introduction of the latest generation titanium orthopedic alloys including Ti12Mo6Zr2Fe TMZF [57,58], Ti15Mo5Zr3Al [59] and Ti15Sn4Nb2Ta0.2Pd alloys [60], as well as the completely biocompatible Ti13Nb13Zr alloy [61,62]. Meanwhile, several implant designers have developed $\beta$-titanium alloys with lower Young's modulus around 70 GPa. The latest developments showing minimum elastic moduli have been achieved by TNZT alloys based on the TiNbTaZr system, specifically by the development of the biocompatible Ti29Nb13Ta4.6Zr alloy [25]. A more detailed overview on the current state of the art on the mechanical behavior of titanium based alloys and how thermo mechanical processing can be used to influence the microstructure and on alloying can be found in other recent reviews [24,63].

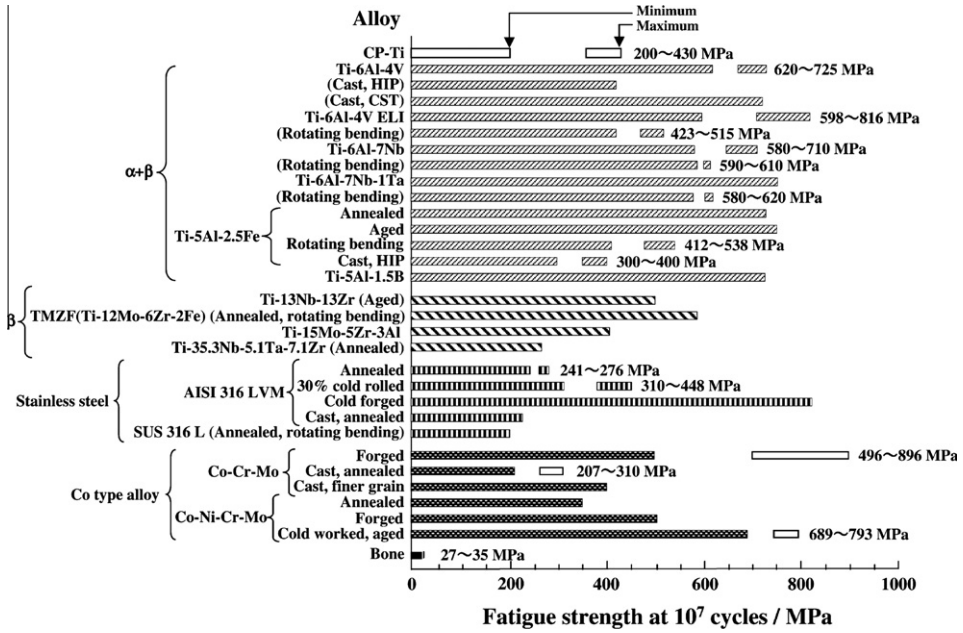


**Fig. 2.** Fatigue strength at $10^7$ cycles of various metallic biomedical materials [28].

In must be emphasized however that values as tabulated in Table 9 are all obtained from standard samples with simple and regular geometries and may not fully represent the actual stress or loading conditions occurring on a complex shaped implant under close to reality conditions.

With regard to the fracture of metallic implant materials, fatigue fracture is considered to be the most crucial problem among the various types of fractures. Fatigue characteristics are closely related with the microstructure of the metallic phases and therefore also with the processing and heat treatment employed. In other words, fatigue characteristics of metallic structural biomaterials must be considered always for specific microstructures or processing parameters [64].

Niinomi et al. compared the fatigue limits of stainless steels, CoCr-alloy, and titanium and its alloys as representative metallic biomaterials in air as shown in Fig. 2 [28]. The shown fatigue limits are compiled according to factors such as the fabricating process, surface condition, microstructure, and fatigue condition. The fatigue limit of bovine bone determined by Kim et al. is also given in Fig. 2 [65]. The fatigue limits decrease with the material in the order that CoCr-alloys show the highest limits, whereas for example Ti6Al4V is lower and AISI 316L stainless steel shows even lower limits. However, the limit of each metallic biomaterial shows a fairly large scatter due to the above mentioned broad range of factors. The fatigue limits of each metallic biomaterial tested are much higher than that of bovine bone.

### 2.2.2. Ceramics

$Al_2O_3$ and $ZrO_2$ are the most prominent bioinert oxide ceramics used in biomedical applications as they possess an attractive combination of a high corrosion resistance, low friction, high wear resistance and a high strength. In particular, alumina ceramic devices have been used in biomedical applications for more than 30 years in load-bearing hip prostheses and dental implants [33,66,67]. Mechanical properties of some biomedical ceramics are summarized in Table 10 [17,33,68–70].

Alumina devices are made from very fine grained polycrystalline $\alpha$-$Al_2O_3$ fabricated by hot isostatic pressing and subsequent sintering at $T = 1600–1800\ ^\circ C$. To limit grain growth during sintering, small

**Table 10**
Mechanical properties of oxide ceramic materials used in biomedical applications [17,33,68–70]

| Property | $\alpha$-$Al_2O_3$ | $ZrO_2$ (Y-TZP) | $ZrO_2$ (Mg-PSZ) | $ZrO_2$ toughened $Al_2O_3$ (ZTA) | $Al_2O_3$ matrix composite (AMC) | Dense Hydroxy-apatite (HA) |
|---|---|---|---|---|---|---|
| Bending strength (MPa) | 595 | 1000 | 800 | 912 | 1150 | 20–80 |
| Compressive strength (MPa) | 4250 | 2000 | 1850 | – | 4700 | 100–900 |
| Young's modulus (GPa) | 400 | 150 | 208 | 285 | 350 | 70–120 |
| Hardness (HV) | 2400 | 1200 | 1120 | 1500 | 1975 | 500–800 |

amounts of MgO are added. This aids to increase strength, fatigue resistance and fracture toughness of such polycrystalline $\alpha$-$Al_2O_3$ devices as these pararmeters are a function of grain size [17]. An average grain size of less than 4 μm at a sufficiently high purity results in a proper flexural strength and excellent compressive strength as recommended in bearing balls of hip replacements. An increase of grain size to levels higher than 7 μm is reported to decrease the mechanical properties by about 20% [1]. The outstanding high friction and wear properties of alumina occur only when the grains are at average sizes smaller than 4 μm at very narrow size distribution [17]. The addition of sintering aids must be held at low levels to avoid precipitations at the grain boundaries that lead to a degradation of the fatigue resistance. Ample testing has shown that alumina implants that fulfill the described requirements show excellent resistance to dynamic and impact fatigue and also resist subcritical crack growth [71]. Stress shielding owing to the high Young's modulus of alumina (Table 10), may be responsible for the loosening of the acetabular cup in analogy to biomedical implant materials based on metals [66].

Lifetime predictions and statistical design of proof tests for load-bearing ceramics have shown that specific prosthesis loads limits of 30 years at 12 kN loads can be set for an alumina device based upon the flexural strength of the material and its environment [66,72]. Other clinical applications of alumina include knee prostheses, bone screws, alveolar ridge, maxillofacial reconstructions and post dental implants [67].

Zirconia is also exceptionally inert in physiological environments [73,74]. The potential advantages of zirconia in comparison to alumina in load bearing prostheses are that zirconia shows higher values in fracture toughness and flexural strength but at the same time a lower Young's modulus [17,75,76]. Zirconia ceramics chosen for biomedical applications can be divided into two types. Partially stabilized zirconia (PSZ) and tetragonal zirconia stabilized with yttria (TZP). Mechanical properties of these bioceramics are listed in Table 10.

Pure zirconia shows a monoclinic phase at room temperature up to 1170 °C. At higher temperatures it transforms into the tetragonal and then into cubic phase at 2370 °C. As sintering temperatures require these high temperatures, the phase transformations during cooling induce mechanical stress (as phase transformations are associated with a volume expansion of approximately 3–5%). Thus, stress generated by the expansion leads to initiation of cracks in pure zirconia ceramics after sintering and thus makes these materials unsuitable for load bearing applications. A way out is to stabilize the high temperature phases during cooling to avoid any stress in the volume [77]. The addition of oxides like MgO, CaO and $Y_2O_3$ allows the generation of multiphase ceramics known as partially stabilized zirconia (PSZ) with a microstructure that consists in majority of cubic zirconia with monoclinic and tetragonal zirconia precipitates as minor phases. A specific feature of such ceramics is that when stress is applied to such a ceramics and crack propagation occurs, the metastable tetragonal zirconia grains located at the crack tip can transform to the stable monoclinic phase and thus expand. As a result an enhancement in toughness can be obtained, by the counteracting compression stress at the crack tip (transformation toughening) [78]. The development of such tetragonal metastable precipitates may be obtained for example by the addition of 8%-mol of MgO to zirconia (Mg-PSZ). This partially stabilized zirconia can also be obtained with the addition of $Y_2O_3$, however, in this system it is also possible to stabilize a tetragonal phase at room temperature. Only zirconia with lower additions of $Y_2O_3$ is known as tetragonal zirconia polycrystal (TZP) [77]. Common additions range in between 2% and 3%-mol $Y_2O_3$ and result in an average grain size distribution of smaller than 1 μm [5]. The fraction of tetragonal

phase retained at room temperature is dependent on the size of grains, on yttria content and on the degree of constraint exerted on them by the matrix. The mechanical properties of such TZP ceramics depend on such parameters [33,79].

The increase of the relevant strength values realized in zirconia ceramics led to attempts to apply such a phase transformation toughening to alumina ceramics. One approach is to disperse zirconia particles in an alumina matrix to achieve a mechanical prestressing of the alumina via the phase transition induced volume change of the zirconia particles during cooling [69,80]. The bending strength of these ceramics show already significantly higher values than pure alumina, however, the probability of crack initiation and propagation is still not sufficient. An example of values for such a zirconia toughened alumina (ZTA) ceramic is also given in Table 10. The wear behavior of such ceramic mixtures was studied as a function of zirconia content in case for application as bearing balls in hip joints and was found to show higher wear rates with increasing zirconia contents. The insufficient resistance behavior was improved by the use of nanometer sized zirconia particles in combination with other additives that lead to the introduction of alumina matrix composites (AMCs) ceramics. The mechanical properties of such AMC ceramics open the possibility to fabricate much thinner walled components with comparable load bearing abilities and at the same time with a higher reliability (Table 10) [70,80–82].

Calcium-phosphate-based bioceramics have been used steadily in the last decades, as crystallographically hydroxyapatite is the dominant lattice structure of hard tissue. Therefore, there has been a tremendous interest in using synthetically derived hydroxyapatite for regenerating bone at the defect sites [67,83].

The stable phases of calcium phosphate ceramics depend considerably upon temperature and the presence of water, either during processing or in the used environment. At body temperature, only two calcium phosphates are stable in contact with aqueous media such as body fluids. At pH values lower than 4.2, the stable phase is $CaHPO_4 2H_2O$, while at values higher than 4.2 the stable phase is $Ca_{10}(PO_4)_6(OH)_2$, known as hydroxyapatite. At higher temperatures phases such as ß-tricalcium phosphate or TCP ($Ca_3(PO_4)_2$) and tetracalcium phosphate ($Ca_4P_2O_9$) are present [17]. The unhydrated high temperature calcium phosphate phases can interact with water or body fluids at 37 °C to form physiological hydroxyapatite [1].

The mechanical behavior of calcium phosphate ceramics strongly influences their application in implants. Bending strength, compressive strength and fatigue resistance depend on phase purity, grain size, sintering temperature [84] and especially the total volume of porosity either in form of micropores smaller than 1 μm due to an incomplete sintering or in form of macropores with diameters bigger than 100 μm created artificially to enable bone ingrowth [85]. An example for dense synthetically derived hydroxyapatite is given in Table 10.

### 2.2.3. Polymers

Polymers play a minor role in the field of load bearing hard tissue replacements compared to metals or ceramics. Therefore in this paragraph only a brief overview on the mechanical aspects of some polymers will be given. In case of the use of a polymer system load carrying device the key parameters are tensile strength, Young's modulus as well as the uptake of water. In contrast to the stiffness of inorganic metals or ceramics, polymers show according to their organic nature a high freedom of motion based on the fact that polymer chains are retained at a local level while a superior network structure resulting from chemical cross links and chain entanglements prevents large scale movement or flow. The description of stress–strain behavior for polymers is similar to that of metals, but a very important consideration for polymers is that the mechanical properties depend remarkably on the applied strain rate, temperature or environmental conditions. Depending on the chemical or crystalline nature of the polymer, the stress–strain behavior can be brittle, plastic or highly elastic. Young's moduli and tensile strengths are orders of magnitude smaller than those of metals, but elongations can be up to several 100% in some cases [1,86,87]. Mechanical properties of some biomedical polymers are summarized in Table 11.

Polyethylene is widely used in biomedical applications. But only in the configuration of ultrahigh-molecular-weight polyethylene (UHMWPE) with a molecular weight of 2–10 million g/mol it can be used as cup for high load bearing balls in joint replacements [5]. Therefore powders of polyethylene

**Table 11**
Mechanical properties of polymer materials used in load bearing hard tissue applications [86–89,91,92].

| Property | UHMWPE | PMMA | PEEK | PEEK 30% short fibers |
|---|---|---|---|---|
| Young's modulus (GPa) | 0.8–2.7 | 3.3 | 3.6 | 13–21 (flexural) |
| Tensile strength (MPa) | 41 | 80 | 92 | 210 |
| Elongation at break (%) | 450 | 5.5 | 50 | 1.3 |
| Water uptake at 20 °C (%) | 0.01 | 0.35 | 0.5 | 0.15 |

are pressed and sintered under high pressure and temperatures above the melting point to achieve pressure induced crystallization [87]. As a result the grade of crystallinity is highly increased and causes the mechanical properties of UHMWPE to a high stiffness and strength [5].

Another commonly used polymer material is Polymethylmetacrylate (PMMA) which shows a high hardness at high values of strength and stiffness. Moreover, the uptake of water is remarkably low. All common molding processes may be used to process PMMA, including injection molding, compression molding and extrusion. Rubber toughening has been used to increase the strength of PMMA owing to its brittle behavior in response to applied loads by copolymerizing elastomeric chains during manufacturing. As a consequence of the mechanical properties PMMA, is widely used in dental applications such in dental fillings and prothesises [88,89]. Additionally PMMA is used as bone cement for the stabilization of cavities in total hip replacements to guarantee load transmission between implant and bone as it shows a Young's modulus between cancellous bone and cortical bone [90].

Polyetheretherketone (PEEK) is now routinely used in longterm medical implant applications because of its versatility, mechanical strength and biocompatibility. PEEK possesses a high grade of crystallinity at a maximum of close to 50% that results in a highly ductile material with a good chemical stability. The mechanical properties of grade PEEK can be increased drastically by carbon fiber reinforcement (CF-PEEK) [91,92]. Examples of application for these toughened PEEK composites are acetabular cups used for articulation against a ceramic femoral head. Hip joint simulator testing showed that wear of the CF-PEEK polymer composite cups is much less than that of UHMWPE cups [93].

## 3. Surfaces of implant materials

### *3.1. Surface versus bulk*

In previous paragraphs the focus was on mechanical properties of materials used for biomedical devices and components. This is the primary aspect for hard tissue replacements, to establish the mechanical formation of an implant. However, to achieve a high grade of compatibility of a material system with the host tissue, key factors are surface determined such as biocompatibility and corrosion resistance. Indirectly these surface factors also effect mechanical behavior such as stress shielding, wear debris or fatigue failure. But most importantly, the surface of the synthetic device is in direct contact with the living organism. Therefore major attention must be paid to the surface of a material system as its reaction with the host tissue is often decisive on success or failure of implantation.

The various surface parameters that influence the response of the host tissue include wettability, roughness, chemical composition, electrical charge, crystallinity and mobility. Atoms at the surface in many cases are highly unstable but dictate most of the biological reactions at the tissue implant interface.

Depending on the implant material the surface may consist of individual atoms, molecules, crystallographic arrangements, or large polymeric structures. Surfaces consist of molecules or atoms with not fully saturated dangling or strained bonds. Surface atoms show less binding – this leads to an enhanced mobility and higher reactivity of the species. As a result these surface atoms can easily undergo phase transformations, crystallization or corrosion (dissolution) processes. This higher energy and higher reactivity are particularly important in view of adsorbates from the biological system. When such a surface comes in contact with a biological environment it reacts immediately to form new bonds and compounds, thus lowering the surface energy [1]. In contrast to the extended arrangement

of atoms in the bulk state of materials the number of atoms in the "surface" state is limited to some atomic layers. This requires special characterization tools.

### 3.2. Surface phenomena

Surface phenomena are primarily driven by an associated reduction in surface free energy with enhanced chemical reactivity. In the following specific points will be briefly addressed.

#### 3.2.1. Surface segregation and reconstruction

There are some possibilities for surfaces to spontaneously alter their structure and chemistry even in the absence of a specific environment. These are surface segregation and reconstruction. The most basic definition of surface segregation may be expressed as the redistribution of solute atoms between the surface and bulk of a material such that the total energy of the material is minimized. As a result surface reconstruction is often observed – even with single crystal surfaces in the vacuum. In the simplest case the outermost layer of atoms rearranges to minimize the overall surface energy. An example is shown in Fig. 3.

While reconstruction can lead to periodic nanoscopic surface structures – to the best of our knowledge any interaction with biomedically relevant species has not been reported. More biologically relevant are surface segregation effects.

Surface segregation can be seen as an interfacial adsorption phenomenon involving a bulk component of a multi-component material, for example resulting in an environment of a compound at the surface. Metallic materials mostly exist at a microscopic level of more than one phase. An example can be given for Ti6Al4V, a commonly used orthopedic implant material that consists of two different phases, the aluminum rich $\alpha$- and the vanadium rich ß-phase. Not only these different phases but also the grain boundaries may have a different chemical composition [94]. Other examples for surface segregations in inorganic biomedical materials are grain-boundary diffusion and motion or environmental effects such as intergranular corrosion and stress corrosion cracking [1].

In polymers, segregation resulting from folding of macromolecular chains at the surface can provide various microstructural domains. Depending on the chemical species present within these domains, proteins may have different interaction with each phase [95–97]. However, the importance of surface segregations to biomedical applications can be summarized in terms of localized toxicity, impaired corrosion resistance or, concerning the above described adsorption phenomena, a modified protein or cell adhesivity in the host tissue can be evoked.

As a result of surface segregation and other influencing factors, surface chemistries and structures can change in response to an external environment in order to reduce interfacial tension. However, sufficient atomic or molecular mobility must exist to enable changes in surfaces in a reasonable period of time [98]. At the microscopic level, a biomaterial surface may have patches or domains of different functionalities so that a newly formed surface chemistry may migrate from the surface into the bulk, or molecules from the bulk may diffuse or interact and thus rearrange among each other or with surrounding species [99,100]. Such reversals do occur in metallic and other inorganic systems, as well as in polymeric systems. Polymers can also undergo a reorientation of the polymer chains at the outermost layers when their surrounding atmosphere is switched from dry air to aqueous.

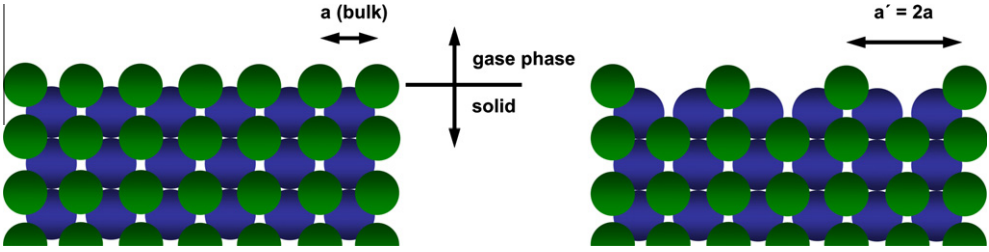


**Fig. 3.** Schematic illustration of surface reconstruction.

Thus surface segregation effects are often used to describe mobility-related alterations in surface structure and chemistry. In fact, a surface reversal must be prevented or inhibited if a modified surface should remain in the state as it was designed. To gain a stable modification of surface chemistry or structure that can be used as surface modification for biomedical devices cross-linking, sterically blocking of the ability of surface states to move, or incorporating a rigid, impermeable layer between the substrate material has to be introduced [1].

*3.2.2. Surface charge*

The origin of charge localized at a solid surface can be either due to charge equilibration with a surrounding or contact medium (such as space charge layers in semiconductor-junctions) or due to intrinsic defects at the surface.

The first case is based on charge relatively for two media in contact – in other words if a metal, semiconductor or insulator are in contact with a second phase (material), the Fermi-levels (the chemical potentials) of the two phases will equilibrate and this will lead typically to charged surfaces. In the case of contacts with liquids, for metals typically the characteristic charge lies in a double layer (Helmholtz-layer), for semiconductors and insulators a space charge layer forms that extends considerably into the solid material [101].

Another source of charges is the disrupted crystal structure of surfaces – i.e. at a surface the unsaturated bonds (dangling bonds) contribute to charge that needs to be accounted for.

Charge accumulated at solid surfaces needs to be balanced by species in the solution. Main carriers of charges in solutions are ions but also species solvatized such as colloids or proteins in the solution must be considered or can even become dominant. The general description of the contribution of a particular solution species to a surface potential has typically the form:

$$\Delta\mu_i = \frac{RT}{zF\ln\frac{C_i}{C_i^{PZC}}}$$

where $C_i^{PZC}$ represents the concentration at the point of zero charge (PZC), $C_i$ the normal concentration and $\Delta\mu_i$ the chemical potential.

For colloids (protein solutions) the PZC or the isoelectric point represents the situation when microscopically no net charge can be measured [102].

Excess charge on surfaces promotes adsorbtion of outer charge. As proteins are major carriers of charge in a biomedical environment, extensive work has been carried out to relate surface charge phenomena with surface protein interactions.

*3.2.3. Adsorption phenomena*

Adsorption phenomena at the fluid–solid interface are usually described in terms of physisorption or chemisorption processes [103–106]. Physisorption of molecules at interfaces is based on the surface energy, i.e. the presence of charge at interfaces. The origin may be localized charge in space charge layers, for example of semiconductors (including oxides such as $TiO_2$ or $Fe_2O_3$), or by induced weak van der Waals forces. The latter originates from dipole moments induced in a surface by an adsorbate (interaction with own image charge). This interaction energy may be weak (~100 meV) but it is a key contribution in interactions of solid surfaces with biological molecules.

Chemisorption in its original concept assumes the formation of a rigid covalent bond on the surface (in other words a chemical surface reaction to take place). A most typical example is surface hydroxide groups that react with a surrounding molecule (e.g. R-COOH, R-$NH_2$, R-SiOH) under $H_2O$ split off. This principle is widely used to attach organic material to oxide surfaces (see section 5 on organic monolayers). An interaction somewhere in between pure induced dipoles and formation of chemical bonds are ionic interactions which still may show some degree of surface mobility of an adsorbate and of the substrate. In other words, a strict separation of chemisorption and physisorption in such cases is often not possible.

In general, physisorption is reversible without any chemical change either of the adsorbate or of the surface while chemisorption represents an irreversible chemical adsorption. For physisorption the molar enthalpy of adsorption can be found in between −5 and −40 kJ/mol while chemisorption leads

to values of molar enthalpy of adsorption of about −200 to −800 kJ/mol [107]. Generally, higher energy surfaces are quickly coated or, from the view point of analytical surface science, contaminated by lower energy species.

A given molecule can generally physisorb and chemisorb on the same surface. More precisely, a molecule first physisorbs and then may be converted into a chemisorbed state. The most common equilibrium situation resembles the existence of a mixture of physisorbed and chemisorbed molecules on the surface depending on the availability of suitable surface sites [108,109].

Generally adsorption processes on surfaces are characterized by so-called isotherms [110]; that are mostly based on experimental observations and typically contain semi-empirical parameters. A most general approach is the Langmuir isotherm:

$$\Theta = \frac{KP}{1 + KP}$$

where $\Theta$ is the coverage (number of adsorption sites occupied/available adsorption sites), $P$ is the partial pressure (for gases or molecular concentration in liquid). As this approach is usually oversimplified, a number of more refined desorption and adsorption processes (BET or Kisliuk) have been proposed.

Particularly noteworthy in the context of biomolecules may be the work related to observations for self-assembled monolayers. It was noted that a key assumption in Langmuir isotherms – that is an already adsorbed species does not interact with the adsorption process of a nearby adsorbed species – cannot hold. It was shown that for low surface concentrations molecules tend to adsorb (in a lying down configuration probably dictated by van der Waals forces) while at higher concentrations specific ionic interactions of charged parts in the molecule force an overall switch over to a "standing" configuration. These effects are considered, e.g. in Kisliuk-type of isotherms [111,112].

In the light of surfaces of biomedical materials that are dedicated for the insertion into the living organism, adsorption of ions of the body fluids (e.g, Ca- and phosphate-ions) as well as adsorption of biomolecules (e.g, proteins) is important for the subsequent biological performance. The adsorption behavior of different species depends on the surface properties (chemistry, charge, energy) and can be tailored by specific surface modifications. Regarding protein adsorption it has to be considered that in water based environments a hydrophilic material shows a lower interfacial energy than a hydrophobic one. That means that the adsorption behavior of proteins on a hydrophobic surface will likely turn into denaturation. In fact the charged bonds and the hydrogen bonding groups will orient towards the water, whereas the hydrophobic groups will be more likely oriented towards the hydrophobic surface [1]. As a result of such thermodynamic adhesion phenomena it was demonstrated that adhesion for bovine serum albumin on surfaces with varying wettability in between super-hydrophobic and super-hydrophilic showed the highest values on intermediate hydrophilic conditions [113].

Specific to protein adsorption phenomena is that the protein may change its conformation upon adsorption to the surface [114]. In aqueous solutions hydrophobic portions may not be exposed to the surrounding electrolyte (energetically not favored). However, if the protein "finds" hydrophobic surfaces or surface locations it may be energetically favorable to maximize contact between both hydrophobic interfaces – thus surface induced conformation change or protein denaturation can occur.

Also typically protein surfaces are in nature often bi-polar so that either hydrophilic or hydrophobic surfaces may preferentially coordinate with the surface or a particular surface location. Due to these uncertainties, rather than measuring the adsorption isotherms (by measuring the equilibrium amount of proteins as a function of the solution concentration) often simply the kinetics is followed [115–117].

Various surface sensitive in situ methods can be used to follow the kinetics such as ellipsometry, reflectometry, infrared-spectroscopy, Raman-scattering, circular dichroism, and currently most frequently fluorescence emission or surface plasmon resonance.

Several reviews to such techniques are available for example [118,119].

An example is shown in Fig. 4 where the adsorption of proteins to surfaces was investigated with quartz crystal microbalance with dissipation (QCM-D). The data show the adsorption behavior of four proteins (fibrinogen, $\gamma$-immunoglobulin, albumin, and lysozyme) with different sizes and shapes onto

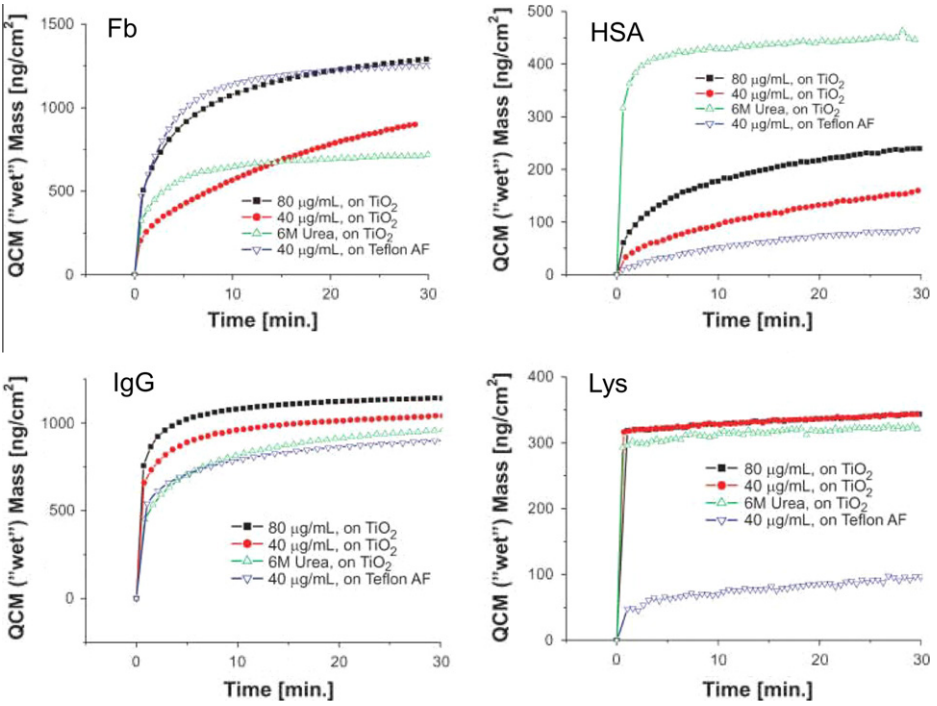


**Fig. 4.** Evolution of adsorbed mass of human fibrinogen (Fb), human serum albumin (HSA), human $\gamma$-immunoglobulin (IgG) and chicken egg white lysozyme (Lys) layers as obtained from the QCM-D. The adsorption of proteins was tested from HEPES (with and without 6 M urea) using 40 and 80 μg/mL concentrations on hydrophilic $TiO_2$ and on hydrophobic Teflon-AF (adapted from [120]).

hydrophilic $TiO_2$ and hydrophobic AF-Teflon surfaces using two different concentrations from two different buffers (HEPES with and without 6 M urea).

The results show that the density of the adsorbed protein layer is changing during the adsorption process and largely depends on the protein, the surface, and the solvent [120].

### *3.3. Aqueous corrosion of biomedical metals*

Red-ox reactions at metal surfaces (in a given environment) lead to the formation of metal cations, depending on the environment oxide layers can be formed (which may slow down further dissolution). In the worse case, the metal ions are permanently solvatized and thus the metal continuously dissolves (it corrodes).

Corrosion reactions of metals in aqueous solutions are therefore of an electrochemical nature. The actual metal dissolution reaction is the oxidation of metal (so-called anodic reaction). This reaction is coupled with a reduction of species in the environment, which are typically dissolved oxygen or protons in acidic solutions. Due to the electroneutrality requirement (i.e, all electrons produced in the anodic reaction must be consumed in the cathodic reaction), the oxidation and reduction reactions must take place simultaneously and with an equal rate. To complete the circuit, the anodic and the cathodic sites must be electrically and electrolytically connected. In case of a metal that is exposed to an aqueous solution or air, the thermodynamic stability is generally only provided for noble metals, as their oxidation potential is more anodic than the reduction potential of species commonly present in the surrounding phase. In contrast, for non-noble metals the situation is reversed, where the difference in reduction and oxidizing potentials of the two phases leads to a driving force for metal oxidation. The environmental conditions then can either favor dissolution (solvation) of the oxidized metal

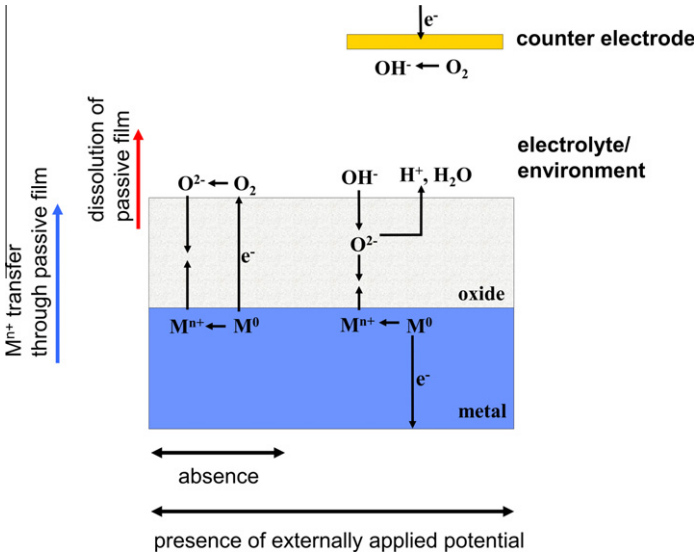


**Fig. 5.** Growth of an oxide film on a metal surface.

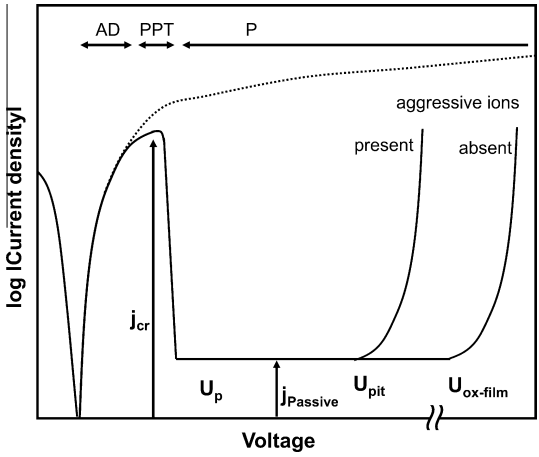


**Fig. 6.** Schematic anodic polarization curves for the typical behavior of a metal exhibiting passivation (solid line) and a nonpassive metal (dashed line).

cation (active corrosion) or the establishment of a second insoluble oxide phase film (passivation) [121].

*3.3.1. Passivity and breakdown of passivity*

Typically used metallic materials in biomedical applications, such as above described, surgical stainless steels, cobalt–chromium-based alloys, titanium and titanium based alloys, show the ability to spontaneously form a stable self-protecting oxide layer (a so-called passive film) on its surface in the reaction with air or most aqueous environments. For example, passive layers form easily on titanium-based alloys and are mostly composed of $TiO_2$ [122]; passive films formed on surgical stainless-steel and cobalt-based alloys are typically $Cr_2O_3$ rich layers [123–125] (during oxide formation often

**Table 12**
Inorganic composition of human blood plasma [141,142].

| Ion | Concentration ($mmol^{-1}$) |
|---|---|
| $Na^+$ | 142.0 |
| $K^+$ | 5.0 |
| $Mg^{2+}$ | 1.5 |
| $Ca^{2+}$ | 2.5 |
| $Cl^-$ | 103.0 |
| $HCO_3^-$ | 27.0 |
| $HPO_4^{2-}$ | 1.0 |
| $SO_4^2$ | 0.5 |

one oxide compound is easier dissolved, the other oxide compound remains enriched on the surface). Passive films typically show only thicknesses of few nanometers, thus, they act as a highly protective surface barrier between the bulk metal and the aggressive biological environment [126]. The protective quality of a passive film is kinetically determined by the ion transfer through the film as well as by the stability of the passive film against dissolution [121,125] (Fig. 5). A variety of factors such as chemical composition, structure, thickness and presence of defects influence the ionic transport through the film as well as the stability of the film in different environments.

Since passivation reactions involve electrochemical steps, it is often convenient to study the active/passive transition by electrochemical methods such as potentiodynamic polarization curves. A schematic example for such polarization curves of a metal showing passivation (solid line) and a nonpassive metal (dashed line) are drawn in Fig. 6. Passivation is manifested in a polarization curve by a drastic drop in current at a particular onset potential defined as passivation potential ($U_p$). With the establishment of a passivation layer the anodic current density (the corrosion reaction rate) is lowered by several orders of magnitude. An indicator for the passivation ability is the critical current density ($j_{cr}$, the maximum current density) reached in the active/passive transition.

The reaction scheme for passivation can be divided into active range, that corresponds to a active dissolution (AD), a transition range and prepassive range (PPT), and a region where the passive layer formation can be observed (P) [127–129]. In the transition and prepassive range the metal becomes increasingly covered by M $(OH)_x$ adsorbates. These adsorbates increasingly block the active dissolution, as apparent in polarization curves in a deviation from the active dissolution behavior. The passivation potential is reached when the surface is completely covered with adsorbates and deprotonization leads to the formation of a primary passivation film that mainly consists of $MO_x$ species. The current flow in the passive range ($j_{Passive}$) is a value for the protectiveness or the quality of the oxide film. In contrast to the described passivation, the polarization behavior of a nonpassive metal shows an active dissolution over the entire anodic potential range. At higher potentials, where the current becomes independent of the potential, dissolution of the metal occurs through a salt layer [121].

Principally, the nature and stability of a passive film on a particular biomedical metal or alloy depend on the environmental conditions, such as the composition of the electrolyte, the redox conditions, the exposure time and temperature [130].

The passive state of a metal can, under certain circumstances, be prone to localized instabilities. Most investigated is the case of localized dissolution events on oxide-passivated surfaces [131–133]. Localized corrosion is triggered by specific aggressive anions – halogenides – and typically starts at sites characterized by inhomogeneities either in the material, or in the surrounding environment. The result is the formation of an active pit in the metal, an example for localized breakdown of passivity. Even though most of the surface is still covered by the intact passive film, the corrosion rate at locally activated sites can reach very high values. Localized corrosion may thus lead to unexpected deterioration of the whole system with disastrous consequences, although the total mass loss is actually small. Therefore, localized corrosion processes are more dangerous in biomedical applications and far less easy to predict than uniform corrosion [121,126]. Fig. 6 gives an alternative example of a polarization curve of a passive metal showing localized breakdown (for example pitting corrosion) of passivity and thus pit growth at $U_{pit}$. The solid line at higher potentials herein represents the polarization

curve of the same material in the absence of aggressive anions, where the current increases at much higher anodic potentials caused by either transpassive oxide film dissolution (breakdown of passive film) or the onset of oxygen evolution at the anodically polarized electrode. For more detailed discussion on fundamentals of passivity, breakdown of passivity and electrochemical fundamentals, the readers are referred to Refs. [121,131,132,134–140].

*3.3.2. Body fluids – corrosive environment for biomedical materials*

In connection with the above described passivity and its breakdown, for biomedical alloys the availability of corrosive media in the living body as well as adequate salt solution for simulated laboratory investigations have to be considered. The inorganic composition of typical human blood plasma is given in Table 12 [141,142]. In order to simulate the biological environment, different types of simulated body fluids have been formulated. Generally, the simulated solutions consist of NaCl (0.14 M), pH buffered to 7.4 and the presence of smaller amounts of other salts representing the inorganic concentrations in typical human blood [141,143]. The presence of chlorine ions and their ability to induce localized corrosion of many important technical alloys makes the human blood plasma a highly aggressive environment for many biomedical metals and alloys.

The inorganic species present in the blood plasma and simulated solutions can also play a critical role in the corrosion process. Besides the accelerating effect of chlorine on the dissolution and failure, calcium and phosphate ions have been shown to slow down the repassivation rate of the protecting oxide layers [144]. This can be of major importance as the repassivation kinetics is determining the metal ion release rates in all cases of cyclic activation/repassivation events on the surface, such as in fretting corrosion (see Section 3.3.3.3). Moreover, it should be considered that the body temperature of 37 °C can accelerate electrochemical reactions and even change the mechanism of corrosion from that occurring at the room temperature, an example is the strong temperature-dependence of the occurrence of metastable pitting on Ti base alloys (see section 3.3.3.1) [145]. A direct extrapolation of reaction kinetics to higher temperatures therefore can be erroneous and the influence of temperature has to be considered if simulations of body environment are conducted.

Another influencing factor, especially for titanium and titanium based alloys, can be found in the formation of $H_2O_2$ in inflammatory reactions in direct contact of an implant with the tissue [146]. It has been shown that the presence of $H_2O_2$ in simulated body solutions changes the thickness and structure of the oxide films and enhances dissolution [147]. In addition to inorganic species, body fluids contain different types of biological relevant species [148–151] and cells [152,153], which may attach to the biomedical alloy surface and affect the surface reactions. For more detailed discussion on simulated body environments in terms of inorganic composition and the addition of proteins and its influence on corrosion behavior of biomedical alloys, the readers are referred to Refs. [126,143].

*3.3.3. Overview of specific cases of corrosion on biomedical alloys*

The most typical modes of corrosion in biomedical alloys will be briefly addressed. The paragraphs below are only intended as introduction and short summary. For readers interested in a particular topic some references for further reading are given. For general literature on localized corrosion the readers are referred to Refs. [121,126,131,132,134–140].

*3.3.3.1. Pitting corrosion.* Pitting occurs with many metals in halide containing solutions and is a type of localized corrosion caused by local dissolution of the passive film and the formation of cavities [135]. In general, halides such as chlorides trigger pitting corrosion and can lead to an autocatalytic localized dissolution. Iron based surgical stainless steels show a higher susceptibility to pitting corrosion as compared with cobalt–chromium- or titanium-based alloys. In biomedical applications failure caused by pitting corrosion is often observed at screw holes after removal of implants based on stainless steel. Alloying components play a major role in increasing the pitting corrosion resistance of stainless steels, especially an increase of the chromium and molybdenum content leads to a higher pitting resistance. Moreover, the impurity concentration, especially the presence of inclusions such as MnS is of major importance for the pitting behavior, as pits typically initiate at MnS inclusions. Therefore, the pitting susceptiblility of different grades of stainless steels strongly varies. The higher the pitting resistance of a material, the higher oxidizing conditions are required to trigger pitting corrosion.

The prevailing redox conditions in the human body are in the range which may lead to pitting corrosion of surgical-grade stainless steels. In contrast, titanium and titanium-based alloys show much higher pitting potentials in simulated biological solutions (in the range of several volts) which are far above the natural redox conditions [145]. The Co–Cr–Mo alloys typically do not fail by pitting corrosion; instead transpassive dissolution by oxidation of the $Cr_2O_3$ passive film into soluble $CrO_4^{2-}$-species takes place at potentials below the oxygen evolution range [154].

As a conclusion, stable pitting corrosion is not a relevant corrosion induced failure mode for Ti based materials in biomedical applications, since the relevant potential region in the body is clearly lower than the pitting potential.

From an electrochemical viewpoint, stable pit growth is maintained as long as the local environment within the pit keeps the pit under active conditions. As mentioned above, stable pitting corrosion (initiation and propagation of pits) takes place above a specific potential (pitting potential), which is a function of the material and the environment. However, already at potentials far below the pitting potential (i.e, under less oxidizing conditions), so called metastable pitting can take place. Under these conditions, pits are initiated but the growth only for a very limited time before repassivation takes place. Metastable pitting has been intensively studied on stainless steels. It is interesting to note that also in the case of titanium, metastable pitting has been reported to take place in physiological media – at potentials far below the pitting potential [145,155–157]. Metastable pitting activity of titanium-based alloys remains high over long exposure time and therefore may have some relevance to the mode of metal ion release from such implants [126]. For more insight literature on pitting corrosion the readers are referred to Refs. [133,158–160].

*3.3.3.2. Crevice corrosion.* Crevice corrosion is a type of localized corrosion that is closely related to pitting corrosion. The appearance of this corrosive attack is preferentially found in regions on metal surfaces where mass transfer is limited such as in narrow crevices or under deposits. This leads to a local enrichment of aggressive species and depletion of oxygen, as well as subsequently to acidification of the crevice solution due to hydrolysis of the dissolving metal cations. These factors can rapidly lead to an activation of the surface in the crevice area. Metals that show an affinity to pitting corrosion also suffer from crevice corrosion; however, the presence of crevices may trigger localized corrosion already under conditions where stable pitting would not take place. As an example of the relevance of crevice corrosion in biomedical applications, the area between the head of a bone screw and counter sink on the fracture fixation plate can suffer from this type of attack. Stainless steel is the most susceptible to crevice induced localized corrosion among the three alloy groups discussed. For cobalt–chromium–molybdenum alloys the very high content of chromium in the passive film leads to a high resistance against activation upon local acidification. Titanium, typically, is claimed to show crevice corrosion only above critical temperatures higher than 80 °C in neutral chloride solutions [161,162]. However, in biomedical applications occurrence of localized corrosion in crevices with strong acidification and oxygen depletion cannot be completely ignored. To avoid crevice-related increased dissolution events on titanium based biomedical alloys the use of bone cements for the fixation of implants composed of such materials should be prevented [163].

*3.3.3.3. Fretting corrosion.* When two closely packed surfaces are subjected to slight oscillations, fretting corrosion may occur at the interface. For passive materials, the mechanical wear can lead to constant removal of the passive film, typically followed by a repassivation process. In detail, the damage is mostly of a localized form and can be a defect at the surface that does not show repassivation, resulting in the formation of a pit, or a continuous cyclic process of activation and repassivation [164]. This type of degradation mechanism is considered to be responsible for corrosion observed between fracture fixation plates and bone screws attaching the plate to bone [165–167]. Moreover, fretting and crevice corrosion have been identified as one of the most important factors in implant corrosion as the risk of metal ion release should be taken into account as a direct consequence of these continuous activation/repassivation events [168,169].

For a more insight information on fretting corrosion of biomedical alloys such as cobalt–chromium-, titanium-based alloys or surgical stainless steel the readers are referred to Refs. [144,170–174].

*3.3.3.4. Galvanic corrosion.* Galvanic corrosion is observed when two dissimilar metals are placed in direct electrical contact within the same environment. If such conditions are given, an enhanced corrosion of the less noble metal of the bimetallic couple may occur. In contrast, corrosion of the more noble metal is reduced or completely suppressed by cathodic protection. The driving force for galvanic corrosion is the difference in corrosion potentials of the components of the couple. Due to the eletroneutrality requirement in corrosion reactions (i.e, the total anodic current must be equal to the total cathodic current), a major factor in determining the danger of galvanic corrosion is the area ratio of the anode and the cathode (a small anode surrounded by a large cathode being most detrimental). Since passive films act as very efficient barriers to corrosion, the danger of galvanic corrosion is lower for materials that show passivation than for the coupling with an actively corroding metal [175]. In analogy with the mechanism for modularity effects, a relative movement of the couple may disturb the interface and cause a modification of the electrolyte composition [167,176].

Some modular orthopedic systems are made of titanium alloys and cobalt-based alloys on the basis that both should remain passive, however, these couplings are a frequent origin of clinical significant corrosion-related problems [177,178].

In contrast, stainless steel coupled with another nobler biomedical alloy could be galvanically destroyed if it suffers pitting corrosion. If both alloys remain within their passive region when coupled in this way and when pitting or crevice corrosion are not initiated, the additional corrosion may be minimal and thus tolerable [179,180].

## 4. Surface modification methods

The field of implantology steadily evolves as more is learned about the specific biological interrelations of the implant and the surrounding. Important factors from the viewpoint of surface engineering include the impact of the surface chemistry, the topography at the micro and nanometer level, physicochemical effects, and biological factors such as biochemically mediated cell differentiation, the unavoidable bacterial colonization of the implant, the biologic dimensions and the histology of surrounding structures. Proper surface modification techniques not only retain the desired bulk attributes of biomedical materials, but also improve specific surface properties required by different clinical applications [181,182].

The focus in the following paragraph is focussed on surfaces of implant materials dedicated for hard tissue replacements. Surface modification techniques will be discussed from the topographic and chemical viewpoint. Bioactive surface modifications and physicochemical parameters such as crystallinity and wettability will be reviewed starting with surface corrugation at the micrometer level and followed by current trends to optimize the topography at the nanometer level.

### *4.1. Surface corrugation at the micrometer level*

The influence of surface roughness on the rate of osseointegration and biomechanical fixation of hard tissue implants has been identified as a key factor. Mainly surface topographies at the micron level were reported as important and several surface modification techniques operating at this length scale were developed. In particular, the observation of more rapid and increased bone contact formation by micron-scale roughened surfaces manufactured through blasting and subsequent acid etching stimulated considerable activities. This observation also leads to the conclusion that hard tissue implants based on alloys, mainly titanium, were not only entirely bioinert or biocompatible, but proper surface conditioning could also influence protein adsorption, cellular activity or tissue response and this in turn could be exploited to achieve a higher level of osseointegration. In various works it has been shown that, morphological features at the micro level control the rate and quality of new tissue formation at the interface [183–187]. Kieswetter et al. reported on the influence of surface roughness on titanium to affect the production of local factors involved in bone formation by osteoblasts, suggesting that the complement of autocrine and paracrine factors produced by cells at the bone–implant interface can be directed by altering the implant surface roughness and to directly effect the type of interface that is formed at the implant site [188].

Numberless other investigations resulted in the finding that an optimal roughness for hard tissue implants is in the range of 1–10 μm. It was concluded that this range of roughness shows the ability to maximize the interlocking between mineralized bone and the surface of the implant [189,190]. Besides the experimental driven results from in vitro and in vivo investigations, theoretical calculations suggested that the ideal surface structure should consist of hemispherical pits of approximately 1.5 μm in depth and 4 μm in diameter [191] that could be supported by numerous in vivo studies on implant topography effects [192,193].

Optimal, mechanical interlocking of implants to the host tissue is required to achieve well accepted and integrated implantations. Not only the geometric requirements and stress distribution factors of the host tissue guide the topographical demands on the implant surface but also the consideration that bone adapts to mechanical loading by osteocytes which act as mechanosensors [194–196].

To meet the demands for an enhanced bone implant contact formation various methods are employed to create and establish such microstructural surface features. Such methods include blasting, acid-etching, anodization and plasma-spraying.

### *4.1.1. Blasting*

Usually blasting is explained as the use of abrasive particles such as hard ceramics against another material under high pressure in order to make it smoother, remove surface contaminants or to roughen the surface [197–199]. The dynamic contact between the forced particles and the surface leads to higher roughness values, increasing metal surface reactivity [185]. The desired roughness can be set up by the particle size. Thus, for the blasting of biomedical materials the particles should be chemically stable and biocompatible. Usually alumina, titania or hydroxyapatite particles are applied for blasting treatments.

In a study on the influence of grit particle size and its influence on surface roughness and torque removal values after 12 week implantation in vivo, two alumina particles sizes (25 and 75 μm) were used. The average roughness after blasting were found at values of 1.1 and 1.4 μm, respectively, where both surfaces showed a rough irregular topography with numerous randomly oriented sharp features (Fig. 7).

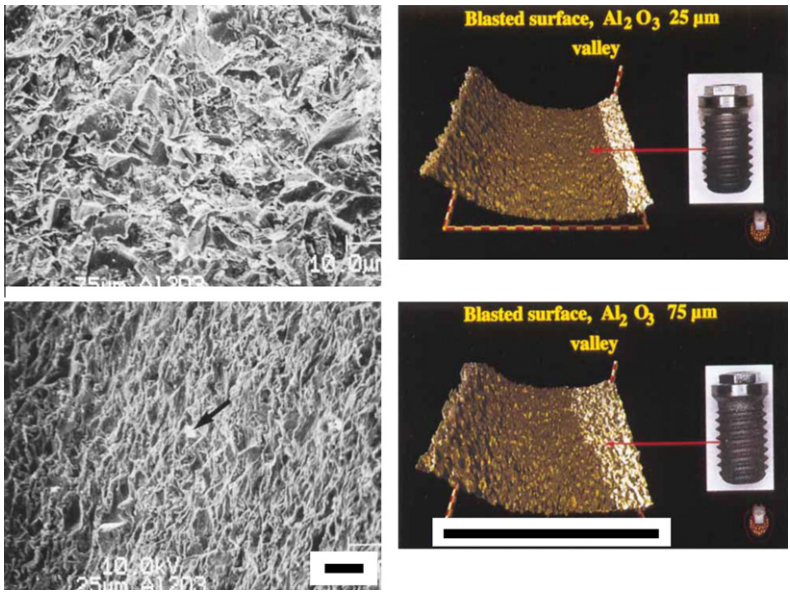


**Fig. 7.** SEM and computer generated topographical images showing the differences in surface structure after blasting titanium implant surfaces with 25 μm and 75 μm particles of alumina (scale bars = 10 μm) [200].

Thus, by increasing the implant-surface topography from an average deviation in height of 1.1–1.4 μm and keeping the isotropic structure with only minor differences in spatial direction, after 12 weeks insertion time in the rabbit tibia and femur, a higher removal torque and more bone implant contact formation were found for the implants blasted with 75 μm particles than with 25 μm particles [200].

Blasting the implant surface with particles other than the implant itself may change the surface composition and the implant biocompatibility. Several studies were reported on the inflammatory response of the host tissue on residual surface contaminants that originate for the blasting material and which may be released. The use of alumina as blasting material bears a potential risk of remnants and thus a dissolution of Al ions into the host tissue that cannot be excluded [185]. Some studies reported that aluminum ions may inhibit normal differentiation of bone marrow stromal cells and normal bone deposition and mineralization [201,202]. However, Wennerberg et al. compared the influence of surface contaminations by analyzing implants blasted with 25 μm particles of $TiO_2$ and $Al_2O_3$ in rabbits. As a result they found no statistically significant differences between the implants in bone implant contact formation or removal torque values and concluded that no differences could be found between the implants blasted with the same size of the particles but using different blasting materials. Moreover, no negative effect of alumina could be detected [185]. These results were confirmed in other studies [189,200,203,204].

The use of biocompatible, osteoconductive and resorbable blasting materials such as hydroxyapatite or beta-tricalcium phosphate has been investigated. Reports on the use of such blasting materials have indicated that roughened surfaces with calcium phosphate blasts show a higher formation of bone implant contacts versus untreated control groups and are comparable to commonly used alumina or titania blasting procedures [205–207].

#### *4.1.2. Acid etching*

Especially titanium based biomedical alloys are widely structured via acid etching procedures. Herein the variety of recipes used to achieve surface modification is wide. However, in all cases strong acids such as HCl, $HNO_3$, $H_2SO_4$ and in particular HF are needed to attack $TiO_2$. Acid etching methods performed on untreated titanium based alloy surfaces have shown to form micro pits at sizes ranging in between 0.5 and 2 μm and have been shown to be beneficial to cell adhesion and enhance osseointegration [195,208,209].

The immersion of titanium implant materials in a mixture of concentrated HCl and $H_2SO_4$ at elevated temperatures (100 °C) for several minutes results in homogeneous micro roughened surfaces. It has been shown that surfaces structured in this way promote a high ability for a rapid osseointegration and a subsequent long term success [210]. HF is known to show a high ability to dissolve the passivation layer, mainly consisting of $TiO_2$, on titanium based materials. Therefore a mixture of HF and $HNO_3$ has been also used to create surface structures at the micro level [211,212]. Moreover, it has been shown that fluoride incorporation into the created surface structures induces an enhanced osteoblastic differentiation and is favorable to the osseointegration of implants [213]. However, fluoride contaminations are known to have an ambivalent influence on the response of the host tissue [214].

Most commonly, acid treatments are carried out after a blasting step to remove blasting damaged surface zones and to refine at the same time surface roughness characteristics. More aggressive mixtures lead to generally finer surface defect distributions, whereas less aggressive acidic solutions induce a finer roughening [215]. After blasting the reactivity of surfaces against the etching solutions is different and thus, remarkably differences in roughness values can be achieved.

SLA surfaces (sand blasted large grit and acid etched) have been reported to show topographies of different scales at the same surface. In several investigations the superior quality of such a combined blasting and acid etching structuring technique has been demonstrated in vitro and in vivo [195,216–218].

#### *4.1.3. Anodization*

Electrochemical anodization represents another typical surface modification method mainly used for titanium based biomedical alloys. In this approach, the implant material is exposed to an anodic voltage in an ionic solution (often $H_2SO_4$, $H_3PO_4$, acetic acid). As a result of polarization (usually

several 10 V), a comparably thick $TiO_2$ layer can be grown on the titanium surface. This treatment is used to increase the oxide thickness and to enhance the corrosion protection. In particular, a possible selective ion release may practically be suppressed if the bulk material represents an alloy, containing soluble compounds, for example vanadium in Ti6Al4V. By altering the process parameters such as anode potential, electrolyte composition, temperature, or under galvanostatic conditions, structural and chemical properties of anodic oxides may be varied.

Under anodic polarization above approximately 100 V the potential may be so high that the oxide thickness substrate does not increase anymore but reaches the dielectric or avalanche breakdown limit. Thus the oxide will locally no longer be resistive but will allow high current flow across the oxide layer. As a result, at such spots the process will lead to an increased gas evolution – oxygen from the electrolyte – and sparking may be observed. This type of high voltage anodization is often referred to as spark anodizing (sparking) or micro-arc oxidation. At the spark locations irregular crystalline oxide forms (at breakdown channels) and after extended time the entire surface may be sparked leading to an irregular porous oxide film. These layers usually have a high micro hardness, strength and wear resistance [219–224].

Yang et al. investigated sparked titanium surfaces in terms of structure in relation of the applied potential and the apatite formation ability of such modified surfaces in simulated body fluid to synthesize bioactive titanium [219]. In this study titanium samples were anodized at different potentials varying from 90 to 180 V in $H_2SO_4$ of different concentrations. The authors indicated that with increasing potential, on the one hand structural features at the micrometer level could be obtained, and on the other hand the crystalline nature of the formed oxide layers changed with the applied potential from anatase to rutile (Fig. 8a and c). Soaking these modified surfaces in simulated body fluid for 6 days leads to an increased hydroxyapatite growth with a higher anodization potential (Fig. 8b and d).

However, no apatite formation could be observed on anodically oxidized titanium that was treated at potentials below the breakdown potential, even though anatase was produced on the surface. Yang et al. concluded that apatite formation on titanium can be initiated on sparked surfaces, indicating that a three dimensional structure of the micro porous titanium oxide structure may be necessary to induce apatite formation on the surfaces. In other investigations such surfaces anodized in the described matter showed a strong augmentation in bone response and histomorphometric test in

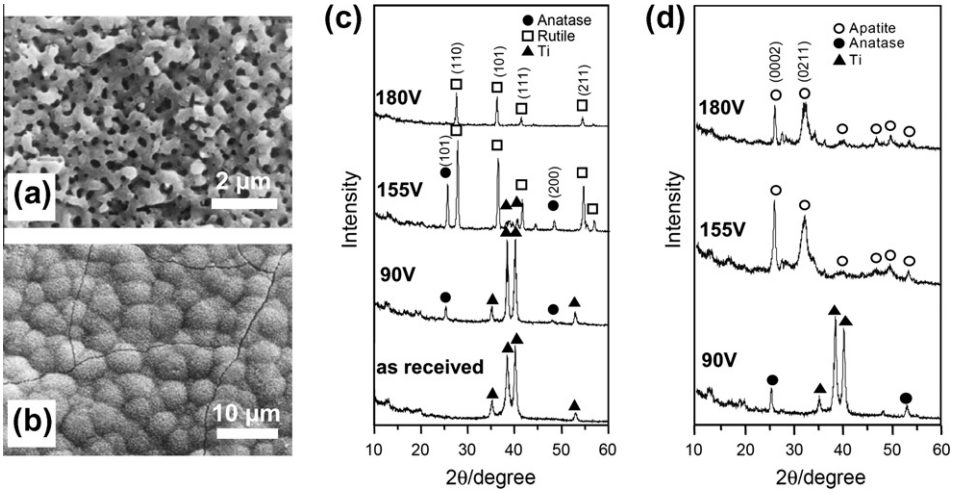


**Fig. 8.** SEM images of an anodically oxidized titanium surface at 155 V in 1 M $H_2SO_4$ for 1 min (a) after soaking for 6 days in SBF (b). XRD patterns taken from titanium surfaces anodically oxidized at 90 V, 155 V and 180 V in 1 M $H_2SO_4$ for 1 min (c) and after soaking these samples in SBF for 6 days (d) [219].

comparison to untreated control groups as explained by an enhanced mechanical interlocking trough bone growth into the pores [220,225].

A further development of spark anodized titanium surfaces used in biomedical applications is constituted by the chemical composition of the formed titanium oxide layers during anodization. Therefore, the addition of calcium ions and phosphates into the electrolyte were investigated to achieve incorporation of Ca/P to induce osseointegration of new bone and to become bioactive [226–228].

#### *4.1.4. Plasma spraying*

Plasma spraying is another method used for the structuring of implant surfaces in the micron-scale level. This method is a version of thermal spraying, a technique for producing coatings using a plasma jet at high temperatures that projects particles onto the surface of the implant where they condense and fuse together. Usually deposits produced with plasma spraying show thicknesses from micrometers to several millimeters and can be produced from a variety of materials. In biomedical applications bioinert ceramics with excellent mechanical properties, such as titania, zirconia or alumina are deposited mostly onto titanium based alloys by plasma spraying to increase the surface roughness and at the same time to modify the surface chemistry. Alumina and zirconia coatings are being used clinically, mostly due to their higher wear resistance than titania. However, alumina and zirconia coatings cannot bind directly to bone tissues due to their bio-inert nature, thus limiting their use in hard tissue applications [229]. Plasma spraying of titania has been used to produce rough implant surfaces – such coatings may show an average roughness of around 20 μm (using high deposition thicknesses to achieve uniform deposits) [230]. Buser et al. demonstrated that such coatings induce an increase in the bone to implant contact formation by measuring the tensile strength at the interface [183]. However, there is a controversy on the binding strength and on particle release from plasma sprayed coatings into the host tissue, caused by either dissolution or fretting [231]. Plasma sprayed surfaces are often used in combination with other modifications such as blasting or etching [230,232]. More recently, plasma spraying is increasingly used for hydroxyapatite coatings as these coatings show beside the structural influence also improved abilities in terms of bioactivation [233].

For an optimal and true ingrowth of bone into porous structures of biomedical material, typically a macro porosity in the range between 100 and 500 μm is required [234,235]. Thus the above described surface modification methods (with smaller scale ranges) are more directed towards the development of a proper interlocking of the host tissue with the biomedical implant material rather than an ingrowth of bone [236,237]. Indeed, micrometer scale topographic modification of implant surfaces have been shown to induce an improvement of the bone implant contact formation and further more to accelerate the development of a stiff interface in vivo [238,239]. Another direction of studies at the patterned surface – cell interaction is provided by the engineering of micropatterns to address patterns of single or multiple cells through precise surface engineering, mainly used for in vitro investigations of cellular bioassays that provide also new insights into cell behavior controlling factors. Excellent reviews exist and interested readers are referred to [240–244]. For more detailed discussion on the above described methods on surface modifications of biomedical implant materials at the micron level and other mechanical surface modification methods, such as grinding and polishing, the readers are referred to [183,197,229,245–247].

### *4.2. Surface topographies at the nanometer level*

In previous paragraph an introduction to techniques to alter the surface topography at the micron-scale was given. Such surfaces mostly show random topographies with surface structures ranging in a wide range from nanometers to millimeters. Zinger and coworkers showed that combining surface patterning techniques at the sub-micrometer level with subsequent sandblasting and etching led to surface roughnesses with combined micrometer and nanometer structures and thus showed an enhanced osteoblast activity [209,248]. From such studies it was deduced that cell attachment in vitro and the bone implant interface in vivo may be influenced by both nanoscale and microscale parameters of topography, where osteoblasts showed an enhanced attachment on submicron-scale structures [249,250]. The role of surface roughnesses at both length scales, either micron or nanometer level, requires the consideration that molecular interactions with the surface occur and as a direct

consequence, cell adhesion phenomena and local biomechanical features of the established interface are directly influenced by this length scale. Modifications of surfaces at the nanoscale will have an effect on the chemical reactivity of a biomedical material and thus affect ionic or biomolecular interactions of the surface with the host tissue. Such changes in surface properties altered by modifications at the nanoscale may change wetting properties, lead to a different protein adsorption, or have an influence on the mineralization of de novo bone formation. The importance of topography at the nanometer scale has been emphasized, where one interpretation of the sensitive reaction to nanotopography occurs because there are small differences in chemistry between one part of the topography and another. An opposite view is that even when small local differences in chemistry are made by techniques such as nanoprinting, there is also a small difference in topography [251–254].

Up to now there is no absolute knowledge on the influence of such features on the biological environment, because of the absence of standardized surfaces with repetitive topography at the nanoscale level with highly controllable lateral resolution. The increasing availability of well understood and standardized surface structures in the sub-100 nm scale will strongly help to understand the interactions between specific proteins and cells.

In the past years reports have been published on the tailored adjustment of surface features at the nanometer level to explore a possible impact of surface structures in the sub-100 nm region. The most promising approaches to fabricate surface roughnesses in the desired structural sub-100 nm region with an adequate lateral resolution in a reproducible manner at the nanometer scale, as well as comparable surface chemistries will be discussed in the following paragraph.

*4.2.1. Photo, electron beam and colloidal lithography*

Photolithographic approaches are commonly used for micron-scale structuring of semiconductor devices. Hence, this approach has also been reported as structuring technique to fabricate well-defined surface features in materials ranging from silicon and quartz to polystyrene and silicone elastomer of distinct lateral resolutions. To achieve such surface structures, commonly used approaches in the silicon wafer industry are used, representing a light sensitive photoresist, a patterned mask to transcript any geometry to the surfaces which is then developed under the influence of light and further sequentially removed, thus leaving a topography of resist around areas of exposed substrate. In a further abrasive step the exposed areas can then be chemically wet etched or reactively removed under ion bombardment. For nanoscale structuring shorter wavelength sources such as deep UV and X-rays are used. Short wavelength writing techniques are based on ion or electron beams. Depending on the treatment and composition of the substrate, a variety of areas of nanostructured surfaces can be embedded into micropatterns [255–257].

Turner and coworkers reported on textured silicon surfaces at the nanoscale that were fabricated using a reactive ion etch process designed to produce nanometer scale columnar structures in silicon that they called silicon grass. Standard photolithographic techniques were used to pattern the surface,

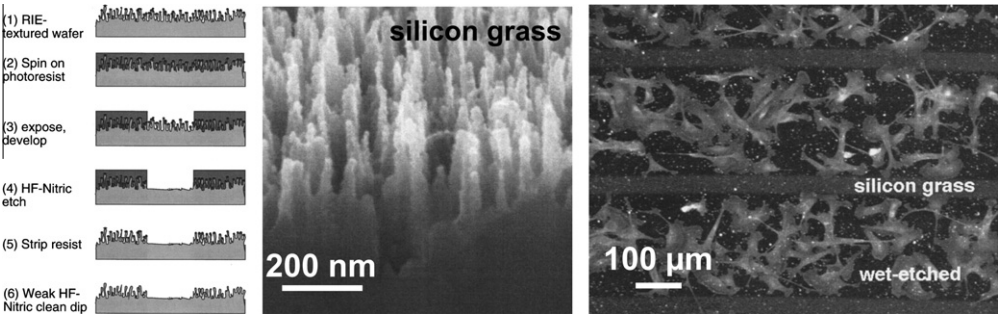


**Fig. 9.** Schematic outline of the steps used to produce silicon substrates with patterned surface features at the nano level, SEM image of the synthesized silicon grass and scanning confocal micrograph of cells from LRM55 cell line adhering preferentially to the wet-etch smoothed regions [254].

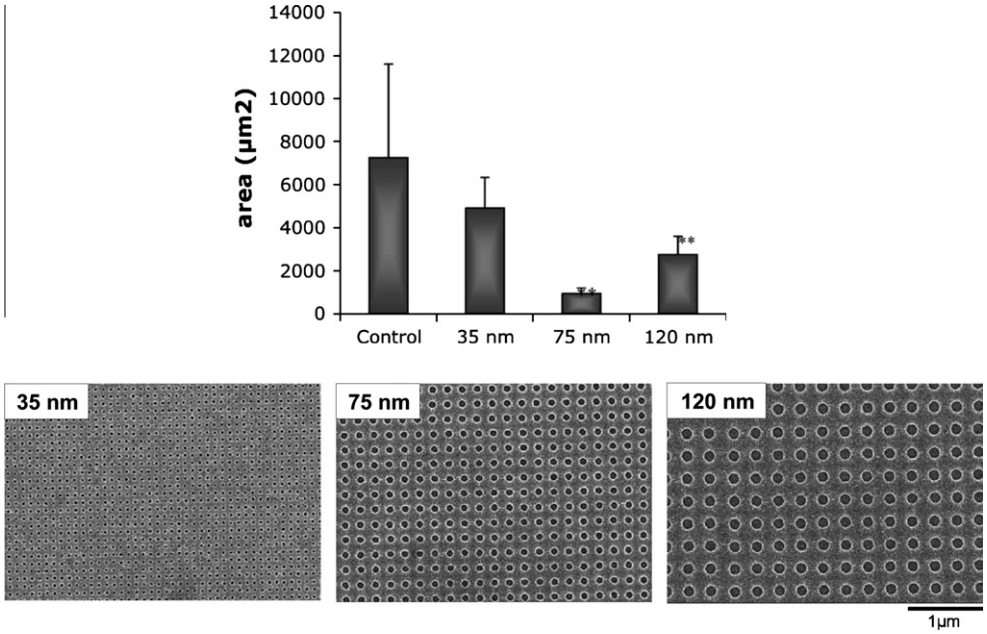


**Fig. 10.** SEM images of different nanopitted silicon masters of different pit sizes produced by high-resolution e-beam lithography and quantification of cell areas of primary human fibroblasts to the same types of nanopitted regular arrays made in polycaprolactone against plane control surfaces (adapted from [270]).

thereby allowing selective modifications of the surface texture by a wet chemical etching for silicon. The resulting surface allowed a side-by-side presentation of different surface textures to cells grown in culture (Fig. 9). In this study, besides other cells investigated, cells from cell line LRM55 showed on such textured surfaces a preferred attachment and growth on the smoother surface compared to the silicon grass surface whereas primary cortical astrocytes preferentially attached and grew on the very rough silicon grass areas [254,258].

Photolithography has been used by many pioneers in the field of cell response to study the influence of microtopography. However, its usefulness for producing nanotopography is very limited and more precise methods have been introduced to come over the need for highly ordered surface topographies at the nanometer level.

Wilkinson et al. reported on the use of electron beam lithography to fabricate surface patternings in the range of several 10 nm [259,260]. Then a nickel die fabrication and hot embossing into polymers was used. With this technique it is possible to achieve different pit sizes at the several 10 nm range. Fig. 10 shows examples for three different patterns of pits with diameters of 35, 75 and 120 nm, respectively. In the reports the pitch between the pits rose from 100 nm over 200 nm to 300 nm with increasing pit size. In this study, it was reported that such ordered surface arrays of nanopits in polycaprolactone or polymethylmethacrylate show marked effects in reducing primary human fibroblasts adhesion compared with less regular arrays or planar surfaces. It was deduced from the results that the investigated cells might be able to distinguish between the different symmetries of the fabricated arrays [251,261].

Most direct and promising is e-beam lithography as structuring technique for the investigation of surface roughnesses at the nanometer scale. However, the challenge remains in establishing long range order (i.e. over large sample areas) as the de-focussing of the beam becomes a main limiting factor at (sticking) deflections of more than 1 mm. Repeated moving the sample during writing by interferometric control has been used to enable the fabrication of large areas of patterns to be produced for cell testing (and stitch accuracies of approximately 20 nm can currently be achieved) [259]. Moreover,

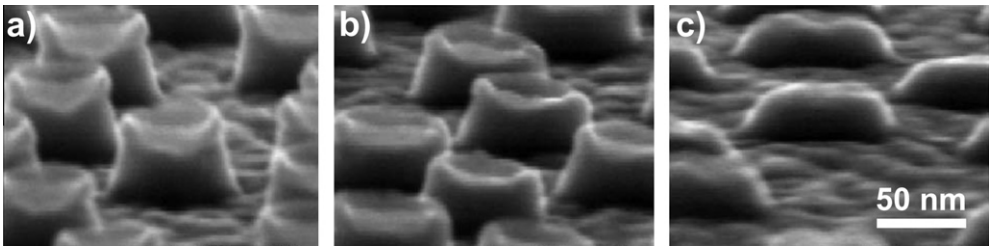


**Fig. 11.** Nanostructured gold surfaces showing different shapes of the upper part of the columns achieved by different heat pretreatments of the PMMA particles before argon ion etching. (a) not heated particles, (b) particles heated to 106 °C and (c) 112 °C [262].

e-beam lithography is in general comparably expensive (in vacuum) and time consuming technique (as each feature has to be written sequentially and considering that for proper cell tests an area in the range of several $cm^2$ is needed) to achieve surface structures for in vitro investigations.

In contrast, colloidal lithography offers the possibility to produce nanostructured surfaces on large scale areas at relatively low prices. The main principle of this technique is based on the dispersing and electrostatical self organization of nanocolloids on a substrate. Often these surfaces are then treated by bombardment with reactive ions leading to an etching (removal) of the surrounding material as well as the colloids themselves [262–264]. As a result, nanocolumns can be achieved in a highly reproducible manner (Fig. 11). Surface structures that are fabricated in the above described way can be used for in vitro investigations directly, in contrary to the other lithographic processes. However, such surfaces are mostly used as die for imprinting into various material systems. Gallagher and coworkers reported on such structuring methods by using $SiO_2$ dies on polycaprolactone [265]. Dalby et al. summarized various reports on the use of nanocolums produced by colloidal lithography [266] and concluded that cells are highly responsive to nanotopography produced with e-beam lithographic nanopits, and colloidal nanocolumns were found to reduce adhesion and more gentle nanoislands to increase adhesion. Up to now the presented lithographic surface structuring techniques do not show sufficiently small structures, either of the cavities themselves or of the distance in between as shown in Figs. 9–11, for authentic investigations on the influence of nanofeatures in vitro.

*4.2.2. Demixing of polymers*

Another method described for the fabrication of structured surfaces at the nanometer scale without altering the material chemistry is based of a controlled demixing of polymers. Therefore, spontaneous demixing of polystyrene and poly (4-bromostyrene) during spin coating on silicon wafers is used to produce islands or different heights [267]. It has been shown that polystyrene shows a strong segregation towards the surface when annealing the film. This means that despite the topography being formed by polymer blends, after the films are annealed the cells only interact with a single chemistry, in this case polystyrene [268]. Fig. 12 shows AFM images of three different surfaces with island heights of 13, 35 and 95 nm. It has been reported that on islands with 95 nm height a decreased endothelial response was observed, compared to 13 nm high islands where cells were seen to give the largest

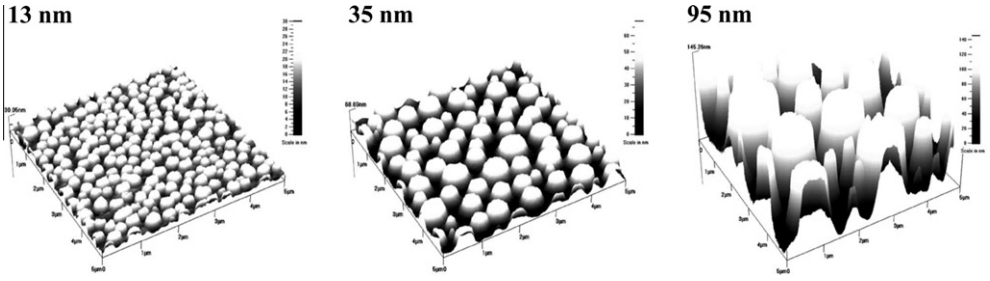


**Fig. 12.** Atomic force microscopical images of demixed polystyrenes with 13 nm, 35 nm and 95 nm high islands [269].

response, with highly spread cell morphologies containing well-defined cytoskeleton [269]. Moreover, the cells were seen to be more spread on the manufactured topographies than that on flat surfaces of similar chemistry.

The structurization of surfaces is classified according to the vertical dimensions. This means that the vertical length scales reported fit to the recommended sub-100 nm region. However, at an island height of 13 nm the average diameter of such islands is already at 140 nm [269]. With increasing height of the islands the lateral dimensions are increasing as well, as indicated in the AFM images of same magnification taken from the surfaces in Fig. 12. Other reports have shown comparable results on using demixed polymer surfaces for the use in in vitro investigations [270–272].

*4.2.3. Nanophase biomedical ceramics, metals and alloys*

To achieve a structurization in the desired sub-100 nm scale range Webster and coworkers fabricated nanophase ceramics [273] and metals [274]. In principle, ceramic or metal powders that show an average grain size distribution at the nanometer level are pressed and further sintered. Thus, surfaces of materials synthesized via this processing procedure can be used for in vitro response investigations. In case of ceramics, powders of alumina and titania have been used. By sintering the pressed powders in air for 2 h at either 1000 or 600 °C the ceramics were successfully produced. Depending on the temperature the starting average grain sizes of 23 nm and 32 nm can be enlarged to values up to 177 nm and 2.12 μm [273]. In addition, the created surfaces of different grain sizes possess the same crystallinity and surface chemistry, altering only in degree of nanometer surface features. Fig. 13 shows such surface roughnesses recorded by AFM. Webster and coworkers reported on a significantly increased adhesion behavior on nanophase alumina surfaces compared to grain sizes in the range of 177 nm, and to cover slide glasses used as control. Comparable results could be found for nanophase grain sizes in case of titania surfaces [273]. At the same time, an increase of adherent fibroblasts was reported on nanophase ceramics [275]. Supporting evidence of decreased fibroblast function on nanophase ceramics has been presented [276–278].

The adhesion behavior of osteoblasts has been reported to show a comparable behavior in relation to the average grain size of biomedical alloys such as cp-titanium, Ti6Al4V and CoCrMo [274]. Webster and coworkers concluded that the adhesion behavior of cells in dependence of the average grain sizes of the used surfaces may be independent of any surface chemistry, as this topographical dependency could be found on either ceramics or metals and other materials [279–282].

These methods for fabricating surface topographies with high lateral resolution in the sub-100 nm range show limitations. Many of the presented approaches are not based on biomedical implant materials that can be used for hard tissue applications or are not clinically relevant. Although this plays a major role in case of transferring the identified dependencies or influencing factors of surface model topographies at the nanometer level to real biomedical material surfaces, the most important task is to have a material system that possesses a good adjustability of nanometer scaled features in the sub-100 nm range in a highly reproducible manner. Moreover, most of the shown examples for structuring techniques are very time consuming, difficult to process and the generated surface structures are somewhat not sufficiently defined. The majority of the shown structures do not fit into the demand of nanometer features in the sub-100 nm range as they are often much bigger than 100 nm. Although numerous investigations have been reported by using the presented surface structures and by using various cell types, up to now it is somewhat difficult to compare the observations, as the investigations have been proceeded on totally different material systems with nanofeatures of different sizes which makes it hard to normalize the results. The desired successful adjustment of nanofeatures of different sizes in narrow alternations has not been described so far. A precise control of defined spacing between adhesive ligands of cells on interfaces at a length scale of 10–100 nm still remains a major challenge. Recently, two methods have been reported to possess the ability to structure nano features at high and distinct lateral resolutions and in a highly reproducible and fairly simple manner. These techniques are either based on a non-clinically relevant material system of gold nanodot arrays that are further coupled with cell adhesive sequences placed in distinct distances on wafers, or the growth of anodic nanoporous or nanotubular oxide structures on valve metals that can be tailored in size for example on biomedical titanium.

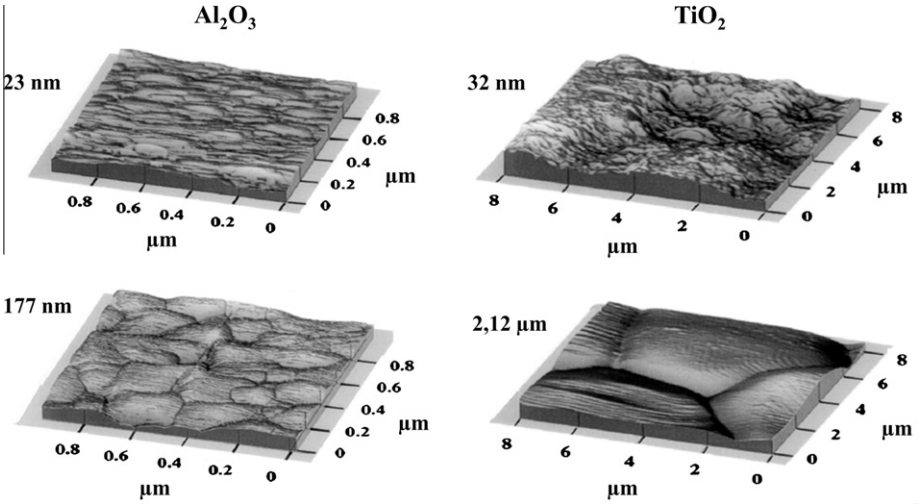


**Fig. 13.** AFM topographies taken from nanophase and conventional alumina and titania surfaces [273].

*4.2.4. Gold nanodot arrays*

Highly ordered arrays of gold nanodots on silicon wafers or glass slides are achieved by a micelle diblock copolymer lithography technology that represents a nanopatterning strategy which enables the modification of substrate topographies at the desired length scale. This technique is mainly based on the self-assembly of polystyrene-block-poly (2-vinyl pyridine) (PS-b-P2VP) diblock copolymers, which form reverse micelles in toluene where the core of the micelle consists of the P2VP blocks which complex the metal precursor ($HAuCl_4$) when added to the micellar solution. Dipping of the substrate into the solution and further plasma treatment to remove any organics, the deposition of highly regular gold nanoparticles forming a nearly perfect hexagonal pattern on solid-state interfaces can be achieved with spacings of the nanoparticles in between 15 and 250 nm (Fig. 14). These nanostructured arrays are used as templates for the spatial arrangement of RGD-based ligands, as indicated in Fig. 14. Since the gold dots are sufficiently small (1–20 nm), it is most likely that only one integrin transmembrane receptor directly interacts with one dot [283,284].

Spatz and coworkers reported in several publications on the cellular behavior of cells on such RGD modified gold nanodot arrays. They observed that MC3T3 osteoblasts showed on 28 and 58 nm spacings well spread cell shapes, whereas on higher spacings the cell shape was found to be much more globular and possessing a migratory morphology. Cell numbers were reported to be directly influenced by the lateral spacings, thus, nanodots separated by 58 nm and not conjugated to RGD did show much less cell numbers (Fig. 15). Furthermore, these observations were repeated with other cell types, like REF52-fibroblasts, 3T3-fibroblasts and B16-melanocytes, indicating a universally characteristic cell adhesion behavior [285].

It was concluded that a critical spacing of the nanodots must not be larger than 58 nm to achieve stable adhesion and the expression of focal adhesion complexes. These nanodots form a very valuable tool, since pattern dimension and geometry control the assembly of single integrins. Thus, uniform patterning of extended substrate areas by diblock copolymer micelle lithography provides access to an important length scale for cell adhesion studies that is hardly accessible with any other technique [286].

*4.2.5. Anodic nanoporous and nanotubular surfaces*

Nanoporous and nanotubular oxide films grown electrochemically on valve metals have received considerable interest in the past decade [287–290]. The use of such surface oxide structures as nanoscaled models for in vitro investigations has been explored widely. Alumina materials as well

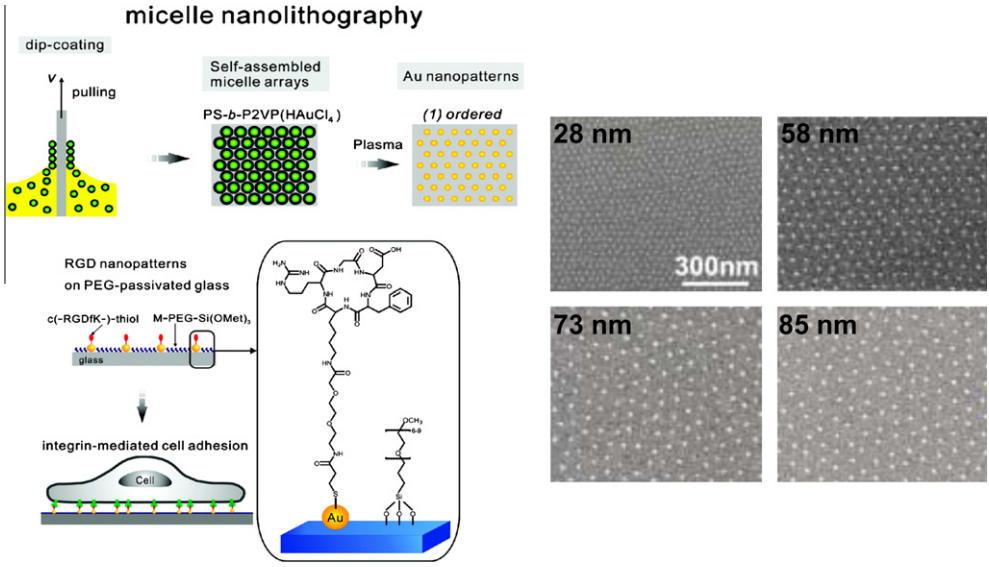


**Fig. 14.** Scheme of diblock copolymer micelle lithography to achieve highly ordered gold nanodot arrays for further biofunctionalization with RGD. SEM images of gold nanodot patterns with spacings of 28, 58, 73 and 85 nm (adapted from [284,285]).

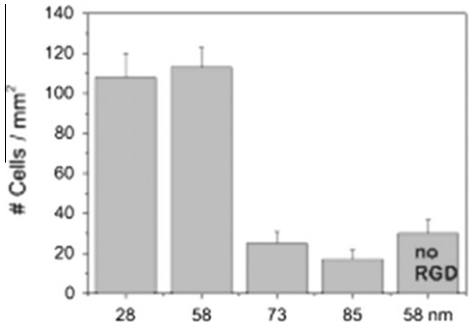


**Fig. 15.** Number of adhering MC3T3 osteoblasts on nanopatterned surfaces with different spacings after 1 day in culture [285].

as titanium, respectively titanium dioxide, represent well accepted biomaterials as these materials have been used extensively as substrates for bone tissue engineering applications.

Anodic porous alumina coatings are part of current research in bone tissue engineering. In a study, alumina membranes with a narrow pore size distribution of 200 nm were used as model surfaces intended to simulate porous anodic alumina converted from aluminum that was deposited on titanium and then anodized to produce pores in the coating [291]. These substrates were cultured with human osteoblasts and seemed to provide a good surface for osteoblastic cell growth, with cells rapidly spreading, flattening and adhering firmly to the surfaces [292]. Using this procedure, pores less than 100 nm diameter where not achieved, i.e. the effect of sub-100 nm topography on osteoblasts could not be investigated. Porous anodic alumina layers converted from sputted deposited aluminum layers have been reported to enhance the interlocking of bone cement to the implant surface in cemented joint applications, especially on bioceramic materials [293]. In further work, when culturing mesenchymal stem cells anodic nanoporous alumina surfaces supported higher cell adhesion, proliferation,

and viability up to 7 days of culture when compared with amorphous alumina surfaces. The long-term effect of these nanoarchitectures on the functionality and phenotypic behavior investigated after a period of 3 weeks showed that the bone-cell performance can be improved using controlled nanoarchitectures [282]. Adhesion and proliferation of epithelial normal cells were investigated on nanoporous alumina surfaces with different porosity adjusted by the electrochemical growth parameter. It was reported that the changes in surface area to which the cells could adhere, and the interactions between small ECM molecules, were influenced by sufficiently small structures on the surface [294].

Titanium, one of the most commonly used implant materials in medicine, when anodized in fluoride containing electrolytes possesses the ability to produce highly ordered $TiO_2$ nanotube arrays with a high adjustability of the lateral dimensions in the sub-100 nm region. Ordered nanotubular structures of $TiO_2$ or other transition metal oxides can be formed, as schematically shown in Fig. 16. In general, the morphology and the structure of nanotubular layers are affected strongly by the electrochemical conditions, particularly the anodization voltage, and the solution parameters such as HF concentration and pH [288,290,295,296]. For more detailed information on growth, structure and applications of anodic oxide nanotube layers in various fields the readers are referred to [297].

A main feature is that the diameter of such $TiO_2$ nanotubes can be directly adjusted by the applied anodization potential [298]. This allows a level of diameter control in the range of 15–100 nm and makes the surfaces an excellent model for the investigation of nanoscale interaction with living matter (Fig. 16).

In recent works, it has been shown that vitality, proliferation, motility and differentiation of mesenchymal stem cells, hematopoietic stem cells, as well as the behavior of osteoblasts, osteoclasts and endothelial cells are critically influenced by the nanoscale $TiO_2$ surface topography with a specific response to nanotube diameters between 15 and 100 nm (Fig. 17). Moreover, it was demonstrated that adhesion, proliferation, migration and differentiation of the investigated cell types were at a maximum for a length scale of 15 nm nanotubes, but minimal at 100 nm nanotubes (this size was found to strongly induce apoptosis). This effect has been proposed to be related to the effective size-scale of the integrin based focal contact formation between cells and surfaces, and the optimum nanotube diameter seems to enhance cellular activities compared to smooth surfaces [299–301].

However, other results were also reported, indicating favored cell adhesion and proliferation on 80 nm [302,303] nanotubes as compared to nanotubes with smaller diameters – this was attributed to differences in surface chemistry or crystallinity. In a further report it could be demonstrated that the response of mesenchymal stem cells to the same nanotubular surface geometries but with different materials such as $ZrO_2$ nanotubes and AuPd-coated nanotube arrays was universal, i.e. less

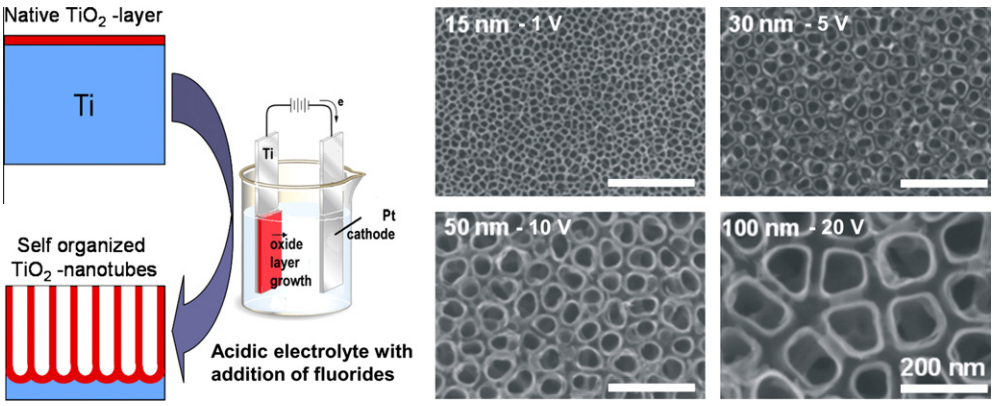


**Fig. 16.** Schematic setup for anodization of titanium in fluoride containing electrolytes. Depending on anodization conditions (mainly potential, electrolyte, temperature), the solid oxide layer can be transformed into nanotubular structures. Exemplary SEM top views of anodically formed $TiO_2$ nanotube layers on biomedical titanium grown at different anodization potentials ranging from 1 to 20 V show indicate the linear potential dependency of the nanotube diameter on the applied potential [298].

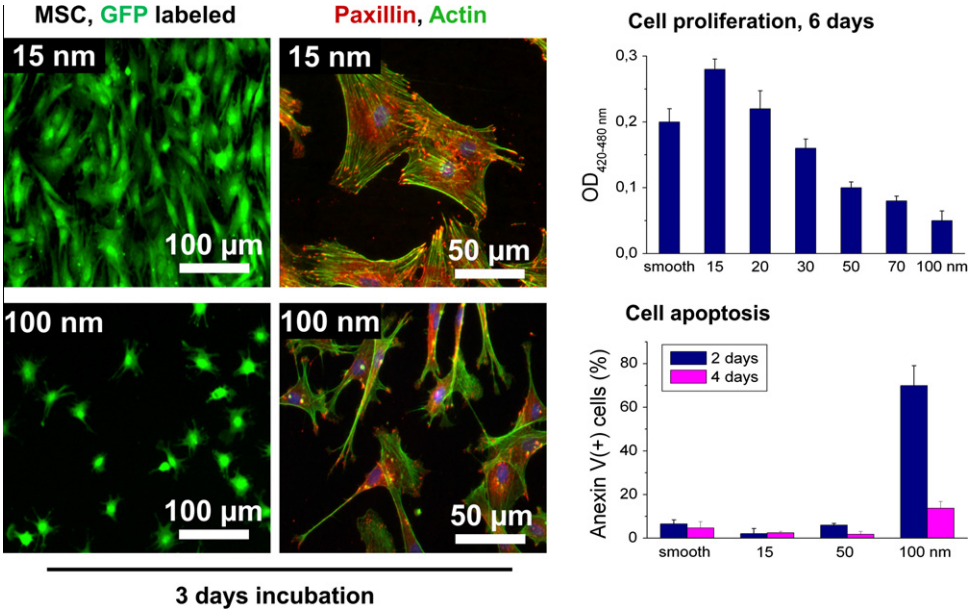


**Fig. 17.** Fluorescence microscopy images of GFP-labeled mesenchymal stem cells after 3 days incubation on 15 nm and 100 nm $TiO_2$ nanotube layers. A 3 days after plating, focal contact formation and stress fiber assembly is extensive on 15 nm nanotubes as shown by anti paxillin staining (red) and anti-actin staining (green), but strongly reduced on 100 nm nanotubes. MSC are well spread on 15 nm nanotubes, but developed a migratory morphology on 100 nm nanotubes with few focal contacts and stress fibers. Cell proliferation rates measured after 6 days by WST-1 assay as well as cell apoptosis show a strong dependency on nanotube diameter [299].

dependent on differences in surface chemistry than on minute topographic structural differences [304]. Remarkable is that for every class of material or post treatment of the nanotubular surfaces a maximum in cell activity was obtained for nanotube diameters of approx. 15 nm [300,301,304,305]. Long term in vivo investigations in the pig on the use of $TiO_2$ nanotubes as implant coatings have shown very promising results in terms of bone implant contact formation and mechanical stability [306]. These findings indicate that nanotubular $TiO_2$ layers are highly promising for tailoring the cell-surface interactions of titanium based implants in a desired manner, as the nanotube formation is also possible on implant alloys such as Ti6Al4V, Ti6Al7Nb or Ti29Nb13Ta4.6Zr and others [307–310].

### *4.3. Chemical surface modifications*

Biological tissue interacts mainly with the outermost atomic layers of an implant. Although secondary and other byproduct reactions will occur, the primary interaction zone is generally defined by the first atomic layers. Therefore, various efforts are directed to modify surfaces of existing biomaterials to achieve desired biological responses [182,311]. Besides morphological modifications of the surface roughnesses of biomedical implant materials, numerous chemical modifications of implant surfaces have been investigated to obtain an optimized tissue interaction. The ideal hard implant should present a surface that will induce osseointegration, a property that is in any case desired regardless of implantation site, bone quantity or bone quality. Hence, physicochemical treatments are designed to cause surface interactions directly with the chemical nature of the bone, in order to enhance and influence the de novo bone formation. In principle, physicochemical approaches are either based on the control of surface composition, surface free energy, wettability or electric charges. These treatments may have the ability to turn a commonly bioinert surface of an implant material, such as metals, into a bioactive character.

*4.3.1. Surface composition*

A most direct approach to modify the chemistry of an implant surface is the application of coatings. Particularly calcium phosphates are known for their bioactive properties and their increased bone-binding effects. Therefore, calcium phosphate coatings, similar to the mineral phase of bone, have been extensively investigated as bioactive coatings on bioinert implant materials [312–314]. For example, metal implants have been coated with layers of calcium phosphates mainly composed of hydroxyapatite. While hydroxyapatite resembles in its chemical structure apatites, carbonate apatite comprises a chemical composition that is more close to the human bone. Incorporation of carbonate into the crystal structure induces a higher reactivity towards bone. The material shows an increased solubility rate in acids [315]. An increased dissolution rate after implantation leads to an enhanced release of calcium and phosphate ions into the per-implant region, hence increases the saturation of body fluids and therefore induces a facilitated precipitation of biological apatite onto the surface of the implant [314,316]. Generally the bone healing process and thus the biological fixation of implants to the host tissue was found to be enhanced with a calcium phosphate coating compared with noncoated implants [317,318]. For the processing of calcium phosphate coatings onto metallic implant surfaces various techniques have been investigated, such as plasma spraying, sol–gel coating, electrophoretic deposition, ion implantation and biomimetic precipitation, in order to combine the mechanical properties of the substrate metals and the biological properties of calcium phosphates.

Plasma spraying is the most commonly used coating technique for calcium phosphates. As mentioned before plasma spraying also leads to a surface modification in terms of higher surface roughnesses. Therefore hydroxyapatite coatings can combine surface topography with chemical effects [319–323].

However, plasma spraying shows some disadvantages in long term investigations. To achieve a dense complete coverage of the substrate material the sprayed depositions must have a minimum thickness of approx. 50 μm. Depending on the field of application – in particular if an orthopedic or dental implant devices is used – this can result in a relatively poor bonding between the plasma sprayed apatite coating and the substrate material [324]. Additional pre-treatments of the substrate material are required to achieve a roughening and thus a better mechanical interlocking of the deposited layers. Moreover, particle release and delamination from the deposited layers and possible inflammatory responses have been reported [324–326]. Furthermore it has been shown that during the coating procedure uncontrollable changes in the composition and crystallinity of the initial calcium phosphate material can occur due to the high energy involved in the process. This means that it is very difficult to coat the desired carbonate apatite, as its structure is decomposed during plasma spraying [327]. To overcome these limitations in apatite coating of implant materials several alternative coating procedures have been investigated.

Most of the problems known from plasma spraying are associated with the excessively high fabrication temperature. In comparison, the sol–gel technique offers certain advantages, because of the high chemical homogeneity, fine grain structure, and low crystallization temperature of the resulting coating. Moreover, it is an economical and technically simple procedure to perform [328,329]. In this method calcium phosphate coatings are prepared by dipping the substrate in calcium (usually nitrate salts) and phosphorus gels. As formed coatings show porous, less dense structures and are reported to show a poor adhesion to the substrate material [330,331]. This poor adhesion is a detrimental factor which limits their use. Therefore, these coatings must be sintered at high temperatures to improve their adhesion strength and density. Depending upon the sintering temperatures different calcium phosphates can be obtained [332,333]. Fluoridated hydroxyapatite coatings with different fluoride contents prepared by sol–gel methods have shown an ambivalent behavior: either to improve the cell viability or at high fluoride contents a decreased calcium release in culture medium due to reduced solubility. For clinical applications, it is suggested that a moderate content of fluorides may be suitable as a compromise among cell attachment, proliferation, apatite deposition and dissolution resistance [334,335].

Cathodic deposition is another type of electrochemical method where hydroxyapatite is formed in situ from an electrolyte containing calcium and phosphate ions where such ions are electrochemically reduced at the cathode. The electrochemical cathodic deposition of calcium phosphates has been reported as a method that can proceed at ambient temperatures with a high controllability and thus

resulting in a good conformability to the shape of the substrate. Adjusting the pH, current density and agitation, it is possible to obtain tailor made calcium phosphate coatings. Post sintering processes are not required in most cases, however a post crystallization of the deposit may be performed for desired phase stabilization [336]. Most commonly deposition is carried out in acidic calcium phosphate solutions that require further aging steps to convert the deposited layers [337–339], other reports have indicated the deposition of apatites from simulated body fluids [340–342]. The current trend in cathodic deposition is the synthesis of calcium phosphate coatings as nanocrystalline deposits, as nanophase grained hydroxyapatite shows greater biological activity. Therefore emphasis is being laid to produce these coatings by using very low concentrations of calcium and phosphates in the depositing solution without the addition of any precursor [343].

In contrast, electrophoretic deposition exhibits a deposition technique based on the movement of charged particles in an electric field that are dispersed in a solution at a particular pH – thus HAp particles are precitipated at the cathode due to local alkalization. Under these adjusted conditions the particles acquire positive charges and thus coatings can be obtained on the cathodically polarized substrate material. However, deposition relies on the coagulation of particles to a dense mass; a post sintering is required to improve the coating strength [344–347]. Electrophoretic deposition enables uniform coatings even on complex geometries at high deposition rates and requires at the same time no expensive apparatus. As disadvantages of electrophoretically driven coatings it has been reported that it is difficult to produce dense crack-free coatings, as the post-sintering is required at elevated temperatures. Moreover, the adhesive strength of such layers has been found to be very low [348].

Physical vapor deposition techniques such as ion plating [349], magnetron sputtering [350] and ion beam dynamic mixing [351] have been introduced to deposit thin calcium phosphate coatings onto implants. The frequent initial amorphous nature of these coatings can be easily improved by a rapid heat treatment [352,353]. The main component of the crystalline structure of these heat-treated films is hydroxyapatite. Various studies already confirmed the favorable bone behavior of calcium phosphate coated implants using such physical vapor deposition techniques. For example, ion beam depositions of calcium and phosphorus onto the surfaces of biomedical materials have been reported to enhance the ability for the formation of hydroxyapatite when exposed into simulated body fluids [354]. It has been concluded that crystalline calcium phoshate rapidly nucleate on the surfaces showing a high adhesive strength and are less prone to crack formation upon further treatment with simulated body fluid medium. However, the deposition of ions onto the surface is an expensive process and moreover a subsequent sintering step at high temperatures is required [351,355]. In a study on the bone implant contact formation in rabbits it was reported that such ion beam treated surfaces may benefit the bone implant response [356].

In order to overcome the drawbacks of the described coating approaches, a biomimetic coating technique has been developed inspired by the natural process of biomineralization. In principle the deposition of apatite by immersion into physiological solutions, known from in vitro biocompatibility testing, is adapted in order to achieve depositions that are close to the composition and chemistry of natural bone [142,318]. This method involves the heterogeneous nucleation and growth of bone like crystals on the surface of the implant at physiological temperatures and under pH conditions which are maintained at around 7.4. In order to accelerate the deposition of coatings from simulated body solutions, several approaches have been put forward. Possible pre-treatments for the acceleration of heterogeneous nucleation can be found in the above described deposition techniques such as cathodic electrochemical deposition in simulated body fluids.

Other surface modification methods, such as alkaline treatment [357–359], acid treatment [360] and $H_2O_2$ treatment [361,362] of $TiO_2$ [363] have been reported in an attempt to form a bioactive surface on metal based implants. Kim et al. [358] reported that amorphous sodium titanate hydrogel, obtained by exposing pure titanium into alkaline solutions and a subsequent heat treatment, would induce apatite formation when soaked in simulated body fluid. It was shown that pure titanium metal formed a bonelike apatite layer on its surface in simulated body fluid within 3 days after being prepared by soaking in 5 M NaOH solution at 60 °C for 24 h with subsequent heat treatment at 600 °C for 1 h [358,364,365].

Others have used high concentrations of calcium and phosphate ions in an increasing pH solution to form a thin layer on the implant surface. In a second step, the desired apatite coating developed

under crystal growth conditions from simulated body fluids [366]. A recent study on the precoating of $TiO_2$ nanotube arrays grown anodically on titanium with calcium phosphate layers by an alternative immersion method indicated a drastically enhanced physiological hydroxyapatite growth in simulated body fluid [367]. It has been reported that such biomimetic coatings show a higher solubility in physiological fluids and are more resorbable by osteoclastic cells like dentin materials than high temperature coatings such as plasma-sprayed apatites [368,369]. From preclinical investigations it has been reported that titanium implants coated with biomimetic calcium phosphates show an accelerated and higher bone implant contact formation than observed in control groups [318,368].

For more detailed information on the reviewed coating techniques of calcium phosphates onto implant materials and their applications the readers are referred to [229,370–372].

*4.3.2. Physicochemical characteristics*

Surface physicochemical characteristics of a biomedical implant material such as wettability, crystallinity and charge may critically influence the host response of an engineered replacement by affecting directly or indirectly protein or cell to implant interactions in vivo [373]. Controlling such surface features can be used to tailor surface related tissue responses such as biomolecule adsorption, cell attachment and vitality.

In order to alter surface physicochemical properties numerous approaches have been reported. Therefore, a brief overview on the most common strategies for the tailoring of surface chemical gradients will be introduced. As a fundamental criteria the methodologies for surface chemistry gradient generation can be divided either in top-down treatments that imply the surface modification and the bottom-up that imply the deposition of species onto the surfaces.

Glow discharge is widely used for the sterilization of biomedical devices prior to implantation and involves the exposure to a highly energized inert gas such as plasma. Besides the generation of hydroxyl free radicals, oxygen and other reactive species used for the killing of bacteria, this atmosphere influences the wetting behavior of implant materials at the same time leading to an increased hydrophilicity [374]. Thus glow discharge has been used to increase surface free energy in order to increase tissue adhesion [375]. However, it has been reported that an increased bone implant contact formation due to an increased surface energy has not been observed. It was proposed that circulating blood could immediately contaminate the implant surface and thus lower the activity (high surface energy) [376]. To overcome this spontaneous contamination Rupp and coworkers have reported on a specific after treatment process of sandblasted acid etched (SLA) titanium surfaces to retain the high surface energy. Therefore, the titanium devices were rinsed after the etching process under a protective $N_2$ gas condition and continuous storage in an isotonic NaCl solution at pH 4–6. It was described that such modified SLA (modSLA) surfaces could retain the high surface energy by reducing the adsorption of potential contaminants from the atmosphere and in the clinical situation, as the hydrophilic condition remains during surgery at contact angles of about 0° compared to about 140° for conventional SLA [377,378].

The influence of hydrophobicity of implant surfaces on tissue and the interaction of different types of cultured cells or blood proteins with various solid substrates showing different wettability have been reported elaborately [379–381]. A considerable number of studies have indicated that cells tend to attach better to hydrophilic surfaces than to hydrophobic surfaces [382–384]. Contradictory reports argue that cells adhere better on intermediate hydrophobic surfaces with contact angles of around 70° [385–387]. These conflicting results may be due to the use of different materials, different surface topographies and especially different surface chemistry applied to alter the wetting behavior.

Grafting with self assembled monolayers (SAM) involves the attachment of specific functional groups onto the surfaces. Monolayers of organosilanes have been successfully used to tailor material surfaces to obtain control over the molecular composition and the resulting integral properties of the surfaces [388,389]. Several studies have described the effect of surface charge, wettability and topography on protein adsorption and cell behavior by using SAMs with different terminal groups for in vitro assay systems [390–393]. McClary et al. reported that hydrophobic methyl-terminated alkanethiol SAMs on gold induce minimal cell attachment and therefore do not support spreading and further focal contact formation of mouse fibroblasts [394]. Faucheux and coworkers reported on the use of a set of SAMs that were prepared differing in their wettability from hydrophobic to hydrophilic

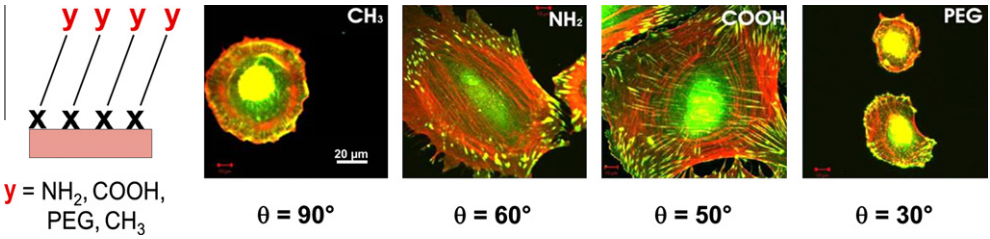


**Fig. 18.** Scanning confocal micrographs of human fibroblasts attached to SAMs with different tail groups (X = $CH_3$, $NH_2$, COOH, PEG) after incubation for 2 h. The cells were double labeled for vinculin (green) and F actin (red). In this example the monolayers were attached on Au surfaces. $\theta$ represents the approximated water-contact angle of the modified surfaces (adapted from [385]).

surfaces by the adsorption of alkylsilanes onto glass or silicon. Primarily the SAMs varied in the type of functional end groups, such as methyl ($CH_3$), amine ($NH_2$), carboxyl (COOH), hydroxyl (OH), and polyethylene glycol (PEG). It was reported that the starting conditions seem to be very important for the subsequent reactions of cells [385]. Fig. 18 illustrates an example of cell spreading on different functionalized SAMs.

One of the key effects of the different terminations is associated to the different surface wetting properties (for example the contact angle varies from 90° to 30° when different terminations are used).

Considering the role of electrostatic interactions in many biological events, charged surfaces have been proposed as being conducive to tissue integration [395,396]. Contradictory results with charged materials in bone have been reported; indeed both positively [395] and negatively [396] charged surfaces were observed to promote bone formation.

Ion implantation involves the bombardment of highly energetic ionic species to the surface of a material. The ions penetrate the surface and thereby bring significant changes in chemical composition and structure at the near surface region. This further may improve wear resistance, corrosion resistance and biocompatibility of implant materials [397,398].

## 5. Functionalization of implant surfaces

Alternatively to surface topography modifications and physicochemical treatments of surfaces to achieve an enhanced bone implant interface formation, biochemical methods offer an alternative path. These functionalization approaches require a deeper understanding of biology and biochemistry of the host tissue at the interface in terms of mechanisms by which cells adhere to surfaces [399], the role of biomolecules, functional peptide sequences and extracellular matrix proteins in influencing or regulating differentiation and remodeling of bone and tissue [400]. Since Pierschbacher and Ruoslahti found that the Arg–Gly–Asp–Ser (RGDS) sequence constituted the active site of several plasma and extracellular matrix proteins such as fibronectin, vitronectin, type I collagen and osteopontin [401], this peptide was immobilized onto surfaces and succeeded in enhancing cell adhesion remarkably [402]. As a consequence, biochemical surface functionalization methods have been investigated in order to immobilize bio attractive molecules such as proteins, peptides or enzymes onto surfaces in order to induce and directly control specific cell and tissue responses at the implant tissue interface [182]. However, a variety of tissue cells possess the same integrins, and therefore nonspecific attachment of those cells to RGD-modified surfaces is a concern, which has to be overcome to develop functionalized surfaces, modified with cell attachment agents, that are more selective on bone forming cells.

### *5.1. Immobilization approaches for bioactive molecules*

Besides the functionalization of surfaces, not only decorating them with cell adhesive sequences but also by biomolecules that are involved in bone development and fracture healing, has become a

wide open field in current research. Numerous growth factors have been identified and are commonly expressed recombinantly and thus are available. The spectrum of growth factors and their effects on tissue responses are widely spread from mitogenicity (IGF-I, FGF-2 or PDGF-BB) to increasing activity of bone cells (TGF-$\beta$1 which enhances collagen synthesis) to osteoinduction (class of BMPs) [403,404].

Different methods have been introduced to immobilize biomolecules onto implant surfaces (Fig. 19) including physical adsorption (e.g. via van der Waals forces or electrostatically), physical entrapment (e.g. via barrier systems or hydrogels) for further controlled release and covalent immobilization via reactive linker molecules.

Adsorption of biomolecules onto surfaces by simple dipping methods resembles the most straight forward approach. However, this bears the drawback that this method provides only little control over the release kinetics and thus delivery, retention and orientation of the adsorbed molecules are hampered. In general, the driving force for the adhesion and stability of such molecules on the surfaces depends only on weak physisorption (van der Waals forces). External parameters such as micro movement of the implant, pH, temperature and solvent conditions in the host tissue represent important factors. Several studies on the adsorption of bio attractive molecules and their influence on tissue regeneration by adsorption of alkaline phosphatase [405] or delivery of TGF-$\beta$ [406,407] into the tissue implant interface have indicated that such approaches may have enhancing effects on bone formation [408]. A conclusive indication whether such simple surface decoration methods with biomolecules may be sufficient for clinical applications is somewhat doubtful in terms of the weak adhering forces and thus the uncertain control over the release kinetics.

In recent years, not only the adsorption of bio attractive molecules has been studied but also the loading of implant surfaces to either avoid inflammatory reactions of the host tissue or to minimize the risk of an uncontrollable bacterial attack. The key requirement is a decelerated release kinetic and sufficiently high amounts of loaded drugs in order to achieve the desired effects. Miscellaneous approaches have been reported to achieve surfaces that show good adhesion properties, provide a sufficient depot volume and decelerated release kinetics. For example in cardiovascular stents, the effects of electrochemically enhanced etching on stainless steel and thus microstructuring of the surface has been suggested to optimize drug-release from drug eluting stents as surface modification prior loading [409]. Porous biomedical ceramics have been investigated as for this class of materials the open porosity can be tailored as a function of sintering conditions. For example, release of hydrocortisone acetate in methanol solutions has been investigated. It has been proposed that two dimensional relevant pore sizes exist with different degrees of efficiency in the release compared to the dimensions of the pores [410].

More recently the formation of self organized nanoporous surfaces on silicon, aluminum and titanium have gained considerable attention, as those nanostructures possess higher surface areas for adsorption and increased depot volume for drug loading. Porous silicon and silica possess several

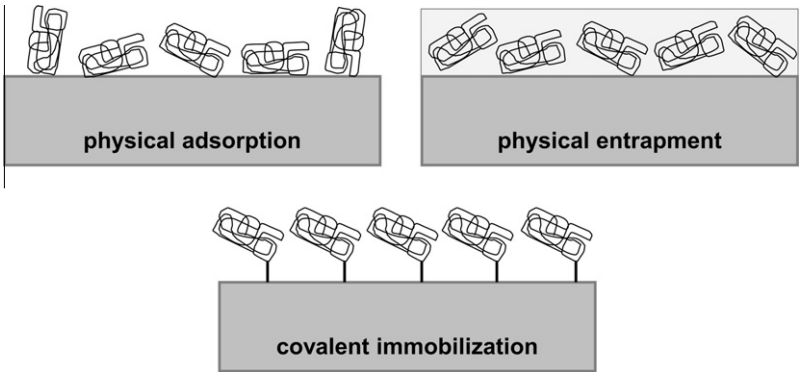


**Fig. 19.** Schematic illustration of different immobilization methods for biomolecules (adapted from [182]) based on physical adsorption, physical entrapment and covalent binding on surfaces.

attractive features, such as stable mesoporous structures, large surface areas, tunable pore size volumes and well-defined surface properties. Such tunable properties are achievable for mesoporous silica materials for hosting molecules of various sizes, shapes, and functionalities [411,412]. Moreover, nanoporous silicon has been shown to exhibit controllable degradation kinetics [413,414]. Besides the conventional loading and release of mesoporous silica it has been shown by using mesoporous silica combined with CdS nanoparticles, that a highly controllable capping and uncapping of the openings can be achieved without any required chemical modification of the molecules of interest. Using such modified mesoporous silica the stimuli-responsive release profiles and the biocompatibility with neuroglial cells in vitro under delivery of vancomycin and adenosine triphosphate encapsulated inside has been reported [412].

Anodically grown nanoporous alumina structures as drug eluting substrates have been described as potential nanoporous coatings on biomedical implant materials [291,415]. However, nanoporous alumina membranes have been synthesized and modified for the use as drug delivery scaffolds [416,417]. In this context nanoporous alumina membranes, with controlled pore sizes, were described as nanoporous scaffolds for the encapsulation of therapeutic cells by investigating the diffusion behavior of glucose, immunoglobulin G (IgG) and insulin. Furthermore, the functionality and viability of encapsulated cells (MIN6) is described and thus a potential alternative encapsulation strategy for the treatment of diabetes [418].

In this context the use of $TiO_2$ nanotube coatings grown anodically on titanium substrates was reported as host for the loading and local delivery of drugs or growth factors on implants at the site of implantation [419]. By altering the dimensions of the nanotubes it has been reported to control the load of different amounts of drugs and the release rates [420]. It has been shown that the loading with gentamicin effectively minimizes initial bacterial adhesion and at the same time supports cell adhesion and proliferation of MCT3T osteoblast precursor cells when compared to titanium surfaces [420]. In another study comparable observations were reported by investigation of loading and release kinetics of bovine serum albumin (BSA) and lysozyme (LYS) as model proteins on $TiO_2$ nanotube arrays [419].

However, even though the release kinetics in the described cases using $TiO_2$ nanotubes have been shown to provide a smart tool for the local drug release on titanium based implant materials, all in all this method shows somewhat unsatisfying results concerning the release kinetics. Therefore a smart encapsulation of biomolecules into $TiO_2$ nanotube coatings with highly controllable release kinetics and higher controllability of the time point of drug release after implantation has been investigated and reported.

The fabrication of amphiphilic $TiO_2$ nanotubular structures that provide a highly controllable drug release system based on a hydrophobic cap (assembly of monolayers with hydrophobic chains) on hydrophilic $TiO_2$ nanotubes has been shown [421]. Moreover, this hydrophobic cap prevents uncontrolled leaching of the hydrophilic drug into an aqueous environment and can be removed by exploiting the photocatalytic nature of $TiO_2$ for UV induced chain scission of attached organic monolayers. By this method the cap is removed and a highly controlled release of drugs can be achieved (Fig. 20).

Furthermore, chain scission induced release from $TiO_2$ surfaces can be triggered not only by UV light but also by suitable X-ray radiation which is important in view of in vivo applications [422]. Additionally to the controlled drug release from surfaces, it has been demonstrated that the fabrication of $TiO_2$ nanotube bundles, that were prior coated with magnetic nanoparticles, can be magnetically guided in three dimensions and used as site-selective drug delivery systems under a directed magnetic field and released also by photo induction [423].

Another strategy for controlled drug release from surfaces is the physical entrapment of biomolecules, where these molecules are retained by a barrier but not chemically bound to it, which makes it a universal technique as it uses extremely mild conditions. This approach bears an attractive method as cell and tissue responses depend on the duration of exposure and concentration of biomolecules, thus it can be used to control release kinetics of biomolecules. Coatings incorporating biomolecules are being explored for delivering biomolecules to the tissue–implant interface by diffusion through or degradation of polymer-based matrices or reservoir systems [424]. Thus, biomolecule release from the implant surface may be controllable, which makes it an attractive approach for the immobilization of bone growth factors. Principally, delivering of biomolecules into the implant interface may be

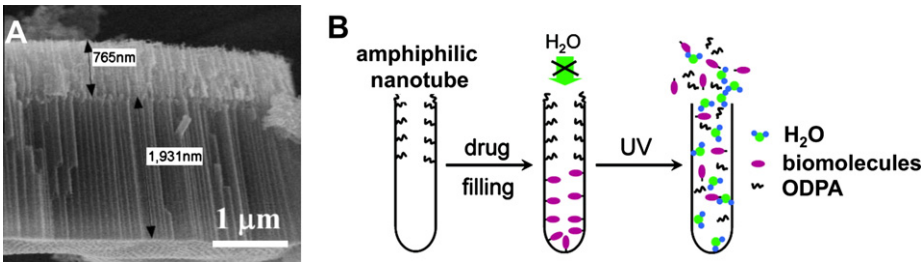


**Fig. 20.** Amphiphilic $TiO_2$ nanotube arrays are fabricated by a two-step anodization procedure combined with hydrophobic monolayers (ODPA, octadecylphosphonic acid). SEM cross-sectional image of the first and the second nanotube layer (A). These tubes can be used as biomolecular carriers, where the outer hydrophobic barrier provides an efficient cap against drug leaching. By utilizing the photocatalytic ability of $TiO_2$, a precisely controlled removal of the cap and a highly controlled release of the loaded drugs can be proceed (B) [421].

carried out by incorporating them into coatings made of materials such as degradable poly (D,L-lactide) (PDLLA) [425] or poly (lactide-co-glycolide) (PLGA) [426,427] or non-biodegradable hydrophobic ethylene vinyl acetate (EVAc) [428] among the coatings being developed. Biodegradable polymeric coatings can be used to release biomolecules for long periods, for example using PLGA as biodegradable carrier and gentamicin as antibiotic [427]. However, there is no overall evidence that perpetual release is required for optimal implant integration.

Collagen coatings have intensively been investigated as they possess the ability to mimic the bone matrix conditions due to their naturally derived origin [429,430]. Moreover, collagen coatings for the incorporation of biomolecules have been investigated and shown a strong ability for cooperative interactions between growth factors such as the class of BMPs [431–433]. In addition, collagen coatings are turned over in vivo and replaced with new tissue during the healing response. Besides the use of organic coatings, in the case of orthopedic implants, bone cements can be used as medium for delivery of bioactive agents to the bone–implant interface and for example loaded with antibiotics [434,435]. However, there are several shortcomings to these proposed localized drug-delivery techniques, including limited chemical stability, local inflammatory reactions due to material composition, and lack of controlled-release kinetics from the coatings. For more detailed information on the drug loading and elution, especially in the field of cardiovascular stents, the readers are referred to following Refs. [424,436].

The covalent binding of biomolecules to surfaces is an alternate way of delivery of such bio promoting molecules to the interface between the host tissue and the implant. In comparison to the above shown approaches, via adsorption or matrix entrapment for surface functionalization, this method is in principal more complex. In contrast to biomolecule adsorption and entrapment, molecules being covalently bound to the surface have some advantages based on the very high loading capabilities and the relatively low-loss rates. Biomolecules being immobilized onto implant surfaces need to interact with the surrounding host tissue for a certain period of time to fully activate cellular responses. Therefore, concentrations immobilized on such surfaces must exceed the threshold levels for cellular activity [182]. However, it has been demonstrated exemplarily, that the biological activity of chemically surface bond insulin and transferrin shows comparable or even accelerated activities than that of soluted ones when investigated with fibroblast cells [437,438]. This effect of enhanced cell growth in vitro on such modified substrates to that observed in the presence of free or simply adsorbed biomolecules has been explained by higher local concentrations and essentially their permanent attachment [439].

The goal of covalent immobilization on hard tissue implants is to induce specific tissue responses by immobilization of selected biomolecules onto the surfaces. For example, protein coupling strategies have been used to manufacture antithrombogenic materials by immobilizing thrombomodulin onto hydrolyzed surfaces [440,441], and related biologically active materials have also been obtained by linking heparin to surfaces bearing amino groups [442]. For example, immobilization of RGD containing peptides has received significant interest because RGD has been identified as the essential

sequence in mediating cell adhesion in many extracellular matrix proteins such as fibronectin and vitronectin [443]. However, RGD containing peptides of different sequences and conformations have been widely immobilized onto biomaterials using surface functional groups [444,445]. In particular, implants based on metals, used for the replacement of hard tissue, do not possess such functional groups needed for the covalent immobilization of biomolecules for most of the binding strategies. However, the passive oxide films on the metals possess in aqueous environments surface hydroxyl groups that provide binding locations for self assembled monolayers (SAMs) and other functionalization [446]. An attachment of organic molecules to inorganic surfaces involves usually the deposition of self assembled monolayers in order to derivatize such surfaces with reactive groups (such as amino groups by coupling of 3-aminopropyltriethoxysilane) [447,448]. Biomolecules then can conjugate to those chemically modified surfaces by reacting with these groups. It has been reported that the biological activity of a surface bound biomolecule can be retained for several days in a simulated physiological environment depending on the substrate and used self assembled monolayer and further the experimental conditions [448]. Moreover, increasing the distance between bound protein and the substrate, as apparent with the presence of self assembled monolayers, has been shown to have a further beneficial effect on cell growth [449].

A variety of immobilizing techniques for the covalent binding of biomolecules onto solid supports for various applications have been explored. In the following paragraph an overview on the most used functionalization chemistries will be given.

### 5.2. Overview on functionalization chemistry

A key technique to combine inorganic materials with organic matter is the use of self-assembled monolayers. The principle of this approach is considerably simple as outlined in Fig. 21a. A bifunctional molecule consisting of a head group that is able to interact strongly with a metal, oxide or polymer, in the ideal case arranges itself on the surface of the material.

Typical molecules that tend to self-organize on surfaces consist of a polar head group such as (–SH, $–NH_2$, –COOH) that may bind to charged surfaces or at least interact by van der Waals forces. In such monolayers the driving force for self-assembly is not only the polar interaction of the head group with the substrate but also the non-polar interaction between the hydrocarbon chains that leads to the parallel alignment of the individual chains.

If the head groups are only interacting with the substrate by comparably weak van der Waals forces or other weak interactions, the molecules still show surface mobility at room temperature (such as

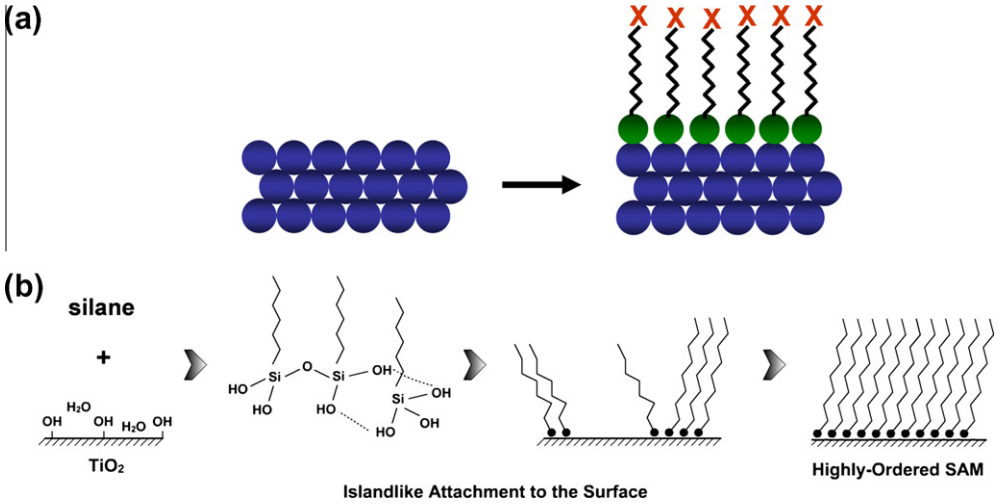


**Fig. 21.** Attachment of self-assembled monolayers to a substrate with variable functionalities (a). Schematic illustration of the attachment of silanes to hydroxide terminated surfaces (b) [459].

thiols on gold), i.e. molecules can move to a next adsorption site. A much stronger linkage to the substrate can be obtained if true surface reactions are used, i.e. a covalent bond between the head group and the substrate is formed. Typical examples for this type of reaction are silanes or silanoles that are attached (grafted) to oxide surfaces by a condensation reaction (splitting off small molecules such as $H_2O$ or HCl as indicated in Fig. 21b). Another typical reaction of this covalent scheme is photo induced alkene or alkine attachment on silicon surfaces.

In many cases important is, however, that in order to link a desired functionality to a surface such monolayers typically carry at their tail (X) a reactive group that can be modified by suitable linking reactions.

However, already by a variation of the termination (X) in polarity of the group (X = $CH_3$, PEG, $NH_2$, COOH, etc.) various degrees of surface energies can be established; in other words for examples the wettability of the surface can be adjusted over a wide range of conditions [450] leading to drastical changes in cell responses under in vitro conditions [385].

Thus, the controlled continuous deposition of self-assembled monolayers enables the generation of molecular gradients on solid surfaces. In principle it has been shown that for different purposes, the same functional groups can be exploited to immobilize biomolecules of interest onto the surface. Utilizing carboxyl or amine terminations to functionalize surfaces has been described as most common paths.

Many commonly used silanes show the ability to hydrolyze into multiple silanol groups, thus, they bear the risk of forming multilayers via Si–OH condensation if the silanization medium contains even low levels of water [450,451]. This may result in an impaired controllability of important properties of the immobilized biomolecules like uniformity, orientation and surface density [452]. Self-assembly of phosphonic acids has been introduced as alternatively immobilization routes on metallic surfaces [453–457]. Advantages of these monolayers compared to silanes can be found at higher hydrolytic stability under physiological conditions which is especially important for coating medical devices [458–460].

Various methods for the covalent immobilization of biomolecules onto biomedical material surfaces have been developed. Common for all is the need of a linker molecule that binds covalently onto the surface and that shows at the same time the ability to bind covalently biomolecules either specifically, for example a free thiol group of a terminal cysteine of the biomolecule, or unspecifically like a free amino group.

In principle the binding of biomolecules is simple but as a fundamental pre-condition the surfaces must provide reactive groups (e.g. –OH, $–NH_2$, –COOH) for the subsequent immobilization steps. Most of the used biomedical materials used in hard tissue replacements such as metals (i.e. surface oxide layers), ceramics or polymers do possess surface terminations as required. Moreover, in case of metal based materials surface oxide layers usually possess hydroxyl groups under wet environmental conditions.

In Fig. 22 a "construction kit" for the covalent immobilization on hydroxyl terminated surfaces is given. However, depending on the linker molecule used, a direct covalent binding to the hydroxyl terminated surface is applicable and then further coupling with biomolecules can be performed. More commonly the chemical immobilization of biomolecules is performed by using the described self assembled monolayers (based on silanes, siloxanes, phosphonic acids or thiols after prior coating with gold) for the tailoring of any desired surface termination (i.e. –OH, $–NH_2$, –COOH). Moreover, the termination of the self assembled monolayer is defined by the biomolecule and furthermore on the linker molecule used for the immobilization. Besides the free selection of the surface termination, such monolayers may also act as spacer groups and thus can provide greater steric freedom and a higher specific activity for the immobilized biomolecules [449].

In principle the main aspect for the successful covalent grafting of biomolecules onto surfaces is determined by the nature of the biomolecule itself. That means that composition and conformation of the biomolecule need to be studied and therefore either a specific binding or an unspecific binding path has to be considered. For example, for the grafting of peptides, such as RGD sequences, maleimide chemistry is commonly involved for the specific binding of a cysteine residue of the peptide sequence. In contrary to this, for example, regarding BMP-2 (bone morphogenic protein 2) all cysteine residues of the monomer are engaged in intramolecular and intermolecular disulfide bonds. Therefore, no

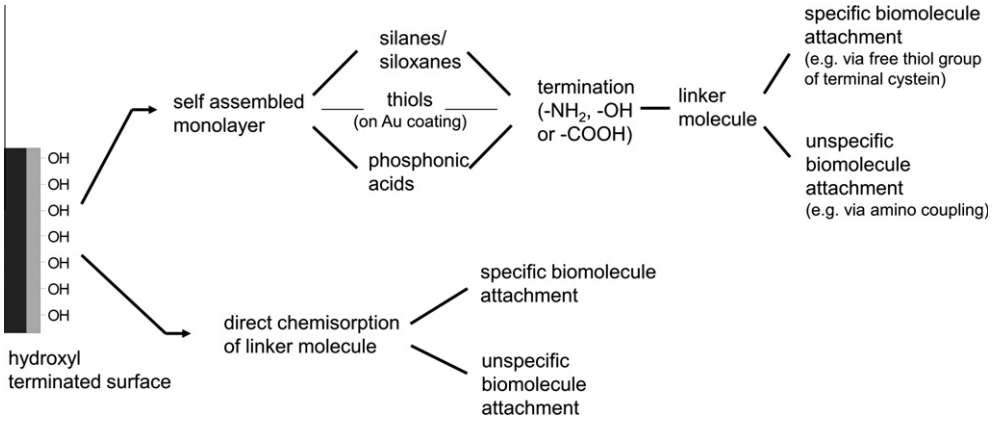


**Fig. 22.** Construction kit for the covalent immobilization of biomolecules onto hydroxyl terminated surfaces of biomedical materials.

residue cysteine is available for this type of maleimide binding approach and alternative coupling strategies need to be considered. However, by employing an unspecific binding to any available amino group of the protein, using for example carbonyldiimidazole chemistry, a successful binding to titanium surfaces has been shown [456,461]. However, a main objective in covalent grafting of biomolecules to surfaces is to preserve the biological activity of the bound molecule (e.g. peptides, proteins, antibodies, enzymes, polysaccharides, DNA). Therefore, a specific linking to a certain end group such as the thiol in cysteine in the RGDC (Arg–Gly–Asp–Cys) peptide sequence is preferable. In the following, examples on the covalent immobilization of biomolecules in respect to their chemical nature will be exemplarily presented.

For the covalent grafting of thiol specific (e.g. cysteine) molecules onto oxide surfaces the use of heterobifunctional cross linkers for coupling of peptides on primary attached SAMs with amine

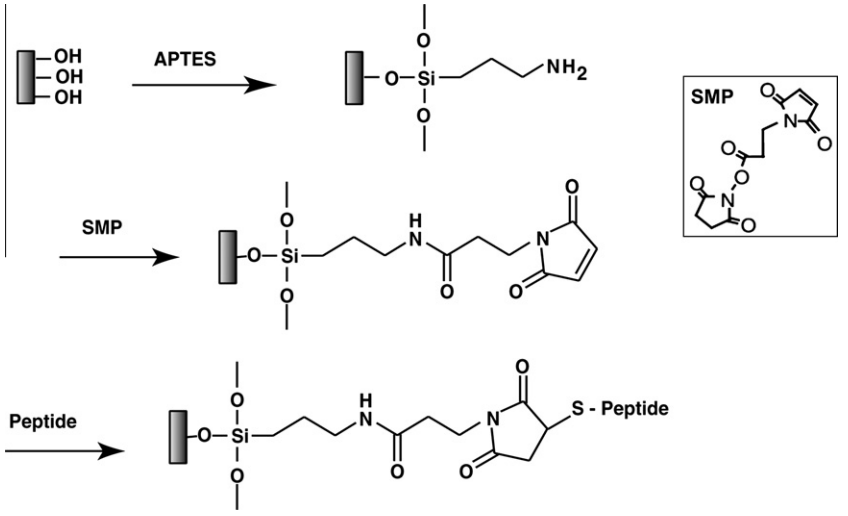


**Fig. 23.** Silanization of an oxide surface with 3-aminopropyltriethoxylsilane (APTES) resulting in a surface with terminal amino groups. Further reaction with a heterobifunctional cross linker, N-succinimidyl-3-maleimidopropionate (SMP) resulting in a surface with maleimide termination. Covalent immobilization of peptides with a cysteine thiol group (–SH) to the maleimide group (adapted from [462]).

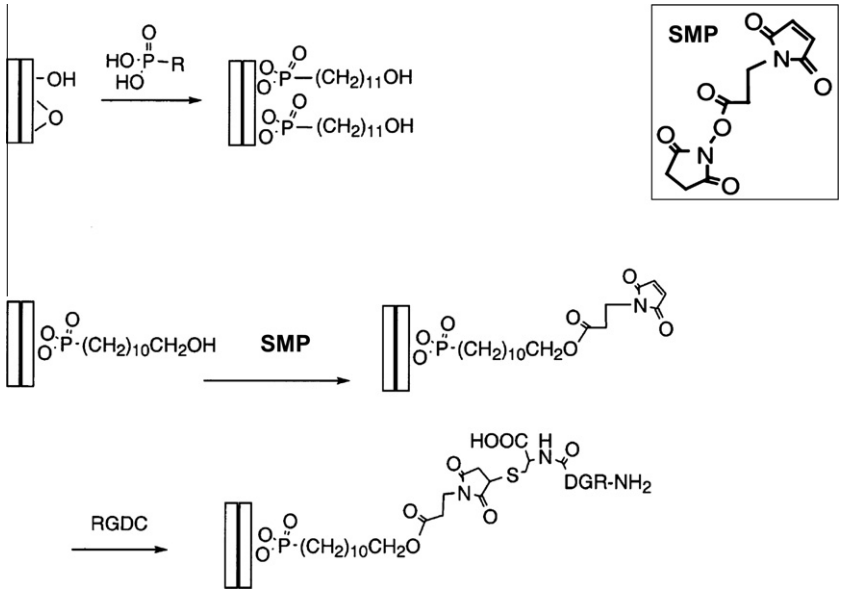


**Fig. 24.** Self-assembly of hydroxyl terminated alkylphosphonic acid and further cross linking with SMP to achieve maleimide functionalization for specific thiol binding (e.g. cysteine) (adapted from [465]).

termination has been reported. Therefore a three step immobilization strategy is commonly utilized to graft those biomolecules on originally hydroxyl terminated surfaces (Fig. 23). In the first step of the synthesis the chemisorption of an amino functional self assembled monolayer (e.g. 3-aminopropylsiloxane) to a hydroxyl terminated oxide surface is carried out [462–466]. In a further step the modification of the terminal amine with a heterobifunctional cross linker molecule is applied to preserve maleimide functional surfaces. As shown in Fig. 23, biomolecules with available thiols can then be coupled to such maleimide terminated substrates either in aqueous and in non-aqueous environments.

The schematic route for the synthetization given in Fig. 23 enables exemplarily N-succinimidyl-3-maleimidopropionate (SMP) as heterobifunctional cross linker and shows that biomolecules can be covalently linked to the substrate via a free thiol group present. Thus, allowing the rest of the immobilized biomolecule to freely interact with the surrounding environment. This functionalization technique has a high flexibility, in the sense that it allows the attachment of any suitable biomolecule having a chemically accessible thiol group. It has been shown that the maleimide group can react with the free thiol group of peptide sequences (i.e. with cysteine of RGDC) [451,466,467] or the mercapto group of cyclo-DfKRG [463].

It has been demonstrated that SMP is also valuable for binding to hydroxyl terminations retaining the described maleimide functionalization for specific binding with free thiols or mercapto groups. Moreover, phosphonic acids with hydroxyl termination (e.g. 11-hydroxyundecylphosphonic acid) have been investigated as monolayers as these acids have been reported to possess a higher stability against hydrolysis [459] and as spacer molecules to sustain steric conformation of the immobilized biomolecules (Fig. 24).

Other routes for specific binding of biomolecules to surfaces via free thiol groups have been demonstrated. For example, the class of maleimide-activated surfaces that enable the grafting of molecules with a free thiol (e.g. cysteine) was created by coupling for example sulfo-SMCC (sulfosuccinimidyl 4-(N-maleimidomethyl) cyclohexane-1-carboxylate) to the terminal amine group of an aminofunctional organosilane (N-(2-aminoethyl)-3-aminopropyl-trimethoxysilane) that was chemisorbed to an oxide surface before [468], as shown in the reaction scheme in Fig. 25.

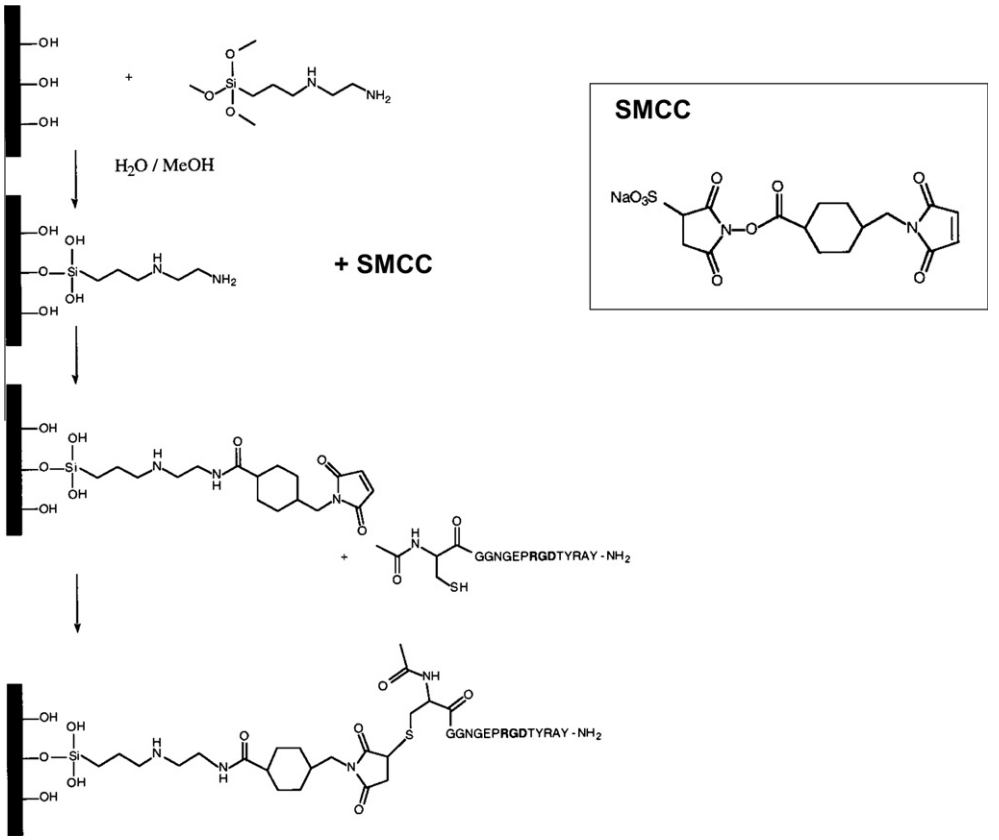


**Fig. 25.** Self-assembly of aminisilane and further cross linking with sulfosuccinimidyl 4-(N-maleimidomethyl) cyclohexane-1-carboxylate (sulfo-SMCC) to achieve maleimide functionalization for specific thiol binding (e.g. cysteine) (adapted from [468]).

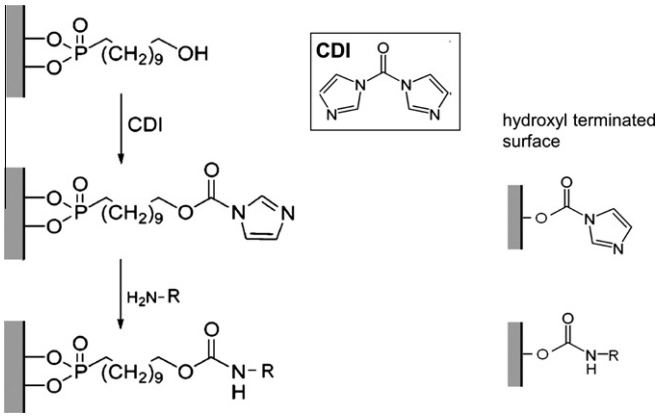


**Fig. 26.** Self-assembly of 11-hydroxy-undecylphosphonic acid and further cross linking with 1,1-carbonyldiimidazole (CDI) or direct activation via CDI in case of hydroxyl terminated surfaces to achieve functionalization for unspecific amino binding (adapted from [456,461]).

Other work used a heterobifunctional cross-linker N-succinimidyl 6-maleimidocaproate (EMCS) to produce oriented metalloprotein nanostructures on silicon wafers modified with an amino-terminated silane. The synthetic route results in more hydrolytically stable maleimide-terminated surfaces prior to the coupling of proteins with oriented thiol-containing cysteine residues [469].

According to the reaction scheme in Fig. 25, Xiao et al. employed a poly (3-aminopropyl) siloxane and a series of heterobifunctional cross-linkers to conjugate cysteine-containing peptides to sputter-deposited titanium films [451,467]. Therefore, the free primary amino groups were linked to three different hetero-cross-linkers, N-succinimidyl-6-maleimidylhexanoate (EMCS), N-succinimidyl-3-maleimidylpropionate (SMP) and N-succinimidyl trans-4-(maleimidylmethyl) cyclohexane-1-carboxylate (SMCC), and compared the results. On the resulting terminal-maleimide surfaces different cell-adhesive peptides could be immobilized. From independent quantitative analysis, an approximate coverage of 0.2–0.4 peptides/nm$^2$ was found [451]. Thiol specific coupling strategies enable accurate construction of model molecular systems with a wide range of surface densities, which can be used to study molecular mechanics and dynamics of such modified surfaces [468] and furthermore the effect of ligand surface density on biological activity [470].

The presented immobilization schemes and methodologies that have been introduced above are based on specific binding via a free thiol group (e.g. cysteine) of biomolecules to surfaces. However, specific immobilization of biomolecules is determined to some extent by the chemical nature of the protein, peptide or enzyme. That means, if for example no free thiol group is accessible, other immobilization routes need to be employed. Examples for unspecific binding routes, targeting for example free amino groups, will be introduced in the following.

Fig. 26 shows an example of a reaction scheme for an unspecific binding approach via binding to free aminogroups of the biomolecules. Carbonyldiimidazole (CDI) chemistry is a commonly used approach to binding to hydroxyl terminated surfaces as well as to free aminogroups belonging to any biomolecule [456,461].

The use of CDI chemistry was investigated as method to bind proteins such as BMP-2 to metal surfaces. The shown reaction scheme in Fig. 26 uses the immobilization of (11-hydroxyundecyl) phosphonic acid to the metal surface. Such surfaces were then further activated for protein binding with carbonyldiimidazole chemistry. The reactivity of these surfaces was tested either with fluorine-tagged molecules or BMP-2 by XPS, ToF-SIMS and ELISA to characterize the chemistry and structure of each surface modification step [456,461,471]. Coupling of BMP-2 and EGF via CDI to anodically grown $TiO_2$ nanotube layers using either a (11-hydroxyundecyl) phosphonic acid as spacer, or direct coupling onto the hydroxylated surfaces, showed no significant beneficial effect on the protein activity of the spacing monolayer [461]. Moreover the conservation of the biological activity of surface bound biomolecules was demonstrated in vitro with mesenchymal stem cells on $TiO_2$ nanotube layers [461,471].

In a further work the influence of different reaction times and concentrations of surface activator CDI on the immobilization of EGF was investigated. It could be shown with XPS and ELISA that the concentration of immobilized EGF increases with the increase of CDI concentration. Immobilized EGF in SAMs was shown to be able to phosphorilate EGFR, demonstrating the biofunctionality of the surfaces [472]. Furthermore, it has been demonstrated by using CDI chemistry that other ECM proteins such as laminin can be covalently linked to agarose hydrogels in a manner that retains their biological function, thus providing biomaterials and drug delivery tools to mimic the strategy of developing and regenerating fibers to enhance neurite extension [473]. Other workers proved the use of CDI to couple lipids onto hydroxyl terminated surfaces. XPS and ToF-SIMS investigations proved the successful chemical coupling of the lipid 1,2-dimyristoyl-sn-glycero-3-phosphoethanolamine (DMPE) to a poly (hydroxyethyl methacrylate) (pHEMA) substrate and that the process enables the retention of the lipid at the interface under harsh conditions [474].

The shown surface activation using CDI chemistry is related to hydroxyl terminations. Other approaches have been introduced to facilitate the covalent immobilization of biomolecules with other surface terminations.

The use of N-hydroxysuccinimide (NHS) has been described in literature as an alternative surface activator. NHS binds unspecifically to free amino groups of biomolecules as shown above, but needs carboxyl groups as reactive surface termination (e.g. self assembled monolayers or polymer surfaces). Fig. 27 shows a typical reaction scheme for the activation of a carboxyl terminated surface. In the

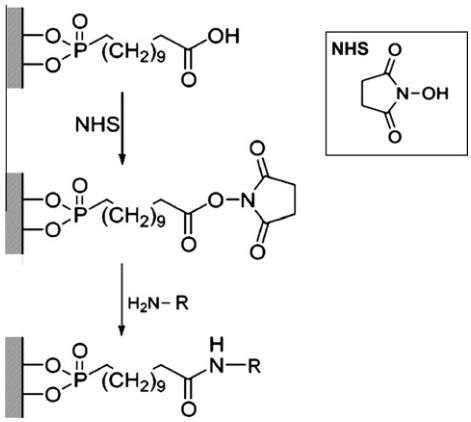


**Fig. 27.** Self-assembly of (12-carboxydodecyl) phosphonic acid and further cross linking with N-hydroxysuccinimide (NHS) to achieve functionalization for unspecific amino binding (adapted from [456]).

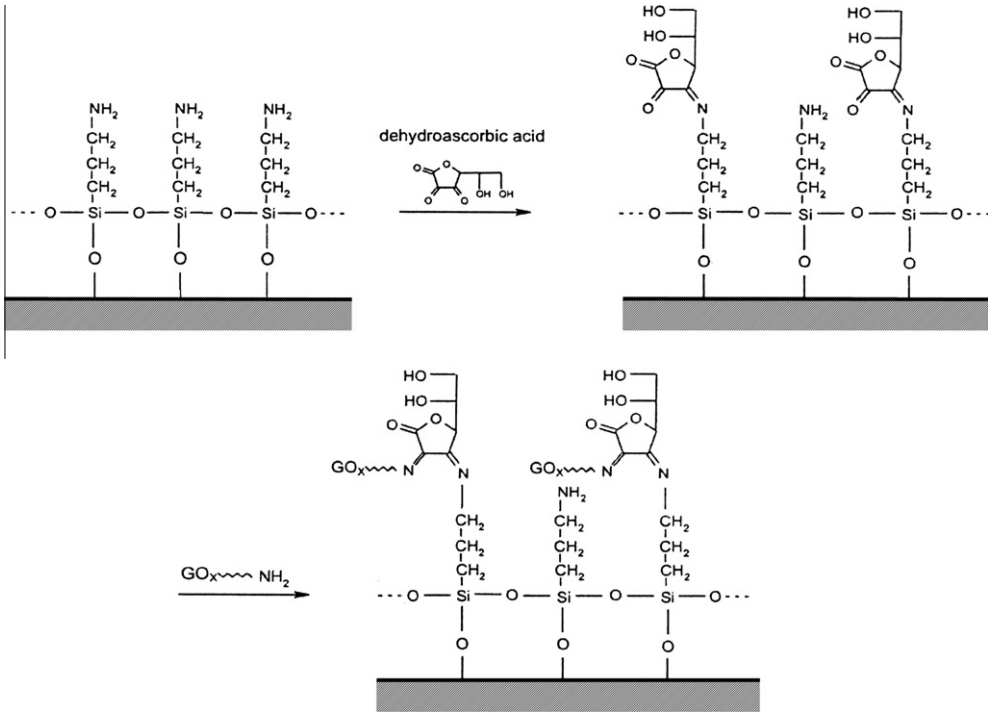


**Fig. 28.** Silanization of an oxide surface with 3-aminopropyltriethoxylsilane resulting in a surface with terminal amino groups. Further reaction with dehydroascorbic acid to achieve functionalization for unspecific amino binding of glucose–oxidase (adapted from [476]).

shown work binding of biomolecules to titanium surfaces was investigated involving the use of a stable phosphonic acid monolayer with carboxyl termination ((12-carboxydodecyl) phosphonic acid).

A method for enzyme-immobilization reaction by means of L-ascorbic acid (ASA) is described using $NH_2$ polymers based on cellulose or poly (vinyl alcohol) with the example of oxidoreductase enzymes.

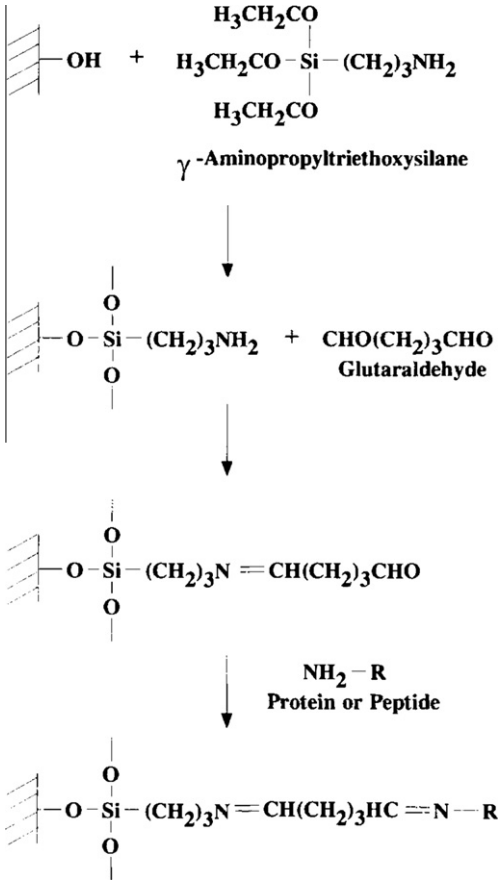


**Fig. 29.** Silanization of an oxide surface with 3-aminopropyltriethoxylsilane resulting in surfaces with terminal amino groups. Further reaction with glutaraldehyde to achieve functionalization for unspecific amino binding of any biomolecule with free amino groups (adapted from [477]).

In this way, enzyme proteins such as glucose oxidase (GOD), glutamate oxidase, lactate oxidase, urate oxidase and peroxidase can be covalently fixed with a high surface loading to ultrathin and transparent $NH_2$-polymer films if their surfaces are previously treated with an ASA solution in DMSO. ASA then obviously reacts like a diketo compound with amino groups of the $NH_2$-polymer film and enzyme protein, forming dehydroascorbic acid derivatives with neighboring Schiff's-base structures. In a subsequent fragmentation reaction, the latter presumably form stable oxalic acid diamide derivatives as coupling structures between enzyme protein and $NH_2$-terminated surfaces [475].

However, Oliveira et al. transferred this binding approach to metal oxide surfaces by silanization of titanium oxide surfaces with 3-aminopropyltriethoxylsilane. The presence of immobilized enzymes on titanium dioxide layers which were chemically or electrochemically generated with possible application as chemical sensors and biosensors. With such modified surface terminations glucose oxidase (GOx) and horseradish peroxidase (HRP) were immobilized by the ascorbic acid route as shown in Fig. 28 [476].

In a further work Song et al. transferred the described approach to anodic nanotubular $TiO_2$ nanotube layers by immobilizing horseradish peroxidase into such porous surface structures [421].

Another route for unspecific immobilization of biomolecules has been described by employing glutaraldehyde as linker. Therefore, amino termitated surfaces are a pre-condition. Fig. 29 shows a

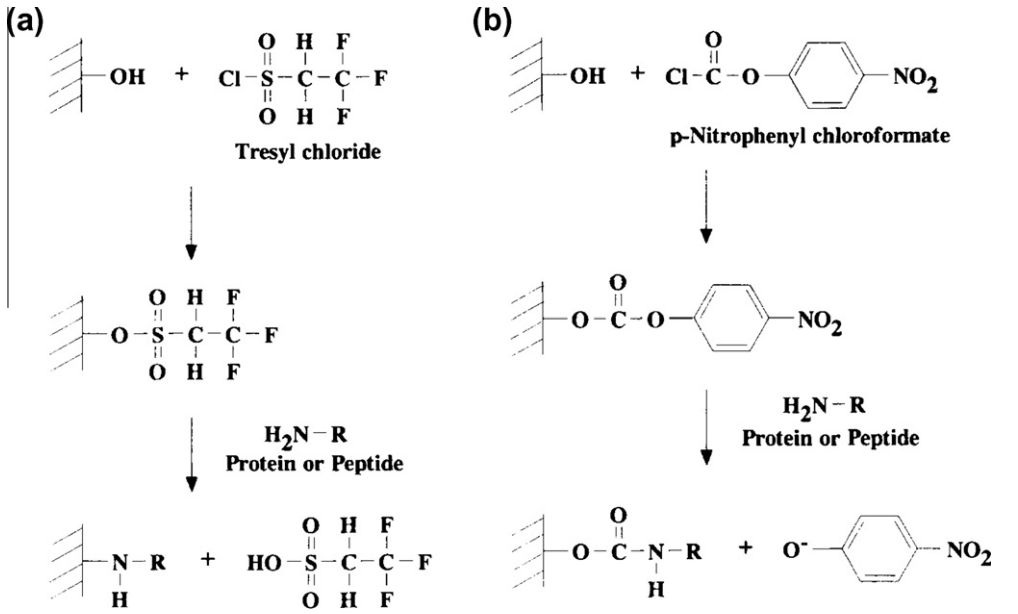


**Fig. 30.** Illustrations of two immobilization schemes tresyl chloride (a) and p-Nitrophenyl chloroformate (p-NPC) (b) for unspecific amino binding of biomolecules with free amino groups (adapted from [477]).

reaction scheme where, via silinazation comparable to before described immobilization routes, has been applied to a hydroxyl terminated oxide surface. Thus, having an amino terminated surface glutaraldehyde can act as activator of the surface by binding (e.g. networking) to amino groups of either the surface or the desired biomolecule [477].

However, the described method is relatively hard to control. Several investigations on the successful immobilization of biomolecules retaining their biological activity have been reported. Proteins such as fibronectin and albumin were covalently coupled to the silane complex with glutaraldehyde without affecting their activity [446,478]. Comparable studies were performed for the immobilization of enzymes such as trypsin to metal oxide surfaces via the described route [448].

Some more exotic linker systems have been described in literature such as tresyl chloride and chloroformates that allow the binding to hydroxyl terminated surfaces and further to free amino groups of biomolecules, similar to the carbonyldiimidazole chemistry routes described above. Here, tresyl chloride (2,2,2-trifluoroethanesulphonyl chloride) interacts with surface hydroxyl species to form tresylate leaving groups that can be displaced by nucleophiles, such as amines and thiols. This method does not leave a spacer arm between protein and substrate (Fig. 30a). However, chloroformate techniques such as p-Nitrophenyl chloroformate (p-NPC) generate reactive carbonates on the substrate which react with nucleophiles, such as amino groups on proteins. This technique results in a urethane linkage with a one atom spacer arm between the biomolecule and substrate (Fig. 30b) [477].

For a more insight information on the immobilization of biomolecules onto biomedical implant surfaces the readers are referred to Ref. [479].

## References

[1] Ratner BD. Biomaterials science: an introduction to materials in medicine. In: Ratner BD, Hoffmann AS, Schoen FJ, Lemons JE, editors. An interdisciplinary endeavour. San Diego: Academic Press; 1996. p. xi, 484 p.
[2] Temenoff JS, Mikos Antonios G. Biomaterials: the intersection of biology and materials science. Upper Saddle River, N.J.: Pearson/Prentice Hall; 2008.
[3] Williams DF. Consensus and definitions in biomaterials. In: de Potter C, de Lange K, de Groot K, Lee AJC, editors. Advances in biomaterials. Amsterdam: Elsevier; 1987. p. 11–6.

[4] Ratner BD. A perspective on titanium biocompatibility. In: Brunette DM, Tengvall P, Textor M, Thomson P, editors. Titanium in medicine |material science, surface science, engineering, biological responses and medical applications. Berlin: Springer; 2001. p. 2–12.
[5] Wintermantel Erich, Ha Suk-Woo. Medizintechnik mit biokompatiblen Werkstoffen und Verfahren. 3, überarb. und erw. Aufl. ed. Berlin [u.a.]: Springer; 2002.
[6] Buschow KHJ, Cahn RW, Flemings MC, Ilschner B, Kramer EJ, Mahajan S. Encyclopedia of materials. In: Buschow Kurt H. Jürgen, editor. Online-Ausg. ed. Amsterdam [u.a.]; Norwich, NY: Elsevier; Knovel [Online-Anbieter]; 2001.
[7] Schenk RK. Bone response to grafts and implants. In: Lin OCC, Chao EY, editors. Perspectives on biomaterials: proceedings of the 1985 international symposium on biomaterials. Taipei, Taiwan, February 25–27, 1985. Amsterdam; New York New York, NY, USA: Elsevier; Distributors for the US and Canada, Elsevier Science; 1986. p. 121–36.
[8] Tirrell DD. Hierarchical structures in biology as a guide for new materials technology. National research council (US) committee on synthetic hierarchical structures, vol. xii. Nmab; 1994. p. 130.
[9] Hancox NM. Biology of bone. Cambridge Eng.: University Press; 1972.
[10] Currey John D. The mechanical adaptations of bones. Princeton, N.J.: Princeton University Press; 1984.
[11] Lakes R. Materials with structural hierarchy. Nature 1993;361:511–5.
[12] Frasca P, Harper RA, Katz JL. Isolation of single osteons and osteon lamellae. Acta Anat (Basel) 1976;95:122–9.
[13] Enderle John D, Bronzino Joseph D, Blanchard Susan M. Introduction to biomedical engineering. second ed. Amsterdam; Boston: Elsevier Academic Press; 2005.
[14] Hench LL. Bioceramics. J Am Ceram Soc 1998;81:1705–28.
[15] Cao WP, Hench LL. Bioactive materials. Ceram Int 1996;22:493–507.
[16] Hench LL. Bioceramics – from concept to clinic. J Am Ceram Soc 1991;74:1487–510.
[17] Hench LL. An introduction to bioceramics. World Scientific Publishing Cooperation; 1993.
[18] Mark James E. Physical properties of polymers handbook. Woodbury, NY: AIP Press; 1996.
[19] Menges Georg. Werkstoffkunde der Kunststoffe. München: Hanser; 1985.
[20] Williams DF. The toxicology of additives in medical plastics. In: Williams DF, editor. Systemic aspects of biocompatibility. Boca Raton, Fla: CRC Press; 1981. p. 145–57.
[21] Williams DF. The Williams dictionary of biomaterials. Liverpool: Liverpool University Press; 1999.
[22] Davis JR. ASM International. Handbook of materials for medical devices. Materials Park, OH: ASM International; 2003.
[23] Mcgrory BJ, Morrey BF, Cahalan TD, An KN, Cabanela ME. Effect of femoral offset on range of motion and abductor muscle strength after total hip-arthroplasty. J Bone Joint Surg – British Vol 1995;77B:865–9.
[24] Long M, Rack HJ. Titanium alloys in total joint replacement – a materials science perspective. Biomaterials 1998;19:1621–39.
[25] Niinomi M. Fatigue performance and cyto-toxicity of low rigidity titanium alloy, Ti–29Nb–13Ta–4.6Zr. Biomaterials 2003;24:2673–83.
[26] Teoh SH. Fatigue of biomaterials: a review. Int J Fat 2000;22:825–37.
[27] Long M, Crooks R, Rack HJ. High-cycle fatigue performance of solution-treated metastable-$\beta$ titanium alloys. Acta Mater 1999;47:661–9.
[28] Niinomi M. Fatigue characteristics of metallic biomaterials. Int J Fat 2007;29:992–1000.
[29] Pruitt LA. Deformation, yielding, fracture and fatigue behavior of conventional and highly cross-linked ultra high molecular weight polyethylene. Biomaterials 2005;26:905–15.
[30] Semlitsch M, Willert HG. Clinical wear behaviour of ultra-high molecular weight polyethylene cups paired with metal and ceramic ball heads in comparison to metal-on-metal pairings of hip joint replacements. Proc Inst Mech Eng, Part H: J Eng Med 1997;211:73–88.
[31] Park J, Lakes RS. Biomaterials an introduction. Springer; 2007.
[32] Bills P, Blunt L, Jiang X. Development of a technique for accurately determining clinical wear in explanted total hip replacements. Wear 2007;263:1133–7.
[33] Hulbert SF. The use of alumina and zirconia in surgical implants. In: Hench LL, Wilson June, editors. An introduction to bioceramics. Singapore; River Edge, NJ: World Scientific; 1993. p. 25–40.
[34] Dörre E. Problems concerning the industrial production of alumina ceramic components for hip joint prothesis. In: Ravaglioli Antonio, Krajewski A, editors. Istituto di ricerche tecnologiche per la ceramica (Italy), Agenzia Polo Ceramico. Bioceramics and the human body. London; New York New York, NY, USA: Elsevier Applied Science; Sole distributor in the USA and Canada, Elsevier Science Pub. Co.; 1992. p. 454–60.
[35] Hulbert SF. The use of alumina and zirconia in surgical implants. In: Hench LL, Wilson June, editors. An introduction to bioceramics. Singapore; River Edge, NJ: World Scientific; 1993. p. 25–40.
[36] Smith Alison J, Dieppe Paul, Vernon Kelly, Porter Martyn, Blom Ashley W. Failure rates of stemmed metal-on-metal hip replacements: analysis of data from the National Joint Registry of England and Wales. The Lancet 2012;12:60353–5.
[37] Ingham E, Fisher J. Biological reactions to wear debris in total joint replacement. Proc Inst Mech Eng H 2000;214:21–37.
[38] Hernandez-Rodriguez MAL, Mercado-Solis RD, Perez-Unzueta A, Martinez-Delgado DI, Cantu-Sifuentes M. Wear of cast metal–metal pairs for total replacement hip prostheses. Wear 2005;259:958–63.
[39] Wang A, Yue S, Bobyn JD, Chan FW, Medley JB. Surface characterization of metal-on-metal hip implants tested in a hip simulator. Wear 1999;225:708–15.
[40] Affatato S, Goldoni M, Testoni M, Toni A. Mixed oxides prosthetic ceramic ball heads. Part 3: effect of the $ZrO_2$ fraction on the wear of ceramic on ceramic hip joint prostheses. A long-term in vitro wear study. Biomaterials 2001;22:717–23.
[41] Ratner BD, Hoffman AS, Schoen FJ, Lemons JE. Biomaterials science. Amsterdam: Elsevier; 2004.
[42] Leyens C, Peters M. Titanium and titanium alloys. Weinheim: Wiley; 2003.
[43] Williams DF. Biocompatibility of clinical implant materials. Boca Raton, Fla: CRC Press; 1981.
[44] Zhuang LZ, Langer EW. Effects of cooling rate control during the solidification process on the microstructure and mechanical-properties of cast Co–Cr–Mo alloy used for surgical implants. J Mater Sci 1989;24:381–8.
[45] Dobbs HS, Robertson JLM. Heat-treatment of cast Co–Cr–Mo for orthopedic implant use. J Mater Sci 1983;18:391–401.

[46] Vander Sande JB, Coke JR, Wulff J. A transmission electron microscopy study of the mechanisms of strengthening in heat-treated Co–Cr–Mo–C alloys. Metall Trans A 1976;7:389–97.
[47] Niinomi Mitsuo. Recent metallic materials for biomedical applications. Metall Mater Trans A 2002;33:477–86.
[48] Ko YG, Jung WS, Shin DH, Lee CS. Effects of temperature and initial microstructure on the equal channel angular pressing of Ti–6Al–4V alloy. Scripta Mater 2003;48:197–202.
[49] Semiatin SL, Seetharaman V, Weiss I. Flow behavior and globularization kinetics during hot working of Ti–6Al–4V with a colony alpha microstructure. Mater Sci Eng A 1999;263:257–71.
[50] Seshacharyulu T, Medeiros SC, Frazier WG, Prasad YVRK. Hot working of commercial Ti–6Al–4V with an equiaxed $\alpha - \beta$ microstructure: materials modeling considerations. Mater Sci Eng A 2000;284:184–94.
[51] Black J. Does corrosion matter? J Bone Joint Surg – British Vol 1988;70:517–20.
[52] Semlitsch MF, Weber H, Streicher RM, Schon R. Joint replacement components made of hot-forged and surface-treated Ti–6A1–7Nb alloy. Biomaterials 1992;13:781–8.
[53] Borowy KH, Kramer KH. On the properties of a new titanium alloy (TiAl5Fe2.5) as implant material. Titanium Science and Technology. Munich: Deutsche Gesellschaft Fuer Metallkunde e.V; 1995. p. 1381–6.
[54] Steinemann SG. Corrosion of titanium and titanium alloys for surgical implants. Titanium Science and Technology. Munich: Deutsche Gesellschaft Fuer Metallkunde e.V; 1985.
[55] Steinmann SG, European Society for Biomaterials. Corrosion of surgical implants-in vivo and in vitro tests. In: Winter George D, Leray Jean L, Groot Klaas de, editors. Evaluation of biomaterials. Chichester; New York: J. Wiley; 1980. p. 1–34.
[56] Laing PG, Ferguson Jr AB, Hodge ES. Tissue reaction in rabbit muscle exposed to metallic implants. J Biomed Mater Res 1967;1:135–49.
[57] Wang K, Gustavson L, Dumbleton J. The characterization of Ti12Mo6Zr2Fe. A new biocompatible titanium alloy developed for surgical implants. Beta titanium in the 1990s. Warrendale: The Minerals, Metals and Materials Society; 1993. p. 49–60.
[58] Wang K, Gustavson L, Dumbleton J. Low modulus, high strength, biocompatible titanium alloy for medical implants. Titanium science and technology. Warrendale: The Minerals, Metals & Materials Society; 1993. p. 2697–704.
[59] Steinemann SG, Maeusli P-A, Szmukler-Moncler S, Semlitsch M, Pohler O, Hintermann H-E, et al. Beta-titanium alloy for surgical implants. Titanium science and technology. Warrendale: The Minerals, Metals & Materials Society; 1993. p. 2689–96.
[60] Okazaki Y, Ito Y, Ito A, Tateishi T. Effect of alloying elements on mechanical-properties of titanium-alloys for medical implants. Mater Trans Jim 1993;34:1217–22.
[61] Kovacs P, Davidson JA. The electrochemical behavior of a new titanium alloy with superior biocompatibility. Titanium science and technology. Warrendale: The Minerals, Metals& Materials Society; 1993. p. 2705–12.
[62] Mishra AK, Davidson JA, Kovacs P, Poggie RA. Ti13Nb13Zr: a new low modulus, high strength, corrosion resistant near-beta alloy for orthopaedic implants. Beta titanium in the 1990s. Warrendale: The Minerals, Metals& Materials Society; 1993. p. 61–72.
[63] Geetha M, Singh AK, Asokamani R, Gogia AK. Ti based biomaterials, the ultimate choice for orthopaedic implants – a review. Progr Mater Sci 2009;54:397–425.
[64] Niinomi M. Mechanical properties of biomedical titanium alloys. Mater Sci Eng a – Struct Mater Prop Microstruct Process 1998;243:231–6.
[65] Kim JH, Niinomi M, Akahori T. Influence of bone structure on mechanical properties of bovine and swine compact bones. In: Pricm 5: the fifth Pacific rim international conference on advanced materials and processing, Pts 1–5., vol. 475–479; 2005. p. 2407–10.
[66] Christel P, Meunier A, Dorlot JM, Crolet JM, Witvolet J, Sedel L, et al. Biomechanical compatability and design of ceramic implants for orthopedic surgery. In: Ducheyne P, Lemons J, editors. Bioceramics: material characteristics versus in vivo behavior. New York: Acad. Sci; 1988. p. 234. 1988/01/01.
[67] Hulbert SF Bokros IC, Hench LL, Wilson J, Heimke G. Ceramics in clinical applications: past, present, and future. In: Vincenzini P, editor. High tech ceramics: proceedings of the world congress on high tech ceramics, the 6th international meeting on modern ceramics technologies (6th CIMTEC), Milan, Italy, 24–28 June 1986 Materials science monographs. Amsterdam; New York New York, NY, USA: Elsevier; Distributors for the US and Canada, Elsevier Science Pub. Co.; 1987. p. 189–213.
[68] Hench LL, Ceramics Best S. Glasses and glass–ceramics. In: Ratner BD, Hoffman AS, Schoen FJ, Lemons JE, editors. Biomaterials science. An introduction to materials in medicine. Amsterdam: Elsevier; 2004. p. 153–69.
[69] Affatato S, Testoni M, Cacciari GL, Toni A. Mixed oxides prosthetic ceramic ball heads. Part 1: effect of the $ZrO_2$ fraction on the wear of ceramic on polyethylene joints. Biomaterials 1999;20:971–5.
[70] Willmann G, von Chamier W, Pfaff HG, Rack R. Biocompatibility of a new alumina matrix biocomposite AMC. Bioceramics 2000;192-1:569–72.
[71] Dorre E, Dawihl W, Biological Engineering Society. Biomaterials Group, British Ceramic Society, European Society for Biomaterials. Ceramic hip endoprostheses. In: Hastings Garth W, Williams DF, editors. Mechanical properties of biomaterials. Chichester; New York: J. Wiley; 1980. p. 113–27.
[72] Ritter Jr JE, Greenspan DC, Palmer RA, Hench LL. Use of fracture mechanics theory in lifetime predictions for alumina and bioglass-coated alumina. J Biomed Mater Res 1979;13:251–63.
[73] Garvie RC, Urbani C, Kennedy DR, McNeuer JC. Biocompatibility of magnesia-partially stabilized zirconia (Mg-PSZ) ceramics. J Mater Sci 1984;19:3224–8.
[74] Tateishi T, Yunoki H. Research and development of advanced bio-composite materials and application to the artificial hip joint. Bull Mech Eng Lab 1987:1–9.
[75] Streicher RM, Semlitsch M, Schom R. Ceramic surfaces as wear partners for polyethlene. In: Bonfield W, Hastings GW, Tanner KE, editors. Bioceramics 4. London: Butterworth-Heinemann; 1991. p. 281–6.
[76] Streicher RM Semlitsch M, Schom R. Articulation of ceramic surfaces against polyethylene. In: Ravaglioli Antonio, Krajewski A, editors. Bioceramics and the human body. London; New York New York, NY, USA: Elsevier Applied Science; Sole distributor in the USA and Canada, Elsevier Science Pub. Co.; 1992. p. 118–23.

[77] Scott HG. Phase relationships in the zirconia–yttria system. J Mater Sci 1975;10:1527–35.
[78] Butler EP. Transformation-toughened zirconia ceramics. Mater Sci Technol 1985;1:417–32.
[79] Lange FF. Transformation-toughened $ZrO_2$ – correlations between grain-size control and composition in the system $ZrO_2$–$Y_2O_3$. J Am Ceram Soc 1986;69:240–2.
[80] Rack R Pfaff HG. A new ceramic material for orthopaedics. In: Willmann Gerd, editor. Bioceramics in hip joint replacement |proceedings 5th international CeramTec symposium, February 18/19, 2000; 25 tables. Stuttgart: Thieme; 2000. p. 141–5.
[81] Burger W. Umwandlungs und platelet verstärkte Aluminiumoxidmatrixwerkstoffe. Keram Z 1998;50:18–22.
[82] Kaddick C, Pfaff HG. Wear study in the alumina–zirconia system. In: Willmann G, Zweymüller K, editors. Bioceramics in hip joint replacement. Stuttgart: Thieme; 2000. p. 146–50.
[83] Le Geros RZ, Le Geros JP. Dens hydroxyapatite. In: Hench LL, Wilson J, editors. An introduction to bioceramics. Singapore; River Edge, NJ: World Scientific; 1993. p. 139–80.
[84] Best S, Bonfield W, Doyle C. Optimization of toughness in dense ceramics. In: Heimke G, editor. Bioceramics. Cologne: German Ceramic Society; 1990. p. 57–64.
[85] de Groot K, Klein CPAT, Wolke JGC, de Blieck-Hogervorst J. Chemistry of calcium phosphate bioceramics. In: Yamamuro T, Hench LL, Wilson J, editors. Handbook on bioactive ceramics. Boca Raton: CRC Press; 1990.
[86] Ebeling FW, Schirber H, Huberth H, Schlör N. Kunststoffkunde. Würzburg: Vogel; 1988.
[87] Dominghaus Hans. ¬Die Kunststoffe und ihre Eigenschaften. Düsseldorf: VDI; 1988.
[88] Franck Adolf, Biederbick K. Kunststoff-Kompendium. Würzburg: Vogel; 1988.
[89] Jones DW. Materials for fixed and removable phrostodontics. In: Chan RW, Haasen P, Kramer EJ, editors. Materials science and technology. Weinheim: Wiley; 1992. p. 429–57.
[90] Miller Mark D. Review of orthopaedics |Orthopaedics. fifth ed. Saunders; 2008.
[91] Wenz LM, Merritt K, Brown SA, Moet A, Steffee AD. In vitro biocompatibility of polyetheretherketone and polysulfone composites. J Biomed Mater Res 1990;24:207–15.
[92] Williams DF, Mcnamara A, Turner RM. Potential of polyetheretherketone (Peek) and carbon-fiber-reinforced peek in medical applications. J Mater Sci Lett 1987;6:188–90.
[93] Scholes SC, Unsworth A. Wear studies on the likely performance of CFR-PEEK/CoCrMo for use as artificial joint bearing materials. J Mater Sci-Mater Med 2009;20:163–70.
[94] Dhlamini MS, Swart HC, Terblans JJ, Terblanche CJ. A comparative study of the impurity segregation from commercially pure Ti, Ti6Al4V and Ti3Al8V6Cr4Zr4Mo. Mater Sci Eng B: Solid-State Mater Adv Technol 2006;130:210–4.
[95] Gray JE, Norton PR, Griffiths K. Surface modification of a biomedical poly(ether)urethane by a remote air plasma. Appl Surf Sci 2003;217:210–22.
[96] Steiner U, Eiser E, Budkowski A, Fetters LJ, Klein J. Surface segregation and wetting from polymer mixtures. In: Teramoto A, Kobayashi M, Norisuye T, editors. Ordering in macromolecular systems |Proceedings of the OUMS'93, Toyonaka, Osaka, Japan, 3–6 June 1993. Berlin: Springer; 1994. p. 313–22.
[97] Dee KC, Puleo DA, Bizios R. An introduction to tissue biomaterial interactions. Hoboken: Wiley; 2002.
[98] Garbassi F, Morra M, Occhiello E, Barino L, Scordamaglia R. Dynamics of macromolecules – a challenge for surface-analysis. Surf Interf Anal 1989;14:585–9.
[99] Ratner BD, Yoon SC. Polyurethane surfaces: solvent and temperature induced structural rearrangements. In: Andrade Joseph D, editor. Polymer surface dynamics |[proceedings of a topical symposium held at the eighth rocky mountain regional meeting of the American chemical society on June 9, 1986 in Denver, Colo]. New York: Plenum; 1988. p. 137–52.
[100] Somorjai GA. The flexible surface – correlation between reactivity and restructuring ability. Langmuir 1991;7:3176–82.
[101] Roy Morrison S. Electrochemistry at semiconductor and oxidized metal electrodes. New York: Plenum Press; 1980.
[102] Lyklema J. 2. Fundamentals of interface and colloid science. Solid–liquid interfaces. San Diego: Academic Press; 1995.
[103] Adamson Arthur W, Gast Alice P. Physical chemistry of surfaces. New York: Wiley; 1997.
[104] Masel Richard I. Principles of adsorption and reaction on solid surfaces. New York: Wiley; 1996.
[105] Naraoka R, Kaise G, Kajikawa K, Okawa H, Ikezawa H, Hashimoto K. Nonlinear optical property of hemicyanine self-assembled monolayers on gold and its adsorption kinetics probed by optical second-harmonic generation and surface plasmon resonance spectroscopy. Chem Phys Lett 2002;362:26–30.
[106] Kornherr A, French SA, Sokol AA, Catlow CRA, Hansal S, Hansal WEG, et al. Interaction of adsorbed organosilanes with polar zinc oxide surfaces: a molecular dynamics study comparing two models for the metal oxide surface. Chem Phys Lett 2004;393:107–11.
[107] Jakubke HD, Karcher R. Lexikon der Chemie. Heidelberg: Spektrum; 2008.
[108] Ruthven Douglas M. Principles of adsorption and adsorption processes. New York: Wiley; 1984.
[109] Zola RS, Freire FCM, Lenzi EK, Evangelista LR, Barbero G. Kinetic equation with memory effect for adsorption–desorption phenomena. Chem Phys Lett 2007;438:144–7.
[110] Oura K, Lifshits VG, Saranin AA, Zotov AV, Katayama M. Surface science |an introduction; with 16 tables. Berlin: Springer; 2003.
[111] Henderson AP, Seetohul LN, Dean AK, Russell P, Pruneanu S, Ali Z. A novel isotherm, modeling self-assembled monolayer adsorption and structural changes. Langmuir 2009;25:931–8.
[112] Kisliuk P. The sticking probabilities of gases chemisorbed on the surfaces of solids. J Phys Chem Solids 1957;3:95–101.
[113] Ikada Y, Suzuki M, Tamada T. Polymer surfaces possessing minimal interaction with blood components. In: Shalaby WS, Hoffman AS, Ratner BD, Horbett TA, editors. Polymers as biomatierials |[proceedings of a symposium on polymers as biomaterials, held March 22–25, 1983, at the American Chem Society meeting in Seattle, Wash]. New York: Plenum Press; 1984. p. 135.
[114] Lee CS, Belfort G. Changing activity of ribonculease A during adsorption: a molecular explanation. Proc Natl Acad Sci USA 1989;86:8392–6.
[115] Israelachvili Jacob N. Intermolecular and surface forces: with applications to colloidal and biological systems. London; Orlando, Fla: Academic Press; 1985.
[116] Lin YS, Hlady V. Human serum albumin adsorption onto octadecyldimethylsilyl-silica gradient surface. Coll Surf B: Biointerf 1994;2:481–91.

[117] Lin YS, Hlady V. The desorption of ribonuclease A from charge density gradient surfaces studied by spatially-resolved total internal reflection fluorescence. Coll Surf B: Biointerf 1995;4:65–75.
[118] Andrade JD. 2. Surface and interfacial aspects of biomedical polymers. 2nd ed. New York: Plenum Press; 1985.
[119] Ramsden JJ. Experimental methods for investigating protein adsorption-kinetics at surfaces. Quart Rev Biophys 1994;27:41–105.
[120] Vörös J. The density and refractive index of adsorbing protein layers. Biophys J 2004;87:553–61.
[121] Schmuki P. From bacon to barriers: a review on the passivity of metals and alloys. J Solid State Electrochem 2002;6:145–64.
[122] Milošev I, Metikoš-Huković M, Strehblow HH. Passive film on orthopaedic TiAlV alloy formed in physiological solution investigated by X-ray photoelectron spectroscopy. Biomaterials 2000;21:2103–13.
[123] Milošev I, Strehblow HH. The composition of the surface passive film formed on CoCrMo alloy in simulated physiological solution. Electrochim Acta 2003;48:2767–74.
[124] Milosev I, Strehblow HH. The behavior of stainless steels in physiological solution containing complexing agent studied by X-ray photoelectron spectroscopy. J Biomed Mater Res 2000;52:404–12.
[125] Schultze JW, Lohrengel MM. Stability, reactivity and breakdown of passive films. Problems of recent and future research. Electrochim Acta 2000;45:2499–513.
[126] Virtanen S, Milošev I, Gomez-Barrena E, Trebše R, Salo J, Konttinen YT. Special modes of corrosion under physiological and simulated physiological conditions. Acta Biomaterial 2008;4:468–76.
[127] Lorbeer P, Lorenz WJ. The kinetics of iron dissolution and passivation. In: Frankenthal RP, Kruger J, editors. The passivity of metals. Princeton: The Electrochemical Society; 1978. p. 607–13.
[128] Keddam M, Mattos OR, Takenouti H. Mechanism of anodic dissolution of iron-chromium alloys investigated by electrode impedances – I. Experimental results and reaction model. Electrochim Acta 1986;31:1147–58.
[129] Keddam M, Mattos OR, Takenouti H. Mechanism of anodic dissolution of iron-chromium alloys investigated by electrode impedances—II. Elaboration of the reaction model. Electrochim Acta 1986;31:1159–65.
[130] Epelboin I, Keddam M, Mattos OR, Takenouti H. The dissolution and passivation of Fe and Fe{single bond}Cr alloys in acidified sulphate medium: Influences of pH and Cr content. Corr Sci 1979;19:1105–12.
[131] Böhni H. Localized corrosion. In: Mansfeld F, editor. Corrosion mechanisms. New York: Dekker; 1988. p. 285–327.
[132] Boehni H. Breakdown of passivity and localized corrosion processes. Langmuir 1987;3:924–30.
[133] Strehblow HH. Mechanisms of pitting corrosion. In: Marcus P, Oudar J, editors. Corrosion mechanisms in theory and practice. New York: Dekker; 1995. p. 201–38.
[134] Natishan Paul M, Electrochemical Society. Corrosion Division. Critical factors in localized corrosion IIproceedings of the symposium on critical factors in localized corrosion II. Proceedings of the Symposium on Critical Factors in Localized Corrosion II Pennington, NJ: Electrochemical Society; 1996. p. xvi, 456 p.
[135] Szklarska-Smialowska Z. Pitting corrosion of metals. Houston: National Association of Corrosion Engineers; 1986.
[136] Hine F, Komai K, Yamakawa K. Localized corrosion. London: Elsevier; 1988.
[137] Tousek Jaromír. Theoretical aspects of the localized corrosion of metals. Aedermannsdorf, Switzerland; Rockport, MA: Trans Tech Publications; 1985.
[138] Brown BF, Kruger J, Staehle RW. Localized corrosion. Houston: NACE; 1974.
[139] Frankenthal J, Kruger RP. Equilibrium diagrams of localized corrosion. Proc Electrochem Soc 1998:84.
[140] . Isaacs HS Bertocci U, Kruger J, Smialowska S. Advance; 1990.
[141] Oyane A, Kim HM, Furuya T, Kokubo T, Miyazaki T, Nakamura T. Preparation and assessment of revised simulated body fluids. J Biomed Mater Res Part A 2003;65A:188–95.
[142] Muller L, Conforto E, Caillard D, Muller FA. Biomimetic apatite coatings – carbonate substitution and preferred growth orientation. Biomol Eng 2007;24:462–6.
[143] Virtanen S. Corrosion of biomedical implant materials. Corros Rev 2008;26:147–71.
[144] Hanawa T, Asami K, Asaoka K. Repassivation of titanium and surface oxide film regenerated in simulated bioliquid. J Biomed Mater Res 1998;40:530–8.
[145] Burstein GT, Liu C, Souto RM. The effect of temperature on the nucleation of corrosion pits on titanium in Ringer's physiological solution. Biomaterials 2005;26:245–56.
[146] Tengvall P, Elwing H, Sjoqvist L, Lundstrom I, Bjursten LM. Interaction between hydrogen-peroxide and titanium – a possible role in the biocompatibility of titanium. Biomaterials 1989;10:118–20.
[147] Pan J, Thierry D, Leygraf C. Electrochemical and Xps studies of titanium for biomaterial applications with respect to the effect of hydrogen-peroxide. J Biomed Mater Res 1994;28:113–22.
[148] Hanawa T, Kohayama Y, Hiromoto S, Yamamoto A. Effects of biological factors on the repassivation current of titanium. Mater Trans 2004;45:1635–9.
[149] Kocijan A, Milosev I, Pihlar B. The influence of complexing agent and proteins on the corrosion of stainless steels and their metal components. J Mater Sci-Mater Med 2003;14:69–77.
[150] Munoz AI, Mischler S. Interactive effects of albumin and phosphate ions on the corrosion of CoCrMo implant alloy. J Electrochem Soc 2007;154:C562–70.
[151] Hiromoto S, Mischler S. The influence of proteins on the fretting-corrosion behaviour of a Ti6Al4V alloy. Wear 2006;261:1002–11.
[152] Hanawa T. Evaluation techniques of metallic biomaterials in vitro. Sci Technol Adv Mater 2002;3:289–95.
[153] Hiromoto S, Hanawa T. Corrosion of implant metals in the presence of cells. Corros Rev 2006;24:323–51.
[154] Hodgson AWE, Kurz S, Virtanen S, Fervel V, Olsson COA, Mischler S. Passive and transpassive behaviour of CoCrMo in simulated biological solutions. Electrochim Acta 2004;49:2167–78.
[155] Burstein GT, Souto RM. Observations of localized instability of passive titanium in chloride solution. Electrochim Acta 1995;40:1881–8.
[156] Burstein GT, Liu C, Souto RM, Vines SP. Origins of pitting corrosion. Corr Eng Sci Technol 2004;39:25–30.
[157] Souto RM, Burstein GT. A preliminary investigation into the microscopic depassivation of passive titanium implant materials in vitro. J Mater Sci-Mater Med 1996;7:337–43.

[158] Frankel GS. Pitting corrosion of metals. A review of the critical factors (vol. 145, p. 2186, 1998). J Electrochem Soc 1998;145:2970.
[159] Baroux B. Pitting corrosion of stainless steels. In: Marcus P, Oudar J, editors. Corrosion mechanisms in theory and practice. New York: Dekker; 1995. p. 265–310.
[160] Schmuki P, Lockwood DJ, Fraser J, Graham MJ. Factors in porous GaAs formation. In: Schmuki Patrik International Symposium on Pits, Pores, editors. Proceedings of the international symposium on pits and pores |formation, properties and significance for advanced luminescent materials |Pits and pores; 1997.
[161] Schutz RW, Thomas DE. Corrosion of titanium and titanium alloys. 9 Metals handbook. Metals Park: ASM International; 1988. p. 669–706.
[162] Mckay P, Mitton DB. An electrochemical investigation of localized corrosion on titanium in chloride environments. Corrosion 1985;41:52–62.
[163] Willert HG, Broback LG, Buchhorn GH, Jensen PH, Koster G, Lang I, et al. Crevice corrosion of cemented titanium alloy stems in total hip replacements. Clin Orthop Relat Res 1996:51–75.
[164] Waterhouse RB. Fretting corrosion. Oxford: Peragamon; 1972.
[165] Brown SA, Flemming CA, Kawalec JS, Placko HE, Vassaux C, Merritt K, et al. Fretting corrosion accelerates crevice corrosion of modular hip tapers. J Appl Biomater 1995;6:19–26.
[166] Gilbert JL, Buckley CA, Jacobs JJ. In vivo corrosion of modular hip prosthesis components in mixed and similar metal combinations. The effect of crevice, stress, motion, and alloy coupling. J Biomed Mater Res 1993;27:1533–44.
[167] Khan MA, Williams RL, Williams DF. Conjoint corrosion and wear in titanium alloys. Biomaterials 1999;20:765–72.
[168] Hanawa T. Metal ion release from metal implants. Mater Sci Eng C – Biomim Supramol Syst 2004;24:745–52.
[169] Okazaki Y, Gotoh E. Comparison of metal release from various metallic biomaterials in vitro. Biomaterials 2005;26:11–21.
[170] Khan MA, Williams RL, Williams DF. In vitro corrosion and wear of titanium alloys in the biological environment. Biomaterials 1996;17:2117–26.
[171] Goldberg JR, Gilbert JL. Electrochemical response of CoCrMo to high-speed fracture of its metal oxide using an electrochemical scratch test method. J Biomed Mater Res 1997;37:421–31.
[172] Barril S, Mischler S, Landolt D. Electrochemical effects on the fretting corrosion behaviour of Ti6Al4V in 0.9% sodium chloride solution. Wear 2005;259:282–91.
[173] Duisabeau L, Combrade P, Forest B. Environmental effect on fretting of metallic materials for orthopaedic implants. Wear 2004;256:805–16.
[174] Windler M, MacDougall JE, Schenk R. Investigation into wear induced corrosion of orthopedic implant materials. In: Winters Gary L, Nutt Michael J, editors. Stainless steels for medical and surgical applications. West Conshohocken, PA: ASTM International; 2003. p. 211–21.
[175] Mears DC. The use of dissimilar metals in surgery. J Biomed Mater Res 1975;9:133–48.
[176] Yerby Scott A, Taylor Jeffery K, Park Jun, Shackelford James F. Corrosion at the interface: a possible solution to cobalt—chrome heads on titanium alloy stems. The J Arthropl 1996;11:157–62.
[177] Salvati EA, Barrena EG. The contribution of metallic debris to osteolysis. Orthopedics 1994;17:763–5.
[178] Lieberman JR, Rimnac CM, Garvin KL, Klein RW, Salvati EA. An analysis of the head–neck taper interface in retrieved hip prostheses. Clin Orthopaed Relat Res 1994:162–7.
[179] Reclaru L, Lerf R, Eschler PY, Blatter A, Meyer JM. Pitting, crevice and galvanic corrosion of REX stainless-steel/CoCr orthopedic implant material. Biomaterials 2002;23:3479–85.
[180] Serhan Hassan, Slivka Michael, Albert Todd, Daniel Kwak S. Is galvanic corrosion between titanium alloy and stainless steel spinal implants a clinical concern? The Spine J 2004;4:379–87.
[181] Schwartz Zvi, Boyan BD. Underlying mechanisms at the bone–biomaterial interface. J Cell Biochem 1994;56:340–7.
[182] Puleo DA, Nanci A. Understanding and controlling the bone–implant interface. Biomaterials 1999;20:2311–21.
[183] Buser D, Schenk RK, Steinemann S, Fiorellini JP, Fox CH, Stich H. Influence of surface characteristics on bone integration of titanium implants – a histomorphometric study in miniature pigs. J Biomed Mater Res 1991;25:889–902.
[184] Gotfredsen K, Hjorting-Hansen E, Budtz-Jorgensen E. Clinical and radiographic evaluation of submerged and nonsubmerged implants in monkeys. Int J Prosthodont 1990;3:463–9.
[185] Wennerberg A. The importance of surface roughness for implant incorporation. Int J Mach Tools Manuf 1998;38:657–62.
[186] Deligianni DD, Katsala N, Ladas S, Sotiropoulou D, Amedee J, Missirlis YF. Effect of surface roughness of the titanium alloy Ti–6Al–4V on human bone marrow cell response and on protein adsorption. Biomaterials 2001;22:1241–51.
[187] Degasne I, Basle MF, Demais V, Hure G, Lesourd M, Grolleau B, et al. Effects of roughness, fibronectin and vitronectin on attachment, spreading, and proliferation of human osteoblast-like cells (Saos-2) on titanium surfaces. Calc Tissue Int 1999;64:499–507.
[188] Kieswetter K, Schwartz Z, Hummert TW, Cochran DL, Simpson J, Dean DD, et al. Surface roughness modulates the local production of growth factors and cytokines by osteoblast-like MG-63 cells. J Biomed Mater Res 1996;32:55–63.
[189] Wennerberg A, Albrektsson T, Andersson B, Krol JJ. A histomorphometric and removal torque study of screw-shaped titanium implants with three different surface topographies. Clin Oral Implants Res 1995;6:24–30.
[190] Wennerberg A, Hallgren C, Johansson C, Danelli S. A histomorphometric evaluation of screw-shaped implants each prepared with two surface roughnesses. Clin Oral Implants Res 1998;9:11–9.
[191] Hansson S, Norton M. The relation between surface roughness and interfacial shear strength for bone-anchored implants. A mathematical model. J Biomech 1999;32:829–36.
[192] Albrektsson T, Wennerberg A. Oral implant surfaces: part 1 – review focusing on topographic and chemical properties of different surfaces and in vivo responses to them. Int J Prosth 2004;17:536–43.
[193] Albrektsson T, Wennerberg A. Oral implant surfaces: part 2 – review focusing on clinical knowledge of different surfaces. Int J Prosth 2004;17:544–64.
[194] Hansson S. The dental implant meets bone – a clash of two paradigms. Appl Osseointeg Res 2006;1:15–7.
[195] Wong M, Eulenberger J, Schenk R, Hunziker E. Effect of surface-topology on the osseointegration of implant materials in trabecular bone. J Biomed Mater Res 1995;29:1567–75.

[196] Wennerberg A, Ektessabi A, Albrektsson T, Johansson C, Andersson B. A 1-year follow-up of implants of differing surface roughness placed in rabbit bone. Int J Oral Maxillo Implants 1997;12:486–94.
[197] Hignett B Andrew TC, Downing W, Duwell EJ, Belanger J, Tulinski EH. Surface cleaning, finishing and coating. In: Wood WG, editor. Metals handbook. Metals Park: American Society for Metals; 1987. p. 107–27.
[198] Kern M, Thompson VP. Sandblasting and silica coating of a glass-infiltrated alumina ceramic – volume loss, morphology, and changes in the surface-composition. J Prosth Dent 1994;71:453–61.
[199] Kern M, Thompson VP. Effects of sandblasting and silica-coating procedures on pure titanium. J Dent 1994;22:300–6.
[200] Wennerberg Ann, Albrektsson Tomas, Lausmaa Jukka. Torque and histomorphometric evaluation of c.p. titanium screws blasted with 25- and 75-μm-sized particles of $Al_2O_3$. J Biomed Mater Res 1996;30:251–60.
[201] Stea S, Savarino L, Toni A, Sudanese A, Giunti A, Pizzoferrato A. Microradiographic and histochemical evaluation of mineralization inhibition at the bone–alumina interface. Biomaterials 1992;13:664–7.
[202] Thompson GJ, Puleo DA. Ti–6Al–4V ion solution inhibition of osteogenic cell phenotype as a function of differentiation timecourse in vitro. Biomaterials 1996;17:1949–54.
[203] Wennerberg A, Albrektsson T, Andersson B. An animal study of c.p. titanium screws with different surface topographies. J Mater Sci: Mater Med 1995;6:302–9.
[204] Piattelli Adriano, Degidi Marco, Paolantonio Michele, Mangano Carlo, Scarano Antonio. Residual aluminum oxide on the surface of titanium implants has no effect on osseointegration. Biomaterials 2003;24:4081–9.
[205] Piattelli M, Scarano A, Paolantonio M, Iezzi G, Petrone G, Piattelli A. Bone response to machined and resorbable blast material titanium implants: an experimental study in rabbits. J Oral Implantol 2002;28:2–8.
[206] Novaes Jr AB, Souza SL, de Oliveira PT, Souza AM. Histomorphometric analysis of the bone–implant contact obtained with four different implant surface treatments placed side by side in the dog mandible. Int J Oral Maxillo Implants 2002;17:377–83.
[207] Mueller WD, Gross U, Fritz T, Voigt C, Fischer P, Berger G, et al. Evaluation of the interface between bone and titanium surfaces being blasted by aluminium oxide or bioceramic particles. Clin Oral Implants Res 2003;14:349–56.
[208] Massaro C, Rotolo P, De Riccardis F, Milella E, Napoli A, Wieland M, et al. Comparative investigation of the surface properties of commercial titanium dental implants. Part I: chemical composition. J Mater Sci Mater Med 2002;13:535–48.
[209] Zinger O, Anselme K, Denzer A, Habersetzer P, Wieland M, Jeanfils J, et al. Time-dependent morphology and adhesion of osteoblastic cells on titanium model surfaces featuring scale-resolved topography. Biomaterials 2004;25:2695–711.
[210] Cho SA, Park KT. The removal torque of titanium screw inserted in rabbit tibia treated by dual acid etching. Biomaterials 2003;24:3611–7.
[211] Ellingsen JE. Pre-treatment of titanium implants with fluoride improves their retention in bone. J Mater Sci: Mater Med 1995;6:749–53.
[212] Ellingsen JE, Johansson CB, Wennerberg A, Holmen A. Improved retention and bone-tolmplant contact with fluoride-modified titanium implants. Int J Oral Maxillo Implants 2004;19:659–66.
[213] Cooper Lyndon F, Zhou Yongsheng, Takebe Jun, Guo Juanli, Abron Armin, Holmén Anders, et al. Fluoride modification effects on osteoblast behavior and bone formation at $TiO_2$ grit-blasted c.p. titanium endosseous implants. Biomaterials 2006;27:926–36.
[214] Guo J, Padilla RJ, Ambrose W, De Kok IJ, Cooper LF. The effect of hydrofluoric acid treatment of $TiO_2$ grit blasted titanium implants on adherent osteoblast gene expression in vitro and in vivo. Biomaterials 2007;28:5418–25.
[215] Buser D, Nydegger T, Oxland T, Cochran DL, Schenk RK, Hirt HP, et al. Interface shear strength of titanium implants with a sandblasted and acid-etched surface: a biomechanical study in the maxilla of miniature pigs. J Biomed Mater Res 1999;45:75–83.
[216] Zhao G, Zinger O, Schwartz Z, Wieland M, Landolt D, Boyan BD. Osteoblast-like cells are sensitive to submicron-scale surface structure. Clin Oral Implants Res 2006;17:258–64.
[217] Zinger O, Zhao G, Schwartz Z, Simpson J, Wieland M, Landolt D, et al. Differential regulation of osteoblasts by substrate microstructural features. Biomaterials 2005;26:1837–47.
[218] Perrin D, Szmukler-Moncler S, Echikou C, Pointaire P, Bernard JP. Bone response to alteration of surface topography and surface composition of sandblasted and acid etched (SLA) implants. Clin Oral Implants Res 2002;13:465–9.
[219] Yang B, Uchida M, Kim HM, Zhang X, Kokubo T. Preparation of bioactive titanium metal via anodic oxidation treatment. Biomaterials 2004;25:1003–10.
[220] Sul YT, Johansson C, Wennerberg A, Cho LR, Chang BS, Albrektsson T. Optimum surface properties of oxidized implants for reinforcement of osseointegration: surface chemistry, oxide thickness, porosity, roughness, and crystal structure. Int J Oral Maxillo Implants 2005;20:349–59.
[221] Schupbach P, Glauser R, Rocci A, Martignoni M, Sennerby L, Lundgren A, et al. The human bone-oxidized titanium implant interface: a light microscopic, scanning electron microscopic, back-scatter scanning electron microscopic, and energy-dispersive X-ray study of clinically retrieved dental implants. Clin Implant Dent Relat Res 2005;7(Suppl. 1):S36–43.
[222] Xiropaidis Andreas V, Qahash Mohammed, Lim Won Hee, Shanaman Richard H, Rohrer Michael D, Wikesjö Ulf ME, et al. Bone–implant contact at calcium phosphate-coated and porous titanium oxide (TiUnite™)-modified oral implants. Clin Oral Implants Res 2005;16:532–9.
[223] Huang YH, Xiropaidis AV, Sorensen RG, Albandar JM, Hall J, Wikesjo UME. Bone formation at titanium porous oxide (TiUnite (TM)) oral implants in type IV bone. Clin Oral Implants Res 2005;16:105–11.
[224] Shibata T, Zhu YC. The effect of film formation conditions on the structure and composition of anodic oxide films on titanium. Corros Sci 1995;37:253–70.
[225] Rocci A, Martignoni M, Gottlow J. Immediate loading of Branemark System TiUnite and machined-surface implants in the posterior mandible: a randomized open-ended clinical trial. Clin Implant Dent Relat Res 2003;5(Suppl 1):57–63.
[226] Ishizawa H, Ogino M. Formation and characterization of anodic titanium oxide films containing Ca and P. J Biomed Mater Res 1995;29:65–72.
[227] Ishizawa H, Ogino M. Characterization of thin hydroxyapatite layers formed on anodic titanium oxide films containing Ca and P by hydrothermal treatment. J Biomed Mater Res 1995;29:1071–9.

[228] Sul YT, Byon ES, Jeong Y. Biomechanical measurements of calcium-incorporated oxidized implants in rabbit bone: effect of calcium surface chemistry of a novel implant. Clin Implant Dent Relat Res 2004;6:101–10.
[229] Liu X, Chu PK, Ding C. Surface modification of titanium, titanium alloys, and related materials for biomedical applications. Mater Sci Eng R: Reports 2004;47:49–121.
[230] Martin JY, Schwartz Z, Hummert TW, Schraub DM, Simpson J, Lankford J, et al. Effect of titanium surface roughness on proliferation, differentiation, and protein synthesis of human osteoblast-like cells (MG63). J Biomed Mater Res 1995;29:389–401.
[231] Urban RM, Jacobs JJ, Tomlinson MJ, Gavrilovic J, Black J, Peoc'h M. Dissemination of wear particles to the liver, spleen, and abdominal lymph nodes of patients with hip or knee replacement. J Bone Joint Surg Am 2000;82:457–76.
[232] Taba Junior M, Novaes Jr AB, Souza SL, Grisi MF, Palioto DB, et al. Radiographic evaluation of dental implants with different surface treatments: an experimental study in dogs. Implant Dent 2003;12:252–8.
[233] Ong JL, Carnes DL, Bessho K. Evaluation of titanium plasma-sprayed and plasma-sprayed hydroxyapatite implants in vivo. Biomaterials 2004;25:4601–6.
[234] Schenk RK, Buser D. Osseointegration: a reality. Periodontol 2000 1998;17:22–35.
[235] Cook SD, Thomas KA, Dalton JE, Volkman TK, Whitecloud 3rd TS, Kay JF. Hydroxylapatite coating of porous implants improves bone ingrowth and interface attachment strength. J Biomed Mater Res 1992;26:989–1001.
[236] Thomas KA, Cook SD. An evaluation of variables influencing implant fixation by direct bone apposition. J Biomed Mater Res 1985;19:875–901.
[237] Thomas KA, Kay JF, Cook SD, Jarcho M. The effect of surface macrotexture and hydroxylapatite coating on the mechanical strengths and histologic profiles of titanium implant materials. J Biomed Mater Res 1987;21:1395–414.
[238] Cochran DL. A comparison of endosseous dental implant surfaces. J Periodontol 1999;70:1523–39.
[239] Shalabi MM, Gortemaker A, Van't Hof MA, Jansen JA, Creugers NH. Implant surface roughness and bone healing: a systematic review. J Dent Res 2006;85:496–500.
[240] Falconnet D, Csucs G, Grandin HM, Textor M. Surface engineering approaches to micropattern surfaces for cell-based assays. Biomaterials 2006;27:3044–63.
[241] Singhvi R, Stephanopoulos G, Wang DIC. Effects of substratum morphology on cell physiology – review. Biotechnol Bioeng 1994;43:764–71.
[242] Folch A, Toner M. Microengineering of cellular interactions. Ann Rev Biomed Eng 2000;2:227–56.
[243] Craighead H. Future lab-on-a-chip technologies for interrogating individual molecules. Nature 2006;442:387–93.
[244] Chen CS, Mrksich M, Huang S, Whitesides GM, Ingber DE. Geometric control of cell life and death. Science 1997;276:1425–8.
[245] Lausmaa J. Mechanical, thermal, chemical and electrochemical treatment of titanium. In: Brunette DM, Tengvall P, Textor M, Thomsen P, editors. Titanium in medicine: material science, surface science, engineering, biological responses and medical applications. Berlin: Springer; 2001. p. 231–66.
[246] Bagno A, Di Bello C. Surface treatments and roughness properties of Ti-based biomaterials. J Mater Sci Mater Med 2004;15:935–49.
[247] Le Guehennec L, Soueidan A, Layrolle P, Amouriq Y. Surface treatments of titanium dental implants for rapid osseointegration. Dent Mater 2007;23:844–54.
[248] Landolt D, Chauvy PF, Zinger O. Electrochemical micromachining, polishing and surface structuring of metals: fundamental aspects and new developments. Electrochim Acta 2003;48:3185–201.
[249] Anselme K, Bigerelle M, Noel B, Iost A, Hardouin P. Effect of grooved titanium substratum on human osteoblastic cell growth. J Biomed Mater Res 2002;60:529–40.
[250] Zhu X, Chen J, Scheideler L, Altebaeumer T, Geis-Gerstorfer J, Kern D. Cellular reactions of osteoblasts to micron- and submicron-scale porous structures of titanium surfaces. Cells Tiss Organs 2004;178:13–22.
[251] Curtis ASG, Gadegaard N, Dalby MJ, Riehle MO, Wilkinson CDW, Aitchison G. Cells react to nanoscale order and symmetry in their surroundings. IEEE Trans Nanobiosci 2004:61–5.
[252] Flemming RG, Murphy CJ, Abrams GA, Goodman SL, Nealey PF. Effects of synthetic micro- and nano-structured surfaces on cell behavior. Biomaterials 1999;20:573–88.
[253] Teixeira AI, Abrams GA, Bertics PJ, Murphy CJ, Nealey PF. Epithelial contact guidance on well-defined micro- and nanostructured substrates. J Cell Sci 2003;116:1881–92.
[254] Turner S, Kam L, Isaacson M, Craighead HG, Shain W, Turner J. Cell attachment on silicon nanostructures, 6th ed. Dana Point, California (USA): AVS; 1997. p. 2848–54.
[255] Dalby MJ, Riehle MO, Sutherland DS, Agheli H, Curtis ASG. Use of nanotopography to study mechanotransduction in fibroblasts – methods and perspectives. Euro J Cell Biol 2004;83:159–69.
[256] Craighead HG, James CD, Turner AMP. Chemical and topographical patterning for directed cell attachment. Curr Opin Solid State Mater Sci 2001;5:177–84.
[257] Wilkinson CDW, Curtis ASG, Crossan J. Nanofabrication in cellular engineering. J Vac Sci Technol B 1998;16:3132–6.
[258] Craighead HG, Turner SW, Davis RC, James C, Perez AM, St. John PM, et al. Chemical and topographical surface modification for control of central nervous system cell adhesion. Biomed Microdev 1998;1:49–64.
[259] Wilkinson CDW, Riehle M, Wood M, Gallagher J, Curtis ASG. The use of materials patterned on a nano- and micro-metric scale in cellular engineering. Mater Sci Eng C-Biomim Supramol Syst 2002;19:263–9.
[260] Curtis A, Wilkinson C. Nantotechniques and approaches in biotechnology. Trends Biotechnol 2001;19:97–101.
[261] Dalby MJ, Gadegaard N, Riehle MO, Wilkinson CDW, Curtis ASG. Investigating filopodia sensing using arrays of defined nano-pits down to 35 nm diameter in size. Int J Biochem Cell Biol 2004;36:2005–15.
[262] Agheli H, Malmström J, Hanarp P, Sutherland DS. Nanostructured biointerfaces. Mater Sci Eng: C 2006;26:911–7.
[263] Hanarp P, Sutherland DS, Gold J, Kasemo B. Control of nanoparticle film structure for colloidal lithography. Coll Surf a – Physicochem Eng Aspects 2003;214:23–36.
[264] Denis FA, Hanarp P, Sutherland DS, Dufrene YF. Fabrication of nanostructured polymer surfaces using colloidal lithography and spin-coating. Nano Lett 2002;2:1419–25.

[265] Gallagher JO, McGhee KF, Wilkinson CDW, Riehle MO. Interaction of animal cells with ordered nanotopography. IEEE Trans NanoBiosci 2002;1:24–8.
[266] Dalby MJ, Riehle MO, Sutherland DS, Agheli H, Curtis AS. Morphological and microarray analysis of human fibroblasts cultured on nanocolumns produced by colloidal lithography. Euro Cell Mater 2005;9:1–8 [discussion].
[267] Affrossman S, Henn G, ONeill SA, Pethrick RA, Stamm M. Surface topography and composition of deuterated polystyrene-poly(bromostyrene) blends. Macromolecules 1996;29:5010–6.
[268] Affrossman S, Stamm M. The effect of molecular weight on the topography of thin films of blends of poly(4-bromostyrene) and polystyrene. Coll Polym Sci 2000;278:888–93.
[269] Dalby MJ, Riehle MO, Johnstone H, Affrossman S, Curtis ASG. In vitro reaction of endothelial cells to polymer demixed nanotopography. Biomaterials 2002;23:2945–54.
[270] Dalby MJ, Berry CC, Riehle MO, Sutherland DS, Agheli H, Curtis ASG. Attempted endocytosis of nano-environment produced by colloidal lithography by human fibroblasts. Experimen Cell Res 2004;295:387–94.
[271] Khor HL, Kuan Y, Kukula H, Tamada K, Knoll W, Moeller M, et al. Response of cells on surface-induced nanopatterns: Fibroblasts and mesenchymal progenitor cells. Biomacromolecules 2007;8:1530–40.
[272] Kriparamanan R, Aswath P, Zhou A, Tang LP, Nguyen KT. Nanotopography: cellular responses to nanostructured materials. J Nanosci Nanotechnol 2006;6:1905–19.
[273] Webster TJ, Siegel RW, Bizios R. Osteoblast adhesion on nanophase ceramics. Biomaterials 1999;20:1221–7.
[274] Webster TJ, Ejiofor JU. Increased osteoblast adhesion on nanophase metals: Ti, Ti6Al4V, and CoCrMo. Biomaterials 2004;25:4731–9.
[275] Webster TJ, Seigel RW, Bizios R. Design and evaluation of nanophase alumina for orthopedic/dental implant efficacy. Scr Mater 2001;44:1639–42.
[276] Webster TJ, Schadler LS, Siegel RW, Bizios R. Mechanisms of enhanced osteoblast adhesion on nanophase alumina involve vitronectin. Tissue Eng 2001;7:291–301.
[277] Webster TJ, Ergun C, Doremus RH, Siegel RW, Bizios R. Specific proteins mediate enhanced osteoblast adhesion on nanophase ceramics. J Biomed Mater Res 2000;51:475–83.
[278] Mustafa K, Oden A, Wennerberg A, Hultenby K, Arvidson K. The influence of surface topography of ceramic abutments on the attachment and proliferation of human oral fibroblasts. Biomaterials 2005;26:373–81.
[279] Price RL, Waid MC, Haberstroh KM, Webster TJ. Selective bone cell adhesion on formulations containing carbon nanofibers. Biomaterials 2003;24:1877–87.
[280] Cai Kaiyong, Bossert Jörg, Jandt Klaus D. Does the nanometre scale topography of titanium influence protein adsorption and cell proliferation? Coll Surf B: Biointerf 2006;49:136–44.
[281] Balasundaram Ganesan, Webster Thomas J. A perspective on nanophase materials for orthopedic implant applications. J Mater Chem 2006;16:3737–45.
[282] Popat Ketul C, Chatvanichkul Kwan-Isara, Barnes George L, Latempa Thomas Joseph, Grimes Craigs A, Desai Tejal A. Osteogenic differentiation of marrow stromal cells cultured on nanoporous alumina surfaces. J Biomed Mater Res Part A 2007;80A:955–64.
[283] Glass Roman, Möller Martin, Spatz Joachim P. Block copolymer micelle nanolithography. Nanotechnology 2003;14:1153–60.
[284] Huang J, Grater SV, Corbellini F, Rinck S, Bock E, Kemkemer R, et al. Impact of order and disorder in RGD nanopatterns on cell adhesion. Nano Lett 2009;9:1111–6.
[285] Arnold M, Cavalcanti-Adam EA, Glass R, Blummel J, Eck W, Kantlehner M, et al. Activation of integrin function by nanopatterned adhesive interfaces. Chemphyschem 2004;5:383–8.
[286] Cavalcanti-Adam EA, Micoulet A, Blummel J, Auernheimer J, Kessler H, Spatz JP. Lateral spacing of integrin ligands influences cell spreading and focal adhesion assembly. Euro J Cell Biol 2006;85:219–24.
[287] Masuda H, Fukuda K. Ordered metal nanohole arrays made by a two-step replication of honeycomb structures of anodic alumina. Science 1995;268:1466–8.
[288] Zwilling V, Darque-Ceretti E, Boutry-Forveille A, David D, Perrin MY, Aucouturier M. Structure and physicochemistry of anodic oxide films on titanium and TA6V alloy. Surf Interf Anal. 1999;27:629–37.
[289] Gong D, Grimes CA, Varghese OK, Hu WC, Singh RS, Chen Z, et al. Titanium oxide nanotube arrays prepared by anodic oxidation. J Mater Res 2001;16:3331–4.
[290] Beranek, #160, R, Hildebrand, H, Schmuki, et al. Self-organized porous titanium oxide prepared in H[2]SO[4]/HF electrolytes. Pennington, NJ, ETATS-UNIS: Institute of Electrical and Electronics Engineers; 2003.
[291] Walpole AR, Briggs EP, Karlsson M, Pålsgård E, Wilshaw PR. Nano-porous alumina coatings for improved bone implant interfaces. Materialwissenschaft und Werkstofftechnik 2003;34:1064–8.
[292] Karlsson M, Pålsgård E, Wilshaw PR, Di Silvio L. Initial in vitro interaction of osteoblasts with nano-porous alumina. Biomaterials 2003;24:3039–46.
[293] Pedimonte J, Travitzky N, Korn M, Kriegelstein S, Greil P. Surface modification of an alumina-based bioceramic for cement application. Adv Eng Mater 2011;13:B306–12.
[294] Chung SH, Son SJ, Min J. The nanostructure effect on the adhesion and growth rates of epithelial cells with well-defined nanoporous alumina substrates. Nanotechnology 2010;21:125104–11.
[295] Macák Jan M, Tsuchiya Hiroaki, Schmuki Patrik. High-aspect-ratio $TiO_2$ nanotubes by anodization of titanium. Ang Chem Int Ed 2005;44:2100–2.
[296] Macak Jan M, Tsuchiya Hiroaki, Taveira Luciano, Aldabergerova Saule, Schmuki Patrik. Smooth anodic $TiO_2$ nanotubes. Ang Chem Int Ed 2005;44:7463–5.
[297] Roy Poulomi, Berger Steffen, Schmuki Patrik. $TiO_2$ Nanotubes: synthesis and applications. Ang Chem Int Ed 2011;50:2904–39.
[298] Bauer Sebastian, Kleber Sebastian, Schmuki Patrik. $TiO_2$ nanotubes: tailoring the geometry in $H_3PO_4$/HF electrolytes. Electrochem Commun 2006;8:1321–5.
[299] Park J, Bauer S, v.d. Mark K, Schmuki P. Size matters: nano-scale microenvironment directs cell fate. 3rd ed. Nano Letters; 2007.

[300] Park J, Bauer S, Schlegel KA, Neukam FW, v.d. Mark K, Schmuki P. $TiO_2$ nanotubes: 15 nm is a universal geometric constant of surface topography supporting cell adhesion and differentiation. Small 2009;5:666–71.
[301] Park Jung, Bauer Sebastian, Schmuki Patrik, von der Mark Klaus. Narrow window in nanoscale dependent activation of endothelial cell growth and differentiation on $TiO_2$ nanotube surfaces. Nano Lett 2009;9:3157–64.
[302] Oh Seunghan, Daraio Chiara, Chen Li-Han, Pisanic Thomas R, Fiñones Rita R, Jin Sungho. Significantly accelerated osteoblast cell growth on aligned $TiO_2$ nanotubes. J Biomed Mater Res Part A 2006;78A:97–103.
[303] Popat Ketul C, Leoni Lara, Grimes Craig A, Desai Tejal A. Influence of engineered titania nanotubular surfaces on bone cells. Biomaterials 2007;28:3188–97.
[304] Bauer Sebastian, Park Jung, Faltenbacher Josef, Berger Steffen, von der Mark Klaus, Schmuki Patrik. Size selective behavior of mesenchymal stem cells on $ZrO_2$ and $TiO_2$ nanotube arrays. Integra Biol 2009:1.
[305] Bauer Sebastian, Park Jung, Mark Klaus von der, Schmuki Patrik. Improved attachment of mesenchymal stem cells on super-hydrophobic $TiO_2$ nanotubes. Acta Biomater 2008;4:1576–82.
[306] von Wilmowsky C, Bauer S, Lutz R, Meisel M, Neukam FW, Toyoshima T, et al. In vivo evaluation of anodic $TiO_2$ nanotubes: an experimental study in the pig. J Biomed Mater Res B Appl Biomater 2009;89:165–71.
[307] Macak Jan M, Tsuchiya Hiroaki, Taveira Luciano, Ghicov Andrei, Schmuki Patrik. Self-organized nanotubular oxide layers on Ti–6Al–7Nb and Ti–6Al–4V formed by anodization in NH4F solutions. J Biomed Mater Res Part A 2005;75A:928–33.
[308] Tsuchiya H, Macak JM, Ghicov A, Schmuki P. Self-organization of anodic nanotubes on two size scales. Small 2006;2:888–91.
[309] Ghicov A, Aldabergenova S, Tsuchyia H, Schmuki P. $TiO_2$–$Nb_2O_5$ nanotubes with electrochemically tunable morphologies. Ang Chem-Int Ed 2006;45:6993–6.
[310] Yasuda K, Schmuki P. Formation of self-organized zirconium titanate nanotube layers by alloy anodization. Adv Mater 2007;19:1757–60.
[311] Kasemo B, Lausmaa J. Surface science aspects on inorganic biomaterials. Crc Crit Rev Biocompat 1986;2:335–80.
[312] Rey C. Calcium phosphate biomaterials and bone mineral. Differences in composition, structures and properties. Biomaterials 1990;11:13–5.
[313] Jarcho M. Calcium-phosphate ceramics as hard tissue prosthetics. Clin Orthopaed Relat Res 1981:259–78.
[314] de Groot K, Wolke JGC, Jansen JA. Calcium phosphate coatings for medical implants. Proc Inst Mech Eng Part H – J Eng Med 1998;212:137–47.
[315] Legeros RZ, Tung MS. Chemical-stability of carbonate-containing and fluoride-containing apatites. Caries Res 1983;17:419–29.
[316] Daculsi G, Laboux O, Malard O, Weiss P. Current state of the art of biphasic calcium phosphate bioceramics. J Mater Sci-Mater Med 2003;14:195–200.
[317] Morris HF, Ochi S, Spray JR, Olson JW. Periodontal-type measurements associated with hydroxyapatite-coated and non-HA-coated implants: uncovering to 36 months. Ann Periodontol 2000;5:56–67.
[318] Barrere F, van der Valk CM, Meijer G, Dalmeijer RA, de Groot K, Layrolle P. Osteointegration of biomimetic apatite coating applied onto dense and porous metal implants in femurs of goats. J Biomed Mater Res B Appl Biomater 2003;67:655–65.
[319] de Groot K, Geesink R, Klein CP, Serekian P. Plasma sprayed coatings of hydroxylapatite. J Biomed Mater Res 1987;21:1375–81.
[320] Geesink RGT, Klein CPAT, de Groot K. Chemical implant fixation using hydroxylapatite coatings. Clin Orthop 1987;225:147–70.
[321] Geesink RGT. Osteoconductive coatings for total joint arthroplasty. Clin Orthopaed Relat Res 2002:53–65.
[322] Dhert WJA. Retrieval Studies on Calcium Phosphate-Coated Implants. Med Progr Technol 1994;20:143–54.
[323] Lacefield WR. Current status of ceramic coatings for dental implants. Implant Dent 1998;7:315–22.
[324] Lee Jessica J, Rouhfar Leyla, Ross Beirne O. Survival of hydroxyapatite-coated implants: a meta-analytic review. J Oral Maxillo Surg 2000;58:1372–9.
[325] Wheeler SL. Eight-year clinical retrospective study of titanium plasma-sprayed and hydroxyapatite-coated cylinder implants. Int J Oral Maxillo Implants 1996;11:340–50.
[326] Chang YL, Lew D, Park JB, Keller JC. Biomechanical and morphometric analysis of hydroxyapatite-coated implants with varying crystallinity. J Oral Maxillo Surg 1999;57:1096–108 [discussion 108–9].
[327] Radin SR, Ducheyne P. Plasma spraying induced changes of calcium phosphate ceramic characteristics and the effect on<i>in vitro stability. J Mater Sci: Mater Med 1992;3:33–42.
[328] Liu DM, Yang QZ, Troczynski T, Tseng WJJ. Structural evolution of sol–gel-derived hydroxyapatite. Biomaterials 2002;23:1679–87.
[329] Weng WJ, Baptista JL. Sol gel derived porous hydroxyapatite coatings. J Mater Sci-Mater Med 1998;9:159–63.
[330] Liu DM, Yang QZ, Troczynski T. Sol–gel hydroxyapatite coatings on stainless steel substrates. Biomaterials 2002;23:691–8.
[331] Kim HW, Kim HE, Salih V, Knowles JC. Sol–gel-modified titanium with hydroxyapatite thin films and effect on osteoblast-like cell responses. J Biomed Mater Res Part A 2005;74A:294–305.
[332] Metikoš-Huković M, Tkalčec E, Kwokal A, Piljac J. An in vitro study of Ti and Ti-alloys coated with sol–gel derived hydroxyapatite coatings. Surf Coat Technol 2003;165:40–50.
[333] Thian ES, Khor KA, Loh NH, Tor SB. Processing of HA-coated Ti–6Al–4V by a ceramic slurry approach: an in vitro study. Biomaterials 2001;22:1225–32.
[334] Cheng K, Weng WJ, Wang HM, Zhang S. In vitro behavior of osteoblast-like cells on fluoridated hydroxyapatite coatings. Biomaterials 2005;26:6288–95.
[335] Montanaro L, Arciola CR, Campoccia D, Cervellati M. In vitro effects on MG63 osteoblast-like cells following contact with two roughness-differing fluorohydroxyapatite-coated titanium alloys. Biomaterials 2002;23:3651–9.
[336] Royer P, Rey C. Calcium-phosphate coatings for orthopedic prosthesis. Surf Coat Technol 1991;45:171–7.
[337] Kumar M, Dasarathy H, Riley C. Electrodeposition of brushite coatings and their transformation to hydroxyapatite in aqueous solutions. J Biomed Mater Res 1999;45:302–10.

[338] Redepenning J, Schlessinger T, Burnham S, Lippiello L, Miyano J. Characterization of electrolytically prepared brushite and hydroxyapatite coatings on orthopedic alloys. J Biomed Mater Res 1996;30:287–94.
[339] Han Y, Fu T, Lu J, Xu KW. Characterization and stability of hydroxyapatite coatings prepared by an electrodeposition and alkaline-treatment process. J Biomed Mater Res 2001;54:96–101.
[340] Rossler S, Sewing A, Stolzel M, Born R, Scharnweber D, Dard M, et al. Electrochemically assisted deposition of thin calcium phosphate coatings at near-physiological pH and temperature. J Biomed Mater Res Part A 2003;64A:655–63.
[341] Peng P, Kumar S, Voelcker NH, Szili E, Smart RS, Griesser HJ. Thin calcium phosphate coatings on titanium by electrochemical deposition in modified simulated body fluid. J Biomed Mater Res Part A 2006;76A:347–55.
[342] Ban SJ, Maruno S. Effect of temperature on electrochemical deposition of calcium-phosphate coatings in a simulated body-fluid. Biomaterials 1995;16:977–81.
[343] Shirkhanzadeh M. Direct formation of nanophase hydroxyapatite on cathodically polarized electrodes. J Mater Sci-Mater Med 1998;9:67–72.
[344] Zhitomirsky I, GalOr L. Electrophoretic deposition of hydroxyapatite. J Mater Sci-Mater Med 1997;8:213–9.
[345] Ducheyne P, Radin S, Heughebaert M, Heughebaert JC. Calcium phosphate ceramic coatings on porous titanium: effect of structure and composition on electrophoretic deposition, vacuum sintering and in vitro dissolution. Biomaterials 1990;11:244–54.
[346] Meng X, Kwon TY, Yang Y, Ong JL, Kim KH. Effects of applied voltages on hydroxyapatite coating of titanium by electrophoretic deposition. J Biomed Mater Res B Appl Biomater 2006;78:373–7.
[347] Stoch A, Brozek A, Kmita G, Stoch J, Jastrzebski W, Rakowska A. Electrophoretic coating of hydroxyapatite on titanium implants. J Mol Struct 2001;596:191–200.
[348] Wei M, Ruys AJ, Swain MV, Kim SH, Milthorpe BK, Sorrell CC. Interfacial bond strength of electrophoretically deposited hydroxyapatite coatings on metals. J Mater Sci-Mater Med 1999;10:401–9.
[349] Yoshinari M, Ozeki K, Sumii T. Properties of hydroxyapatite-coated Ti–6Al–4V alloy produced by the ion-plating method. Bull Tokyo Dent Coll 1991;32:147–56.
[350] Jansen JA, Wolke JG, Swann S, Van der Waerden JP, de Groot K. Application of magnetron sputtering for producing ceramic coatings on implant materials. Clin Oral Implants Res 1993;4:28–34.
[351] Yoshinari M, Ohtsuka Y, Derand T. Thin hydroxyapatite coating produced by the ion beam dynamic mixing method. Biomaterials 1994;15:529–35.
[352] Yoshinari M, Hayakawa T, Wolke JG, Nemoto K, Jansen JA. Influence of rapid heating with infrared radiation on RF magnetron-sputtered calcium phosphate coatings. J Biomed Mater Res 1997;37:60–7.
[353] Yoshinari M, Watanabe Y, Ohtsuka Y, Derand T. Solubility control of thin calcium-phosphate coating with rapid heating. J Dent Res 1997;76:1485–94.
[354] Pham MT, Matz W, Reuther H, Richter E, Steiner G, Oswald S. Ion beam sensitizing of titanium surfaces to hydroxyapatite formation. Surf Coat Technol 2000;128:313–9.
[355] Choi JM, Kim HE, Lee IS. Ion-beam-assisted deposition (IBAD) of hydroxyapatite coating layer on Ti-based metal substrate. Biomaterials 2000;21:469–73.
[356] Hayakawa T, Yoshinari M, Kiba H, Yamamoto H, Nemoto K, Jansen JA. Trabecular bone response to surface roughened and calcium phosphate (Ca-P) coated titanium implants. Biomaterials 2002;23:1025–31.
[357] Kokubo T, Kushitani H, Abe Y, Yamamuro T. Apatite coating on various substrates in simulated body fluids. In: Heimke G, editor. Bioceramics. Cologne: German Ceramic Society; 1990. p. 235–42.
[358] Kim HM, Miyaji F, Kokubo T, Nakamura T. Apatite-forming ability of alkali-treated Ti metal in body environment. J Ceram Soc Jpn 1997;105:111–6.
[359] Kim HM, Miyaji F, Kokubo T, Nakamura T. Bonding strength of bonelike apatite layer to Ti metal substrate. J Biomed Mater Res 1997;38:121–7.
[360] Wen HB, Liu Q, De Wijn JR, De Groot K, Cui FZ. Preparation of bioactive microporous titanium surface by a new two-step chemical treatment. J Mater Sci-Mater Med 1998;9:121–8.
[361] Ha SW, Eckert KL, Gruner H, Wintermantel E. Calcium phosphate formation on chemically treated vacuum plasma sprayed titanium coatings. In: Sedel L, Rey L, editors. Bioceramics. Paris: Elsevier; 1997. p. 451–4.
[362] Tengvall P, Elwing H, Lundstrom I. Titanium gel made from metallic titanium and hydrogen-peroxide. J Coll Interf Sci 1989;130:405–13.
[363] Li PJ, Ohtsuki C, Kokubo T, Nakanishi K, Soga N, Degroot K. The role of hydrated silica, titania, and alumina in inducing apatite on implants. J Biomed Mater Res 1994;28:7–15.
[364] Kokubo T, Miyaji F, Kim HM, Nakamura T. Spontaneous formation of bonelike apatite layer on chemically treated titanium metals. J Am Ceram Soc 1996;79:1127–9.
[365] Kokubo T. Apatite formation on surfaces of ceramics, metals and polymers in body environment. Acta Mater 1998;46:2519–27.
[366] Habibovic P, Barrere F, van Blitterswijk CA, de Groot K, Layrolle P. Biomimetic hydroxyapatite coating on metal implants. J Am Ceram Soc 2002;85:517–22.
[367] Kodama A, Bauer S, Komatsu A, Asoh H, Ono S, Schmuki P. Bioactivation of titanium surfaces using coatings of $TiO_2$ nanotubes rapidly pre-loaded with synthetic hydroxyapatite. Acta Biomater 2009;5:2322–30.
[368] Barrere F, van der Valk CM, Dalmeijer RAJ, van Blitterswijk CA, de Groot K, Layrolle P. In vitro and in vivo degradation of biomimetic octacalcium phosphate and carbonate apatite coatings on titanium implants. J Biomed Mater Res Part A 2003;64A:378–87.
[369] Leeuwenburgh S, Layrolle P, Barrere F, de Bruijn J, Schoonman J, van Blitterswijk CA, et al. Osteoclastic resorption of biomimetic calcium phosphate coatings in vitro. J Biomed Mater Res 2001;56:208–15.
[370] Narayanan R, Seshadri SK, Kwon TY, Kim KH. Calcium phosphate-based coatings on titanium and its alloys. J Biomed Mater Res Part B: Appl Biomater 2008;85B:279–99.
[371] Kim KH, Ramaswamy N. Electrochemical surface modification of titanium in dentistry. Dent Mater J 2009;28:20–36.
[372] de Jonge Lise, Leeuwenburgh Sander, Wolke Joop, Jansen John. Organic–inorganic surface modifications for titanium implant surfaces. Pharmaceut Res 2008;25:2357–69.

[373] Ruardy TG, Schakenraad JM, vanderMei HC, Busscher HJ. Preparation and characterization of chemical gradient surfaces and their application for the study of cellular interaction phenomena. Surf Sci Rep 1997;29:3–30.
[374] Aronsson BO, Lausmaa J, Kasemo B. Glow discharge plasma treatment for surface cleaning and modification of metallic biomaterials. J Biomed Mater Res 1997;35:49–73.
[375] Baier RE, Meyer AE. Implant surface preparation. Int J Oral Maxillo Implants 1988;3:9–20.
[376] Wennerberg A, Bolind P, Albrektsson T. Glow-discharge pretreated implants combined with temporary bone tissue ischemia. Swed Dent J 1991;15:95–101.
[377] Rupp F, Scheideler L, Olshanska N, de Wild M, Wieland M, Geis-Gerstorfer J. Enhancing surface free energy and hydrophilicity through chemical modification of microstructured titanium implant surfaces. J Biomed Mater Res Part A 2006;76A:323–34.
[378] Schwarz F, Wieland M, Schwartz Z, Zhao G, Rupp F, Geis-Gerstorfer J, et al. Potential of chemically modified hydrophilic surface characteristics to support tissue integration of titanium dental implants. J Biomed Mater Res Part B – Appl Biomater 2009;88B:544–57.
[379] Wei J, Yoshinari M, Takemoto S, Hattori M, Kawada E, Liu B, et al. Adhesion of mouse fibroblasts on hexamethyldisiloxane surfaces with wide range of wettability. J Biomed Mater Res B Appl Biomater 2007;81:66–75.
[380] An YH, Friedman RJ. Concise review of mechanisms of bacterial adhesion to biomaterial surfaces. J Biomed Mater Res 1998;43:338–48.
[381] Jones MI, McColl IR, Grant DM, Parker KG, Parker TL. Protein adsorption and platelet attachment and activation, on TiN, TiC, and DLC coatings on titanium for cardiovascular applications. J Biomed Mater Res 2000;52:413–21.
[382] Altankov G, Grinnell F, Groth T. Studies on the biocompatibility of materials: fibroblast reorganization of substratum-bound fibronectin on surfaces varying in wettability. J Biomed Mater Res 1996;30:385–91.
[383] Groth T, Altankov G. Studies on cell-biomaterial interaction: role of tyrosine phosphorylation during fibroblast spreading on surfaces varying in wettability. Biomaterials 1996;17:1227–34.
[384] Chen M, Zamora PO, Som P, Pena LA, Osaki S. Cell attachment and biocompatibility of polytetrafluoroethylene (PTFE) treated with glow-discharge plasma of mixed ammonia and oxygen. J Biomater Sci Polym Ed 2003;14:917–35.
[385] Faucheux N, Schweiss R, Lützow K, Werner C, Groth T. Self-assembled monolayers with different terminating groups as model substrates for cell adhesion studies. Biomaterials 2004;25:2721–30.
[386] Ikada Y. Surface modification of polymers for medical applications. Biomaterials 1994;15:725–36.
[387] Lee JH, Khang G, Lee JW, Lee HB. Interaction of different types of cells on polymer surfaces with wettability gradient. J Coll Interf Sci 1998;205:323–30.
[388] Mrksich M, Whitesides GM. Using self-assembled monolayers to understand the interactions of man-made surfaces with proteins and cells. Ann Rev Biophys Biomol Struct 1996;25:55–78.
[389] Schreiber F. Structure and growth of self-assembling monolayers. Progr Surf Sci 2000;65:151–256.
[390] Ito Y. Surface micropatterning to regulate cell functions. Biomaterials 1999;20:2333–42.
[391] Webb K, Hlady V, Tresco PA. Relationships among cell attachment, spreading, cytoskeletal organization, and migration rate for anchorage-dependent cells on model surfaces. J Biomed Mater Res 2000;49:362–8.
[392] Jenney CR, DeFife KM, Colton E, Anderson JM. Human monocyte/macrophage adhesion, macrophage motility, and IL-4-induced foreign body giant cell formation on silane-modified surfaces in vitro. J Biomed Mater Res 1998;41:171–84.
[393] Arima Yusuke, Iwata Hiroo. Effect of wettability and surface functional groups on protein adsorption and cell adhesion using well-defined mixed self-assembled monolayers. Biomaterials 2007;28:3074–82.
[394] McClary KB, Ugarova T, Grainger DW. Modulating fibroblast adhesion, spreading, and proliferation using self-assembled monolayer films of alkylthiolates on gold. J Biomed Mater Res 2000;50:428–39.
[395] Hamamoto N, Hamamoto Y, Nakajima T, Ozawa H. Histological, histocytochemical and ultrastructural-study on the effects of surface-charge on bone-formation in the rabbit mandible. Arch Oral Biol 1995;40:97–106.
[396] Krukowski M, Shively RA, Osdoby P, Eppley BL. Stimulation of craniofacial and intramedullary bone-formation by negatively charged beads. J Oral Maxillo Surg 1990;48:468–75.
[397] Braceras I, Alava JI, Goikoetxea L, de Maeztu MA, Onate JI. Interaction of engineered surfaces with the living world: ion implantation vs. osseointegration. Surf Coat Technol 2007;201:8091–8.
[398] Pelletier Jacques, Anders Andre. Plasma-based ion implantation and deposition: a review of physics, technology, and applications 2005;33:1944–59.
[399] Albelda SM, Buck CA. Integrins and other cell adhesion molecules. FASEB J 1990;4:2868–80.
[400] Pimentel Enrique. Handbook of growth factors. Boca Raton: CRC Press; 1994.
[401] Pierschbacher MD, Ruoslahti E. Cell attachment activity of fibronectin can be duplicated by small synthetic fragments of the molecule. Nature 1984;309:30–3.
[402] Brandley BK, Schnaar RL. Covalent attachment of an arg–gly–asp sequence peptide to derivatizable polyacrylamide surfaces – support of fibroblast adhesion and long-term growth. Anal Biochem 1988;172:270–8.
[403] Mohan S, Baylink DJ. Bone-growth factors. Clin Orthopaed Relat Res 1991:30–48.
[404] Lind M. Growth factor stimulation of bone healing. Effects on osteoblasts, osteomies, and implants fixation. Acta Orthop Scand Suppl 1998;283:2–37.
[405] Piattelli A, Scarano A, Corigliano M, Piattelli M. Effects of alkaline phosphatase on bone healing around plasma-sprayed titanium implants: a pilot study in rabbits. Biomaterials 1996;17:1443–9.
[406] Lind M, Overgaard S, Nguyen T, Ongpipattanakul B, Bunger C, Soballe K. Transforming growth factor-beta stimulates bone ongrowth. Hydroxyapatite-coated implants studied in dogs. Acta Orthop Scand 1996;67:611–6.
[407] Lind M, Overgaard S, Ongipattanakul B, Nguyen T, Bunger C, Soballe K. Transforming growth factor-beta 1 stimulates bone ongrowth to weight-loaded tricalcium phosphate coated implants – An experimental study in dogs. J Bone Joint Surg – Brit Vol 1996;78B:377–82.
[408] Sumner DR, Turner TM, Purchio AF, Gombotz WR, Urban RM, Galante JO. Enhancement of bone ingrowth by transforming growth factor-beta. J Bone Joint Surg Am 1995;77:1135–47.
[409] Stover M, Renke-Gluszko M, Schratzenstaller T, Will J, Klink N, Behnisch B, et al. Microstructuring of stainless steel implants by electrochemical etching. J Mater Sci 2006;41:5569–75.

[410] Krajewski A, Ravaglioli A, Roncari E, Pinasco P, Montanari L. Porous ceramic bodies for drug delivery. J Mater Sci-Mater Med 2000;11:763–71.
[411] Lu YF, Fan HY, Stump A, Ward TL, Rieker T, Brinker CJ. Aerosol-assisted self-assembly of mesostructured spherical nanoparticles. Nature 1999;398:223–6.
[412] Lai CY, Trewyn BG, Jeftinija DM, Jeftinija K, Xu S, Jeftinija S, et al. A mesoporous silica nanosphere-based carrier system with chemically removable CdS nanoparticle caps for stimuli-responsive controlled release of neurotransmitters and drug molecules. J Am Chem Soc 2003;125:4451–9.
[413] Prestidge CA, Barnes TJ, Lau CH, Barnett C, Loni A, Canham L. Mesoporous silicon: a platform for the delivery of therapeutics. Expert Opin Drug Deliv 2007;4:101–10.
[414] Salonen J, Kaukonen AM, Hirvonen J, Lehto VP. Mesoporous silicon in drug delivery applications. J Pharmaceut Sci 2008;97:632–53.
[415] Briggs EP, Walpole AR, Wilshaw PR, Karlsson M, Palsgard E. Formation of highly adherent nano-porous alumina on Ti-based substrates: a novel bone implant coating. J Mater Sci-Mater Med 2004;15:1021–9.
[416] Martin CR. Nanomaterials – a membrane-based synthetic approach. Science 1994;266:1961–6.
[417] Popat Ketul C, Mor Gopal, Grimes Craig A, Desai Tejal A. Surface modification of nanoporous alumina surfaces with poly(ethylene glycol). Langmuir 2004;20:8035–41.
[418] La Flamme KE, Mor G, Gong D, La Tempa T, Fusaro VA, Grimes CA, et al. Nanoporous alumina capsules for cellular macroencapsulation: transport and biocompatibility. Diab Technol Ther 2005;7:684–94.
[419] Popat KC, Eltgroth M, LaTempa TJ, Grimes CA, Desai TA. Titania nanotubes: a novel platform for drug-eluting coatings for medical implants? Small 2007;3:1878–81.
[420] Popat KC, Eltgroth M, Latempa TJ, Grimes CA, Desai TA. Decreased Staphylococcus epidermis adhesion and increased osteoblast functionality on antibiotic-loaded titania nanotubes. Biomaterials 2007;28:4880–8.
[421] Song YY, Schmidt-Stein F, Bauer S, Schmuki P. Amphiphilic $TiO_2$ nanotube arrays: an actively controllable drug delivery system. J Am Chem Soc 2009;131:4230–2.
[422] Schmidt-Stein Felix, Hahn Robert, Gnichwitz Jan-Frederik, Song Yan Yan, Shrestha Nabeen K, Hirsch Andreas, et al. X-ray induced photocatalysis on $TiO_2$ and $TiO_2$ nanotubes: degradation of organics and drug release. Electrochem Commun 2009;11:2077–80.
[423] Shrestha NK, Macak JM, Schmidt-Stein F, Hahn R, Mierke CT, Fabry B, et al. Magnetically guided titania nanotubes for site-selective photocatalysis and drug release. Angew Chem Int Ed Engl 2009;48:969–72.
[424] Acharya G, Park K. Mechanisms of controlled drug release from drug-eluting stents. Adv Drug Deliv Rev 2006;58:387–401.
[425] Schmidmaier G, Lucke M, Schwabe P, Raschke M, Haas NP, Wildemann B. Collective review: bioactive implants coated with poly(D,L-lactide) and growth factors IGF-I, TGF-beta1, or BMP-2 for stimulation of fracture healing. J Long Term Eff Med Implants 2006;16:61–9.
[426] Agrawal CM, Pennick A, Wang X, Schenck RC. Porous-coated titanium implant impregnated with a biodegradable protein delivery system. J Biomed Mater Res 1997;36:516–21.
[427] Price JS, Tencer AF, Arm DM, Bohach GA. Controlled release of antibiotics from coated orthopedic implants. J Biomed Mater Res 1996;30:281–6.
[428] Walsh WR, Kim HD, Jong YS, Valentini RF. Controlled-release of platelet-derived growth-factor using ethylene-vinyl acetate copolymer (Evac) coated on stainless-steel wires. Biomaterials 1995;16:1319–25.
[429] Fischer U, Hempel U, Becker D, Bierbaum S, Scharnweber D, Worch H, et al. Transforming growth factor beta1 immobilized adsorptively on Ti6Al4V and collagen type I coated Ti6Al4V maintains its biological activity. Biomaterials 2003;24:2631–41.
[430] Puleo DA. Release and retention of biomolecules in collagen deposited on orthopedic biomaterials. Artif Cells Blood Substit Immobil Biotechnol 1999;27:65–75.
[431] Katz RW, Reddi AH. Dissociative extraction and partial purification of osteogenin, a bone inductive protein, from rat tooth matrix by heparin affinity chromatography. Biochem Biophys Res Commun 1988;157:1253–7.
[432] Muthukumaran N, Ma S, Reddi AH. Dose-dependence of and threshold for optimal bone induction by collagenous bone-matrix and osteogenin-enriched fraction. Coll Relat Res 1988;8:433–41.
[433] Suzawa Miyuki, Takeuchi Yasuhiro, Fukumoto Seiji, Kato Shigeaki, Ueno Naoto, Miyazono Kohei, et al. Extracellular matrix-associated bone morphogenetic proteins are essential for differentiation of murine osteoblastic cells in vitro. Endocrinology 1999;140:2125–33.
[434] Frutos Cabanillas P, Dıez Peña E, Barrales-Rienda JM, Frutos G. Validation and in vitro characterization of antibiotic-loaded bone cement release. Int J Pharmac 2000;209:15–26.
[435] Silverman LD, Lukashova L, Herman OT, Lane JM, Boskey AL. Release of gentamicin from a tricalcium phosphate bone implant. J Orthopaed Res 2007;25:23–9.
[436] Wallace DG, Rosenblatt J. Collagen gel systems for sustained delivery and tissue engineering. Adv Drug Deliv Rev 2003;55:1631–49.
[437] Liu SQ, Ito Y, Imanishi Y. Cell-growth on immobilized cell-growth factor. 4. Interaction of fibroblast cells with insulin immobilized on poly(methyl methacrylate) membrane. J Biochem Biophys Meth 1992;25:139–48.
[438] Liu Shu Qin, Ito Yoshihiro, Imanishi Yukio. Cell growth on immobilized cell growth factor: 5. Interaction of immobilized transferrin with fibroblast cells. Int J Biol Macromol 1993;15:221–6.
[439] Ito Y. Cell growth factor immobilized materials. In: Imanishi Y, editor. Synthesis of biocomposite materials: chemical and biological modifications of natural polymers. Boca Raton: CRC Press; 1992. p. 285–305.
[440] Kishida A, Ueno Y, Fukudome N, Yashima E, Maruyama I, Akashi M. Immobilization of human thrombomodulin onto poly(ether urethane urea) for developing antithrombogenic blood-contacting materials. Biomaterials 1994;15:848–52.
[441] Kishida A, Ueno Y, Maruyama I, Akashi M. Immobilization of human thrombomodulin on biomaterials – evaluation of the activity of immobilized human thrombomodulin. Biomaterials 1994;15:1170–4.
[442] Ticha M, Zelezna B, Jonakova V, Filka K. Immobilization of heparin on polyacrylamide derivatives. J Chromatogr B-Biomed Appl 1994;656:423–6.

[443] Ruoslahti E, Pierschbacher MD. New perspectives in cell-adhesion – rgd and integrins. Science 1987;238:491–7.
[444] Healy KE. Molecular engineering of materials for bioreactivity. Curr Opin Solid State Mater Sci 1999;4:381–7.
[445] Verrier S, Pallu S, Bareille R, Jonczyk A, Meyer J, Dard M, et al. Function of linear and cyclic RGD-containing peptides in osteoprogenitor cells adhesion process. Biomaterials 2002;23:585–96.
[446] Nanci A, Wuest JD, Peru L, Brunet P, Sharma V, Zalzal S, et al. Chemical modification of titanium surfaces for covalent attachment of biological molecules. J Biomed Mater Res 1998;40:324–35.
[447] Duan K, Wang RZ. Surface modifications of bone implants through wet chemistry. J Mater Chem 2006;16:2309–21.
[448] Puleo DA. Retention of enzymatic activity immobilized on silanized Co–Cr–Mo and Ti–6Al–4V. J Biomed Mater Res 1997;37:222–8.
[449] Ito Y, Inoue M, Liu SQ, Imanishi Y. Cell growth on immobilized cell growth factor. 6. Enhancement of fibroblast cell growth by immobilized insulin and/or fibronectin. J Biomed Mater Res 1993;27:901–7.
[450] Ulman A. Formation and structure of self-assembled monolayers. Chem Rev 1996;96:1533–54.
[451] Xiao SJ, Textor M, Spencer ND, Sigrist H. Covalent attachment of cell-adhesive, (Arg–Gly–Asp)-containing peptides to titanium surfaces. Langmuir 1998;14:5507–16.
[452] Kouvroukoglou S, Dee KC, Bizios R, McIntire LV, Zygourakis K. Endothelial cell migration on surfaces modified with immobilized adhesive peptides. Biomaterials 2000;21:1725–33.
[453] Tosatti S, Michel R, Textor M, Spencer ND. Self-assembled monolayers of dodecyl and hydroxy-dodecyl phosphates on both smooth and rough titanium and titanium oxide surfaces. Langmuir 2002;18:3537–48.
[454] Viornery C, Chevolot Y, Leonard D, Aronsson BO, Pechy P, Mathieu HJ, et al. Surface modification of titanium with phosphonic acid to improve bone bonding: characterization by XPS and ToF-SIMS. Langmuir 2002;18:2582–9.
[455] Hofer R, Textor M, Spencer ND. Alkyl phosphate monolayers, self-assembled from aqueous solution onto metal oxide surfaces. Langmuir 2001;17:4014–20.
[456] Adden N, Gamble LJ, Castner DG, Hoffmann A, Gross G, Menzel H. Phosphonic acid monolayers for binding of bioactive molecules to titanium surfaces. Langmuir 2006;22:8197–204.
[457] Gawalt ES, Avaltroni MJ, Koch N, Schwartz J. Self-assembly and bonding of alkanephosphonic acids on the native oxide surface of titanium. Langmuir 2001;17:5736–8.
[458] Marcinko S, Fadeev AY. Hydrolytic stability of organic monolayers supported on $TiO_2$ and $ZrO_2$. Langmuir 2004;20:2270–3.
[459] Helmy Roy, Fadeev Alexander Y. Self-assembled monolayers supported on $TiO_2$? Comparison of C18H37SiX3 (X = H, Cl, OCH3), C18H37Si(CH3)2Cl, and C18H37PO(OH)2. Langmuir 2002;18:8924–8.
[460] Silverman BM, Wieghaus KA, Schwartz J. Comparative properties of siloxane vs phosphonate monolayers on a key titanium alloy. Langmuir 2005;21:225–8.
[461] Bauer Sebastian, Park Jung, Pittrof Andreas, Song Yan-Yan, von der Mark Klaus, Schmuki Patrik. Covalent functionalization of TiO2 nanotube arrays with EGF and BMP-2 for modified behavior towards mesenchymal stem cells. Integra Biol 2011;3:927–36.
[462] Balasundaram G, Sato M, Webster TJ. Using hydroxyapatite nanoparticles and decreased crystallinity to promote osteoblast adhesion similar to functionalizing with RGD. Biomaterials 2006;27:2798–805.
[463] Porte-Durrieu MC, Guillemot F, Pallu S, Labrugere C, Brouillaud B, Bareille R, et al. Cyclo-(DfKRG) peptide grafting onto Ti–6Al–4V: physical characterization and interest towards human osteoprogenitor cells adhesion. Biomaterials 2004;25:4837–46.
[464] de Taillac LB, Porte-Durrieu MC, Labrugere C, Bareille R, Amedee J, Baquey C. Grafting of RGD peptides to cellulose to enhance human osteoprogenitor cells adhesion and proliferation. Compos Sci Technol 2004;64:827–37.
[465] Gawalt ES, Avaltroni MJ, Danahy MP, Silverman BM, Hanson EL, Midwood KS, et al. Bonding organics to Ti alloys: facilitating human osteoblast attachment and spreading on surgical implant materials corrections (vol. 19, p. 200, 2003). Langmuir 2003;19:7147.
[466] Nelson M, Balasundaram G, Webster TJ. Increased osteoblast adhesion on nanoparticulate crystalline hydroxyapatite functionalized with KRSR. Int J Nanomed 2006;1:339–49.
[467] Xiao SJ, Textor M, Spencer ND, Wieland M, Keller B, Sigrist H. Immobilization of the cell-adhesive peptide Arg–Gly–Asp-Cys (RGDC) on titanium surfaces by covalent chemical attachment. J Mater Sci Mater Med 1997;8:867–72.
[468] Rezania A, Johnson R, Lefkow AR, Healy KE. Bioactivation of metal oxide surfaces. 1. Surface characterization and cell response. Langmuir 1999;15:6931–9.
[469] Hong HG, Jiang M, Sligar SG, Bohn PW. Cysteine-specific surface tethering of genetically-engineered cytochromes for fabrication of metalloprotein nanostructures. Langmuir 1994;10:153–8.
[470] Rezania A, Healy KE. Biomimetic peptide surfaces that regulate adhesion, spreading, cytoskeletal organization, and mineralization of the matrix deposited by osteoblast-like cells. Biotechnol Progr 1999;15:19–32.
[471] Park Jung, Bauer Sebastian, Pittrof Andreas, Killian Manuela S, Schmuki Patrik, von der Mark Klaus. Synergistic control of mesenchymal stem cell differentiation by nanoscale surface geometry and immobilized growth factors on TiO2 nanotubes. Small 2012;8:98–107.
[472] Goncalves R, Martins MCL, Oliveira MJ, Almeida-Porada G, Barbosa MA. Bioactivity of immobilized EGF on self-assembled monolayers: optimization of the immobilization process. J Biomed Mater Res Part A 2010;94A:576–85.
[473] Yu XJ, Dillon GP, Bellamkonda RV. A laminin and nerve growth factor-laden three-dimensional scaffold for enhanced neurite extension. Tissue Eng 1999;5:291–304.
[474] McArthur SL, Halter MW, Vogel V, Castner DG. Covalent coupling and characterization of supported lipid layers. Langmuir 2003;19:8316–24.
[475] Tiller J, Berlin P, Klemm D. A novel efficient enzyme-immobilization reaction on NH2 polymers by means of L-ascorbic acid. Biotechnol Appl Biochem 1999;30:155–62.
[476] Oliveira EM, Beyer S, Heinze J. SECM characterization of immobilised enzymes by self-assembled monolayers on titanium dioxide surfaces. Bioelectrochemistry 2007;71:186–91.
[477] Puleo DA. Biochemical surface modification of Co–Cr–Mo. Biomaterials 1996;17:217–22.

[478] Middleton CA, Pendegrass CJ, Gordon D, Jacobs J, Blunn GW. Fibronectin silanized titanium alloy: a bioinductive and durable coating to enhance fibroblast attachment in vitro. J Biomed Mater Res Part A 2007;83A:1032–8.
[479] Morra M. Biochemical modification of titanium surfaces: peptides and ECM proteins. Euro Cells Mater 2006;12:1–15.